

83519

OTS: 60-11,661

JPRS: 2690

23 May 1960

AD-A286 617



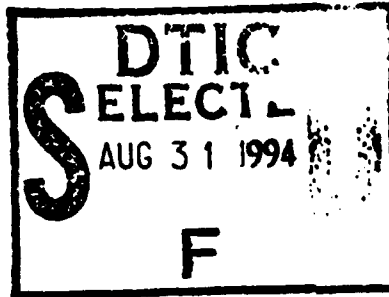
3

C

SHORT WAVE DIRECTION FINDERS

- USSR -

By O. V. Belavin



COPY 1

LIBRARY COPY

JUN 8 1960

94-28180



22387



Distributed by:

OFFICE OF TECHNICAL SERVICES
U. S. DEPARTMENT OF COMMERCE
WASHINGTON 25, D. C.

This document has been approved
for public release and sale; its
distribution is unlimited

~~Price \$5.50~~

U. S. JOINT PUBLICATIONS RESEARCH SERVICE
205 EAST 42nd STREET, SUITE 300
NEW YORK 17, N. Y.

DTIC

04 2 30 2 1

CN-83519

**Best
Available
Copy**

SHORT WAVE DIRECTION FINDERS

[Following is a translation (reproduced, for reasons of speed and economy, directly from the translator's dictation) of the book "Korotkovolnovyye Radiopelengatory" (Short Wave Direction Finders), published in Moscow, 1959, pages 3 - 124.]

TABLE OF CONTENTS

	Page
FOREWORD.....	1
<u>Chapter I</u>	
Methods of Direction Finding and Block Diagrams of	
Long-Base Radio Direction Finders.....	4
1. Short-Wave Radio Navigational Systems.....	4
2. Short-Base Radio Direction Finders.....	6
3. Long-Base Radio Direction Finders.....	8
4. Direction Finding Methods.....	10
Rapid Rotation of the Directivity Pattern.	18
Measurement of the Phase Differences (Phase Method).....	23
5. Antennas of Long-Base Radio Direction Finders.....	27
Single Antennas.....	27
Groups of Antennas.....	30
6. Methods of Measuring Phase Differences....	35
Methods of Direct Measurement of Phase Differences.....	36
Compensation Methods of Measuring Phase Differences.....	38

Dist	d/or
A-1	Special
	Codes

7. Amplification Circuits for Signals in Long-Base Short-Wave Radio Direction Finders...	54
Pure Single-Channel Amplifications.....	55
Single-Channel Amplification with Conversion of Signals by Additional Modulation..	63
Single-Channel Amplification with Signal Conversion by the Heterodyne Method.....	67
Simple Two-Channel Amplification.....	75
Amplification with Use of Driver-Frequency Voltage.....	76
Amplification with Driver Heterodyne.....	82
 <u>Chapter II</u>	
Errors of Short-Wave Direction Finders, Due to Conditions of Radio Wave Propagation.....	85
1. Influence of the Ionosphere on the Propagation of Radio Waves.....	85
2. Bearing Errors Due to Singularities in the Propagation of Short Waves.....	86
3. Methods of Reducing Interference Errors...	99
 <u>Chapter III</u>	
Effect of Channel Unbalance on the Apparatus	
1. Errors of Two-Channel Radio Direction Finders.....	115
Two Versions of Two-Channel Amplification Schemes.....	115
2. Errors in the Post-Amplification Circuit..	118
3. Observation Errors.....	134
 <u>Chapter IV</u>	
Effect of Unequal Channel Parameters on the Apparatus Errors of Two-Channel Radio Direction Finders.	
1. Parameters of Non-Identity.....	138
2. Bandwidth of a Two-Channel Radio Direction Finder.....	145
3. Errors Due to Non-Identity of Tuned Amplifier Channels.....	147
 <u>Chapter V</u>	
Apparatus Errors of a Two-Channel Radio Direction Finder for a Pulsed Radio Signal.....	160
1. Character of the Pattern on the Tube Screen in the Case of a Pulsed Signal.....	160
2. Reading of the Bearing in the Case of a Pulsed Radio Signal.....	168
3. Errors in the Circuit with Pulsed Amplification.....	171

Chapter VI

Apparatus Errors of Phase Meters Operating at	
Low Frequency.....	184
1. Choice of Phase Meter Circuit.....	184
2. Phase Meters with Reading by Means of a Cathode Ray Tube.....	185
3. Phase Meter Error During Change in Signal Amplitude.....	196
4. Apparatus Error of the Phase Meter.....	198
5. Transient Time of Phase Meter Reading.....	203
6. Operation of the Phase Meter in the Presence of Noise.....	210
BIBLIOGRAPHY.....	218

FOREWORD

Short wave direction finders serve as one of the means of long distance radio navigation. Their essential advantage is the ability to cover large distances with relatively little power consumed by the transmitters. The only factor that limits to a certain extent extensive use of short wave radio direction finders is the insufficient direction-finding accuracy. The problem of raising the accuracy of radio direction finding at short waves is therefore quite urgent.

The available literature on short-wave radio navigation is contained essentially in journal articles. Yet, a need is felt for papers that generalize and systematize these varied data, which sometimes are contradictory.

It is the aim of this book to fill to some extent this gap and thereby aid the students in the corresponding sections of courses on radio navigation.

We consider in this text the construction principle and block diagrams of short wave direction finders, we analyze their operating features, and make recommendations concerning the choice of different versions.

Particular attention is paid to direction finders with long

base, which ensure relatively high accuracy of direction finding. This feature makes radio direction finders with long base the most promising.

Since conditions of propagation of radio waves determine to a considerable extent the accuracy of short-wave radio navigation, it is necessary to take into account the features of propagation of radio waves when choosing or designing direction finders.

In Chapter I, written by candidate of technical sciences, lecturer O.V. Belavin, are considered direction finding methods and block diagrams of long-base direction finders. Chapter II, written by candidate of technical sciences V.A. Veytsel¹, gives a brief survey of the most characteristic errors in radio navigation, due to conditions of the ~~next~~ route, and recommendations on means of raising the accuracy of direction finders. In ~~Chapters III, IV, and V~~, written by candidate of technical sciences, V.S. Ul'yanov, are investigated the operating features of two-channel inertialess direction finders, and an analysis is given of the apparatus error when continuous and pulsed radio signals are used.

Chapter VI, written by V.A. Veytsel¹, is devoted to the selection and investigation of the phase-meter block, which is the final stage in the direction finder that operates with signal conversion.

The text contains the first publication of results of original research on the error of the receiving circuits, and phase meters of laboratory models built at the MAI/Moscow Aviation Institute/.

In writing Chapters I and II, use was made of data on foreign long-base radio direction finders, the description of which can be found in the literature cited at the end of the book.

This work, which is the first attempt of dissemination of different material on short wave radio direction finding, is naturally not free of errors. The authors will receive gratefully advice and critical remarks, which should be addressed to the Moscow Aviation Institute.

Chapter I

METHODS OF DIRECTION FINDING AND BLOCK DIAGRAMS OF LONG-BASE RADIO DIRECTION FINDERS

1. SHORT-WAVE RADIO NAVIGATIONAL SYSTEMS

The use of the means of long distance radio navigation makes it possible to guide airplanes over long distances with a minimum number of surface-based radio navigation points. For our country, the development of a system of long-distance radio navigation, operating with satisfactory accuracy at distances of several thousand kilometers, is of great significance.

Radio-navigational means with a range exceeding 2500 kilometers can be attained by using long or short waves. The possibility of using radio waves in the centimeter band (reflected from the troposphere) is still doubtful. However, the use of long radio waves calls for transmitters of considerable power. Radio navigation means operating at these waves are best made in the form of radio beacons, with only radio receivers mounted on the airplanes.

In addition, it is easy to produce in the long-wave band artificial noise, which practically covers the entire band. Even in the

absence of man-made noise, random interference from neighboring radio stations may frequently occur. The high level of atmospheric static at long waves leads unavoidably to an increase in the power of the transmitting devices. The foregoing factors reduce considerably the basic advantage of radio navigational systems at long waves -- the high operating reliability (in the absence of interference).

The use of short radio waves (in the band from 3 to 30 Mcs) requires no high power transmitters, and transmitters with an antenna power on the order of several hundreds of watts are adequate. A short-wave radio navigation system can be produced in a direction-finder version, by locating the radio direction finders on the surface of the earth. In this case the operating time of the system transmitters may be quite insignificant. The operation of such a system is very difficult to detect. The production of man-made static is also made difficult.

The problem of developing a long-range direction finder system at short waves reduces to the solution of problems connected with the possibility of increasing the accuracy of radio direction finding. The existing radio direction finders for short waves, of the Adcock type, produce large errors when operating at distances more than 1,000 kilometers, and frequently cannot operate at weak signals.

It is necessary to consider the possibilities of producing short wave radio direction finders, which result in considerably smaller errors. In such radio direction finders, the distances between antennas

or groups of antennas exceed a wavelength. They are called long-base radio direction finders and are considered in the present book.

Naturally, it must be borne in mind that short-wave radio direction finders cannot insure in general high operating reliability, owing to the characteristic conditions of short wave radio propagation. It may also happen that radio navigation systems operating at short waves will not be able to insure the same accuracy as long-wave systems. Nevertheless, conditions may occur under which the use of short wave systems of navigation may yield the necessary effect. One must therefore consider short-wave radio navigation systems as almost essential supplements to means operating at long waves.

2. SHORT-BASE RADIO DIRECTION FINDERS

Radio direction finders, whose main antenna system element is a loop, operate well in the medium wave band (0.2 -- 1.5 Mcs). They permit radio direction finding with a mean squared error not exceeding 1° , under the best conditions/10/. In the short-wave band, loop-type radio direction finders produce large errors, due primarily to the peculiar features of propagation of short radio waves, which are reflected from the ionosphere. The errors arise as a result of the change in the angle of polarization of the wave upon reflection from the ionosphere.

The appearance of errors in a loop direction finder upon change in angle of polarization of the radio waves is due to the

reception of the electromagnetic field on the horizontal parts of the loop. Therefore, separated antennas were used in the next stage of development of radio direction finders at short waves. Radio direction finders with separated antennas are called Adcock type radio direction finders.

The directivity pattern of an antenna system consisting of two antennas, separated by not more than 0.1 of a wavelength, is the same as that of a simple loop. These are short-base radio direction finders.

Various versions of radio direction finders of the Adcock type have been proposed, in order to reduce further the signal reception level on the horizontal feeders of the antenna system and to reduce the antenna effect. Data on the investigation of various versions of Adcock type radio direction finders are given in the well known work by V.V.Shirkov [13].

Nevertheless, since pickup does exist in the feeders, radio direction finders of the Adcock type are not free of polarization errors.

Matters are improved somewhat by using separated loops instead of separated antennas. This reduces the polarization errors and increases the interference rejection of the radio direction finders, but still does not solve the problem of the effective utilization of these radio direction finders for long distance and exact direction finding at short waves. Owing to the short base of the Adcock type radio direction finders they produce large errors, due to the influence

of scattered reflection. In addition, it is difficult to increase the interference rejection of such radio direction finders, for they must receive signals from all directions. Furthermore, the use of sharply-directional antennas is frequently excluded. All this leads to the conclusion that radio direction finders with short λ base cannot be recommended as a foundation for the construction of exact radio direction finders for short waves, operating at distances of several thousands kilometers. We therefore leave out here the description of various block diagrams of short-base radio direction finders, referring the reader to the literature [8, 10, 13].

3. LONG-BASE RADIO DIRECTION FINDERS

The large errors due to the influence of scattered reflections and variations in the angle of polarization, inherent in short-base radio direction finders, have necessitated a search for a solution to the problem of increasing the accuracy of long distance direction finding at short waves by employing long-base radio direction finders. Already at the beginning of the thirties, in investigations performed at the Central Radio Laboratory on the stability of bearings on the Leningrad-Khabarovsk line [1], a long-base antenna system was employed. Approximately at the start of the forties, radio direction finders with long base have been developed intensely in Germany. In the middle of the forties, radio direction finders with long base found application on a large scale in England. The results of the work by

Ross with such radio direction finders was published in special reports on the investigation of conditions of direction findings at short waves/167.

The known material on radio direction finders with long base has shown that these direction finders must ensure a considerably greater direction finding accuracy at medium waves and a certain increase in accuracy of direction finding at short waves. In spite of this, there is still a lack of literature that considers the possible block diagrams of radio direction finders with long base and direction finding methods. In the design of radio direction finders with long base, questions arise of the advantageous choice of an antenna system, of the direction finding method, of the block diagram of the receiving-indicating apparatus, etc. Furthermore, all these problems must be related to the direction finding conditions. The choice of direction finder parameters must insure a reduction in the different errors due to the definite characteristics of direction findings at short waves. Yet the literature hardly touches upon such questions. There are many books devoted to the investigation of direction finding errors at short waves by means of long-wave radio direction finders. But the authors of these books investigate principally the theoretical problems, without dwelling on practical recommendations regarding the choice of parameters and circuits for radio direction finders with long base. In the present text we consider the principal methods of direction finding at short waves, block diagrams of long-base radio

directionfinders, and recommendations on the design of radio direction finders from the point of view of reducing the apparatus errors.

Long-base radio direction finders can be called sector finders, since usually the bearing is measured within a narrow sector of angles. If the position of the sector can be changed, then, naturally, it is possible to find the bearing to a signal from any direction.

4. DIRECTION FINDING METHODS

Comparison of Amplitudes

Direction finding can be carried out by radio direction finders of long base by using the method of comparison of signal amplitudes.

Assume that we have two groups of antennas, the horizontal section of the directivity patterns of which are shown in Fig. 1.1. The voltages at the outputs of the antennas can be written as

$$E_1 = E_0 f_1(\beta, \theta); \quad E_2 = E_0 f_2(\beta, \theta), \quad (1.1)$$

where β — elevation angle.

θ — bearing measured from the direction chosen as the reference point.

E_0 — amplitude of the voltage in the direction of the maximum of the pattern.

If we take, for example, the ratio or the difference of the amplitudes, we obtain the following formulas

$$v = \frac{E_1}{E_2} = \frac{f_1(\beta, \theta)}{f_2(\beta, \theta)}; \quad (1.2)$$

$$v_1 = E_0 [f_1(\beta, \theta) - f_2(\beta, \theta)] \kappa, \quad (1.3)$$

where v and v_1 — readings of the direction finder indicator in the ~~former~~ former and in the latter cases.

The ratio of the voltages, as seen from (1.2) depends on the bearing of the arriving signal and on the elevation angle. Formula (1.2) can be represented in the form

$$v = f(\beta, \theta). \quad (1.4)$$

Differentiating, we obtain

$$dv = \frac{\partial f(\beta, \theta)}{\partial \beta} d\beta + \frac{\partial f(\beta, \theta)}{\partial \theta} d\theta. \quad (1.5)$$

Relation (1.4) can be called the direction-finding characteristic (Fig. 1.2).

The slope of the direction-finding characteristic determines the direction-finding scale, and the instrumental accuracy. The narrower the lobes of the antenna directivity pattern, the greater this scale.

The advantage of a direction finder employing amplitude comparison is that it takes into account only the amplitude relations of the signals, and the phase relations do not play any role at all. In practice the directivity patterns of antennas contain more or less pronounced side lobes. In addition to the principal sectors, there appear on the direction finding characteristic also false sectors, shown dotted in Fig. 1.2. Considerable difficulties arise also in

connection with eliminating the influence of the "altitude" error, inasmuch as ~~and therefore~~ the elevation angle enters into Eq. (1.2).

A block diagram of the receiving-indicating unit of the radio direction finder for amplitude comparison is shown in Fig. 1.3.

Actually the diagram shows a two-channel receiving-indicating unit. The voltage from the output of the second channel controls in AGC stage, which changes the gains of the channels simultaneously, maintaining the voltage at the output of the second channel constant.

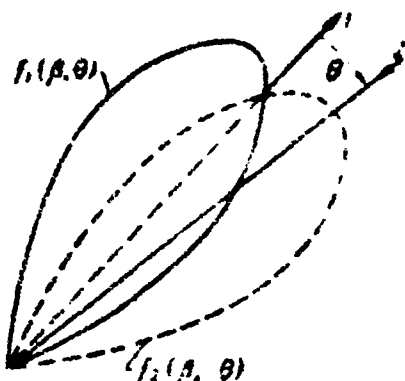


Fig. 1.1. Arrangement of the directivity patterns of two antennas in direction finding by the amplitude-comparison method.

1 — direction of the zero reading of the bearing, 2 -- direction of the incoming signal.

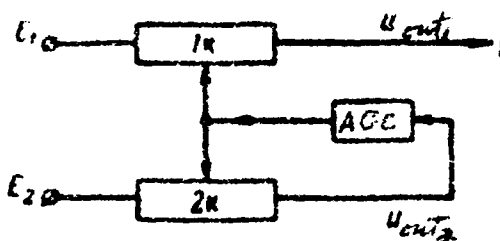
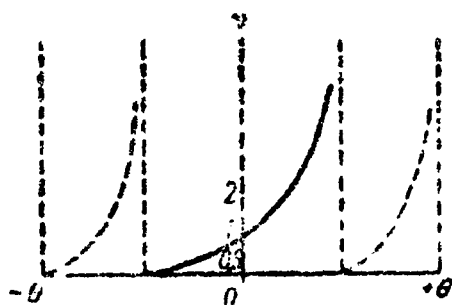


Fig. 1.2. Characteristic of direction finding of a finder operating by the amplitude-comparison method.

θ — signal bearing, γ — reading of radio direction finder.

Fig. 1.3. Block diagram of radio direction finder, operating by the amplitude-comparison method.

E — voltage of the first antenna group, E_2 — voltage of the second antenna group, I — voltage applied to indicator, AGC — automatic gain control stage, $1k$ — first channel, $2k$ — second channel.

The voltage at the output of the first channel is

$$u_{out_1} = E_1 K, \quad (1.6)$$

where K is the gain of the channel.

Accordingly, the voltage at the output of the second channel is

$$u_{out_2} = K E_2 = \text{const} = c. \quad (1.7)$$

Inserting the value of the gain from Eq. (1.6) into (1.7) we see that the voltage at the output of the first channel is proportional to the ratio of the voltages at the input

$$u_{out_1} = c \frac{E_1}{E_2}. \quad (1.8)$$

The magnitude of the apparatus errors of an amplitude-compari-

son radio direction finder is determined by the operating quality of the AGC circuit, which should operate very effectively. When ~~max~~ the input voltage is changed by a factor of 10^3 , the output voltage at the output of the second channel should change only by several percent. Usually ~~contains~~ an amplified AGC circuit is used.

In addition, the apparatus errors of the receiving-indicating unit depend on the field intensity of the received radio station. If the input voltage is insufficient to operate the AGC, the circuit yields large errors.

A variation in the directivity patterns also leads to apparatus errors. This variation should not exceed 1% at a 0.2° bearing accuracy.

The possible occurrence of various apparatus errors makes it impossible to consider the amplitude-comparison method as basic in radio direction finders with long bases. It can play only a subsidiary role. This method ~~is~~ ^{was} ^{more} used ~~more~~ frequently earlier, when the factors that determine the stability of the phase characteristics of the receiving apparatus at short waves were not sufficiently studied.

Slow Rotation of the Directivity Pattern

Another method of direction finding is based on a slow rotation of the directivity pattern. In this case the signal amplitudes are not compared simultaneously, but successively in time.

The directivity pattern of the antenna system, which has a

sharp null, was rotated by smoothly switching the antennas with the aid of a special device. By rotating the pattern, one finds the position at which the signal is not recorded by the indicator.

In the early radio direction finders of this type, the indicator used was an earphone connected to the output of the receiver. Direction finding by slow rotation of the directivity pattern can be readily explained using as an example the Wullenwever radio direction finder with a sine compensator (Fig. 1.4). The antenna system of this radio direction finder consists of broadband antennas, arranged in a circle. Located in the center of the antenna system is a direction finding booth, in which is located the sine compensator and the receiving apparatus.

The antennas are connected in groups of four each and are phased to one direction by means of artificial delay lines, located in the sine compensator (see Fig. 1.4). The delay time from one antenna to another should change sinusoidally, and this is why the phasing apparatus is called a sine-compensator.

The sine compensator consists of a dual cylinder with non-conducting walls. The inner cylinder can rotate independently of the outer one. On the inner and outer cylinders are ~~mounted~~ placed metallic switch blades, between which the necessary capacitive coupling is produced. The delay lines are connected to the blades of the internal cylinder, and cables from the antennas are connected to the blades of the external cylinder. Located on the top of the

sine compensator is a bearing scale. When the internal cylinder of the sine compensator is rotated, the diagram patterns of the groups rotate smoothly.

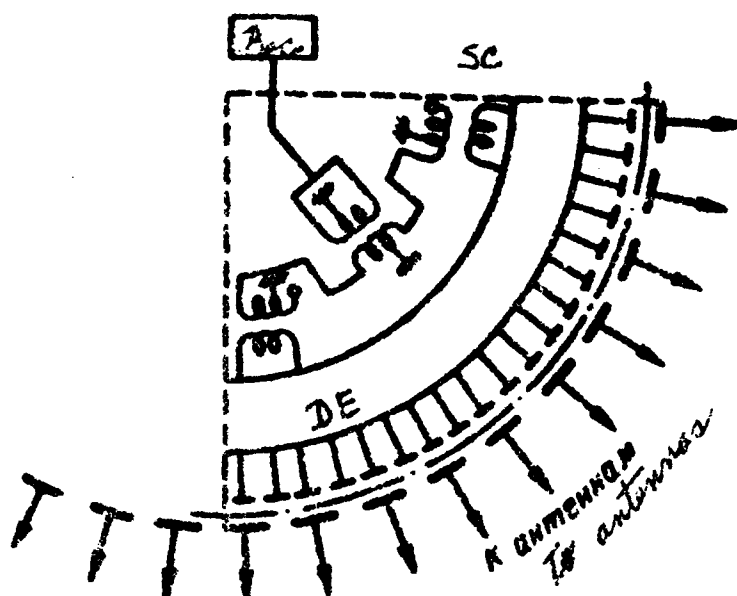


Fig. 1.4. Block diagram of the antenna system of the Wallenwever directionfinder.

Rec — receiver, SC — sine compensator, DE — delay elements.

Smooth rotation of the pattern is attained by the fact that between two blades of the inner cylinder are placed three blades of the outer cylinder. The outputs of the two groups of antennas are fed to a switch, which can connect them either for addition or for maximum difference (Fig. 1.5).

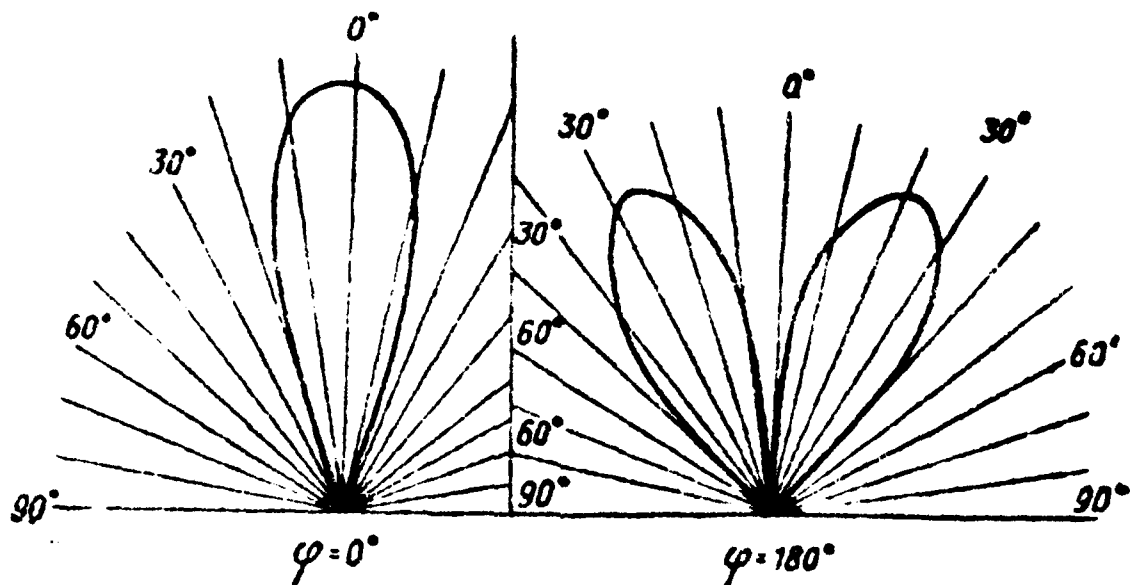


Fig. 1.5. Directivity pattern of antenna groups for different connections (left -- connection for sum, right -- for difference).

The searching for a signal occurs with the directivity patterns connected for summation. In this position the inner cylinder of the sine compensator ~~xxxx~~ rotates until a maximum sound is received, and roughly, accurate to several degrees, one determines the bearing of the radio station.

After the signal is detected, the directivity pattern is switched over for difference and the direction finding is continued for minimum audibility. In the case of a long base, several minima are obtained. The operator selects the minimum corresponding to the readings obtained during the search. The instrumental accuracy of bearing determination is on the order of several tens of minutes and depends here on the patterns of the antenna system and on the signal to noise ratio.

As in the case of audio radio direction finders, we can

speak of a sensitivity modulus, taking this term to mean the product of the angle of silence by the intensity of the signal field.

The instrumental accuracy increases with increasing frequency, since at higher frequencies the directivity patterns are sharper. The presence of apparatus errors is verified by means of an external heterodyne. This makes it possible to introduce the necessary corrections in the bearing readings.

Direction finding is always along a perpendicular to the base, thus insuring maximum instrumental accuracy. A radio direction finder operating by the method of slow rotation of the directivity pattern has low operating efficiency. This shortcoming is inherent in all methods of non-simultaneous comparison of signal amplitudes. There is no instantaneous reading in this case.

Rapid Rotation of the Directivity Pattern

The insufficient operating efficiency in slow rotation of the directivity pattern can be eliminated to a considerable extent by using rapid rotation of the directivity pattern of the antenna system. For example, it is possible to rotate mechanically the internal cylinder of the sine compensator. It is easy to understand that, with this, the input voltage of the receiver will be modulated in amplitude. If the directivity pattern has sharp nulls, then the voltage at the output of the receiver will not contain the carrier frequency, and will have only the side bands. The block diagram of the radio

direction finder, operating on the method of rapid rotation of the directivity pattern, as shown in Fig. 1.6.

Assume that we have a reference generator, the voltage of which is synchronized with the position of the rotor of the motor which rotates the directivity pattern. Let in the simplest case the directivity pattern have the shape of a Fig. 8. Then the ~~dir~~ voltage at the input of the receiver, if the voltage of the carrier frequency is also present, will be proportional to the quantity

$$\sin \omega t [1 + m \sin(\theta + \Omega t)], \quad (1.9)$$

and the reference voltage will be proportional to

$$\sin \Omega t. \quad (1.10)$$

The receiver will separate out the voltage of the envelope, the frequency of which will be equal to the frequency of rotation of the directivity pattern. If we measure the phase differences of the voltages at the output of the receiver and the reference voltage, it will equal the bearing of the signal. We see that in this method use is made of additional forced modulation of the signal as the directivity pattern is rotated, and phase measurement is carried out at a low frequency.

In rotating a diagram which has several minima, as occurs in direction finders with large base, the voltage at the receiver output does not have a fundamental frequency component of the reference voltage, and contains only harmonics of this frequency.

The ~~reading~~ bearing reading becomes ambiguous.

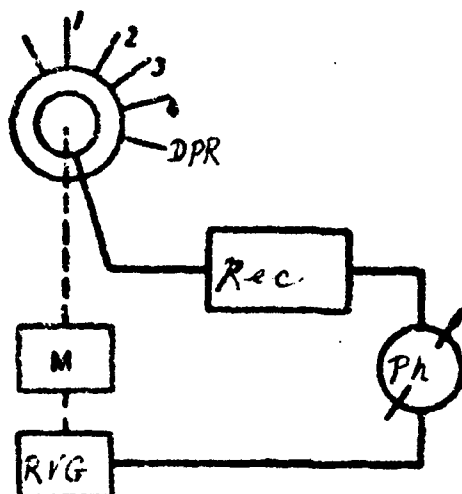


Fig. 1.6. Block diagram of a radio direction finder based on the method of rapid rotation of the directivity pattern.

1, 2, 3, and 4 -- antennas. dpr -- rotating device for directivity pattern. Rec -- receiver. Ph -- phase meter. M -- motor. RVG -- reference voltage generator.

The overall directivity pattern of two groups of antennas connected ~~for~~ differentially can be represented in the form

$$f(\theta) = \sin n\theta, \quad (1.11)$$

where θ -- bearing

n -- an integer, characterizing the directive properties of the resultant pattern (in the case of a long base).

When this pattern rotates, the voltage at the input of the receiver, taking into account the additional carrier-frequency voltage,

will be proportional to the quantity

$$\sin \omega t [1 + m \sin n (\theta + \Omega t)]. \quad (1.12)$$

Obviously the voltage at the output of the receiver will contain the n -th harmonic of the reference voltage. The frequency of the reference voltage must be multiplied by a factor of n . The phase meter measures the phase difference

$$\varphi = n\theta. \quad (1.13)$$

Thus, the coefficient n characterizes also the ambiguity of the reading.

However, the method of rapid rotation of the directivity pattern has substantial shortcomings. First of all, the interference rejection is greatly reduced. At short waves, interference from neighboring radio stations manifest themselves quite strongly. In the case of slow rotation of the pattern, the operator can listen separately to the signals from the radio stations, entering into the pass band of the receiver, and to match the strength of the signal at the output of the receiver with the position of the pointer on the sine-compensator scale. This eliminates to a considerable extent the influence of signals from neighboring radio stations on the results of the direction finding.

In the case of fast rotation of the directivity pattern, all the signals which are received simultaneously by the antenna system are modulated, and the signal of each radio station gives an

envelope of one and the same frequency. The phase meter averages the readings and gives an error in the direction finding. In this method the direction finding is subject to a certain time lag.

Taking these shortcomings into account, the method of rapid rotation of the directivity pattern can be recommended only when it is assumed that the signal from the direction-finding radio station, operating in a continuous mode, will be sufficiently strong compared with the signals of the neighboring stations. A technical realization of this method involves certain difficulties. In the case of a long base the pattern can be rotated either mechanically or by electronic switching of the antennas. The interference rejection is also reduced by the need of employing detection when separating the envelope. In this case, a deterioration of the signal to noise ratio may occur.

When the radio stations operate in the telegraph mode, the method of rapid rotation of the directivity pattern can be employed if the phase meter has low inertia. It must be noted that the rotation of the directivity pattern can be realized by electronic switching of the antennas. Here it is ~~extremely~~ essential that the pattern be rotated by 360° . Modulation of the signal can be obtained also by swinging the antenna characteristics within a specified sector. This idea leads to radio direction finder schemes with long bases, based on different ~~transmission~~ conversions of the signal as they are amplified, principally in one channel.

Measurement of Phase Differences (Phase Method)

A block diagram of the phase method of direction finding is shown in Fig. 1.7. The phase difference is measured between voltages in two antennas and this difference depends on the base (distance between antennas) and on the bearing of the signal (see below, Fig. 2.3). This dependence is expressed by the formula

$$\varphi = \frac{2\pi d}{\lambda} \sin \theta \cos \beta. \quad (1.14)$$

For small bearing angles, the formula can be represented in the form

$$\varphi = \frac{2\pi d}{\lambda} \theta \cos \beta. \quad (1.15)$$

A comparison of this formula with (1.5) discloses that the direction finding scale depends on the ratio of the base of the wavelength. By increasing the base it is possible to increase considerably the accuracy of direction finding. This advantage of the phase method as regards accuracy drops out immediately if the base is taken ~~more~~ shorter than the wavelength. Therefore the phase method of direction finding is not employed in short-base direction finders.

Formula (1.14) leads also to several other features of the phase method of direction finding. The scale of bearing reading is a nonlinear function of the phase shift angle. The linearity of the scale increases the closer the direction of the direction-

finding radio station is to being perpendicular to the base.

If the base is longer than the wavelength, then even when the possible direction of the incoming signal is confined to one half plane (owing to the presence of a screen in the antennasystem, an ambiguity may occur in the reading. Assuming that the bearing of the signal changes by $\pm 90^\circ$, we can see from (1.14) that ^athe phase shift of $\pm \pi$ will be repeated if the base is successively increased by half a wavelength. Consequently, the number of sectors of ambiguity, N_s , will be given by the formula

$$N_s = \frac{a}{\lambda} 2. \quad (1.16)$$

Thus, the phase method ~~ix~~ leads to ambiguity in reading.

Depending on the wavelength, the reading scale will be different. It is therefore necessary to have graphs to convert the indicator readings into bearings of the signal. In these graphs the parameter is the wavelength.

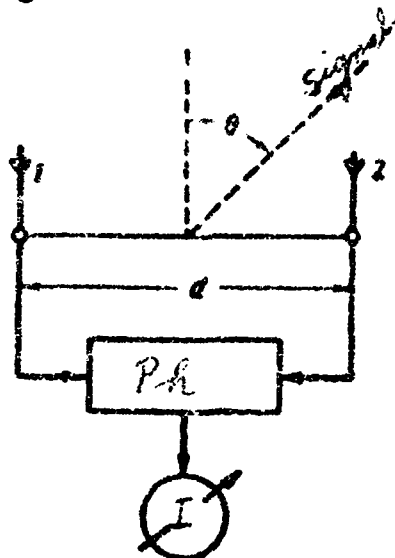


Fig. 1.7. Block diagram of the phase method of direction finding.

1 and 2 — antennas. Ph — phase meter. I — indicator.

Finally, it is easy to see that a change in the angle of arrival of the radio wave leads to errors, which are called "altitude" errors. If the angle of elevation is not measured simultaneously with the direction finding, the operator will assume that the phase shift is due only to the bearing of the signal and will calculate the bearing from the formula

$$\varphi = \frac{2\pi d}{\lambda} \sin \theta', \quad (1.17)$$

where θ' is the bearing measured in an inclined plane.

It is more correct, however, to use (1.14).

Comparing formulas (1.17) and (1.14) it can be noted that the altitude error of the signal

$$\Delta\theta = \theta' - \arcsin(\sin \theta' / \cos \beta). \quad (1.18)$$

It is thus seen that the phase method gives a non-uniform scale of direction finding and altitude errors. However, the non-linearity of the scale and the altitude errors decrease when the direction finding is close to a perpendicular direction to the base. Therefore phase direction finders are sector direction finders. It is simultaneously possible to obtain the bearings of signals only within a narrow sector of angles near the perpendicular

base. The principal advantage of phase direction finder is the possibility of increasing the accuracy by increasing the base.

The need for using graphs to convert the readings of the indicator into bearings for each wavelength reduces somewhat the operating efficiency of the direction finding with a long base. However, if one attempts to realize completely the accuracy in short-base direction finders, then it is also necessary to have graphs of the radio deviation, which in this case should be plotted for each frequency separately.

Consequently, the presence of graphs for the conversion of the readings of the indicator into bearings of the signal in direction finders with long base, in the realization of the maximum possible accuracy, is not a new requirement. The ambiguity in the long-base direction finders is eliminated by certain known methods, such as employing in addition a short base.

If the second base of the radio direction finder is equal to half the wavelength, then the ambiguity will be eliminated within the confines of one half plane.

Consequently, the phase method makes it possible to increase considerably the accuracy of direction finding and is particularly convenient in sector radio direction finders, when the sector of the signal bearing does not exceed several degrees near the direction of the perpendicular to the base of the direction finder. Receiving-indicating apparatus of the direction finder is in this case the

phase meter (see block diagram, Fig. 1.7).

5. ANTENNAS OF LONG-BASE RADIO DIRECTION FINDERS

It is first necessary to consider the features of the antenna systems. The antenna system of long-range radio direction finders should be sufficiently broadband, to insure reception of signals at frequencies from 3 to 30 Mcs. The antenna system should furthermore have a definite directivity (principal lobes of the diagram), and have where possible no considerable side lobes. Finally, the antenna system should be constructed in such a way, that the sector of direction finding can be rotated smoothly or discretely, insuring direction finding of signals within 360° .

Single Antennas

Antenna systems of a radio direction finder with a long base can consist of individual antennas, as well as of groups of antennas so interconnected as to obtain the required directivity patterns.

The antennas included in the groups can be both directional and non-directional. The requirement of switching the sectors leads to the necessity of arranging the antennas in a circle and of using switches.

The requirements that must be satisfied by a single antenna are above all a sufficient coverage of the frequency band. Consequently, the antennas should be broadband. Individual antennas

Fig. 1.8. Asymmetrical
vertical dipole.

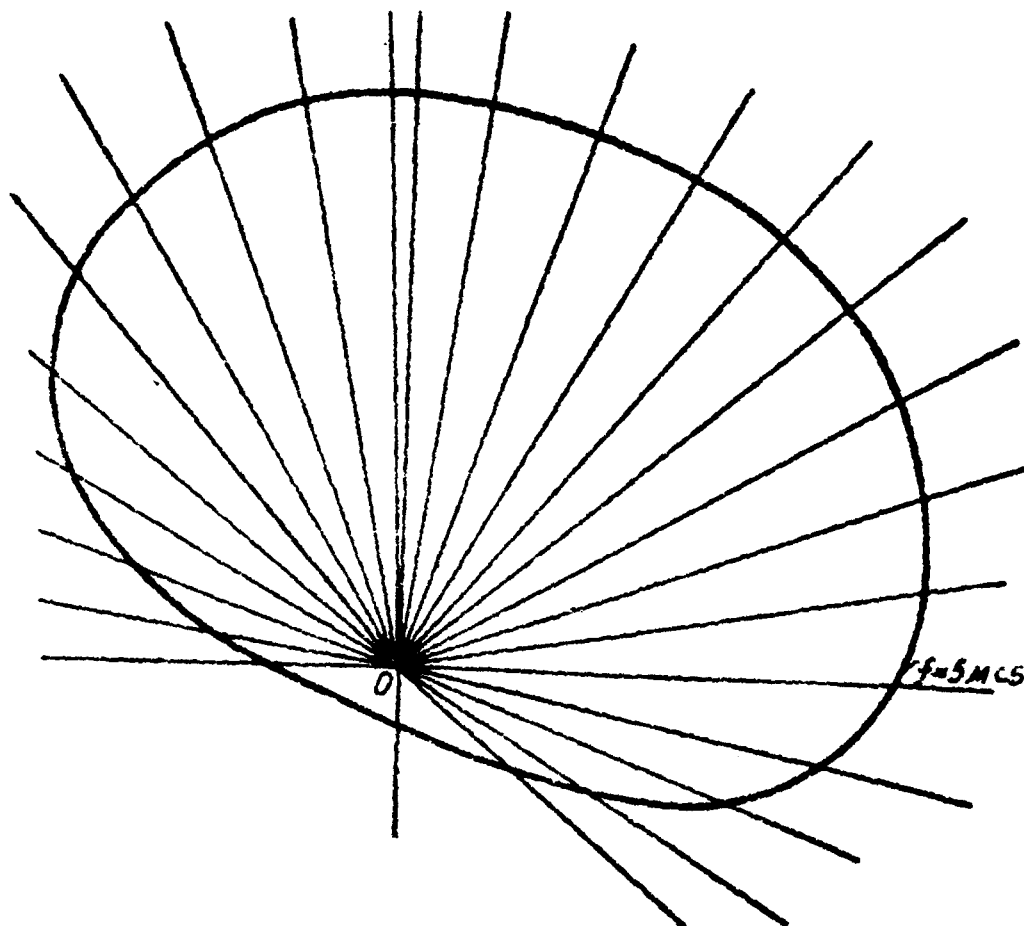
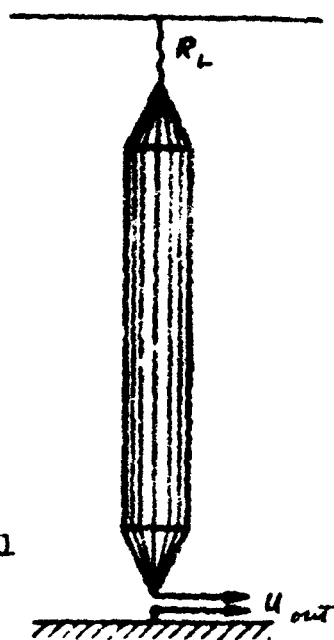


Fig. 1.9. Directivity pattern of asymmetrical vertical dipole
with reduced wave resistance (in the presence of a screen).

should furthermore have a directivity which is determined by the use of the entire antenna system.

The simplest antenna is an asymmetrical vertical dipole (Fig. 1.8), which represents a cylinder made up of a net of vertically suspended wires, suspended vertically on a non-conducting base, and joined below into one common point. The resistance of the antenna matches the feeder employed (usually 75 ohms).

A canopy made of a wooden ring is mounted on the top side, and the conductors are stretched along its radius. A matching resistance is connected between the cylinder and the canopy.

Antenna operation can be improved by using a screen made of wire mesh, stretched behind the antenna at a distance of a quarter of the average wavelength. An approximate directivity pattern of an antenna with screen, consisting of 32 vertical conductors and a canopy, is shown in Fig. 1.9.

It is possible to use in a direction finder a rhombic antenna [6], which makes it possible to obtain considerable directivity, produces a symmetrical output, and is also broadband. However, for a rhombic antenna it is necessary to employ a considerably greater working area. As a single antenna one can use also a long-conductor antenna (Beveridge antenna), which represents a long wire supported on poles. On the end of the wire one connects a matching resistance [11]. The length of the antenna should be several times the wavelength (up to ten times), i.e., approximately 200 meters. Naturally, the installation of a Beveridge antenna calls for a large area.

The calculation of the parameters of broadband antennas for short waves have been discussed sufficiently in detail in the literature [1, 2, 11].

Groups of Antennas

The directivity can be improved by joining individual antennas in groups. This becomes particularly necessary if the single antennas consist of vertical broadband dipoles. For direction finding it is necessary to have two voltages from two groups of antennas and a device for switching the sectors over. The character of the directivity pattern of two groups of antennas may be different, depending on the method of direction finding. It is possible to obtain two directivity patterns, the maxima of which are in the same direction (Fig. 1.10). The antenna groups must be placed in this case in such a way, as to insure the necessary dimension of the base. If a direction finding method based on amplitude comparison is used, it is necessary to obtain voltages from two antenna groups, whose directivity patterns start out in one point, but at different angles (Fig. 1.11).

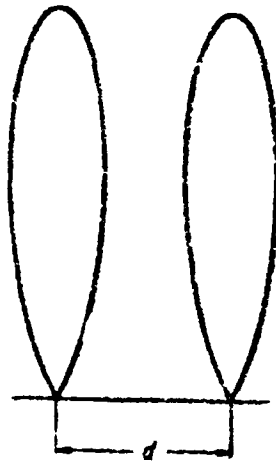


Fig. 1.10

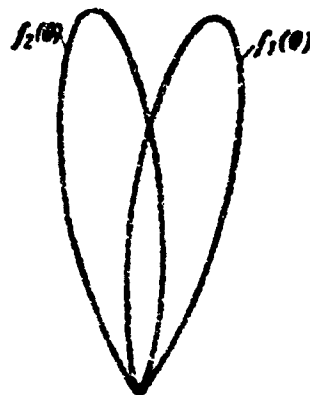


Fig. 1.11

Fig. 1.10. Directivity pattern of two groups of antennas when phased in one direction.

Fig. 1.11. Directivity patterns of two groups of antennas when phased in different directions.

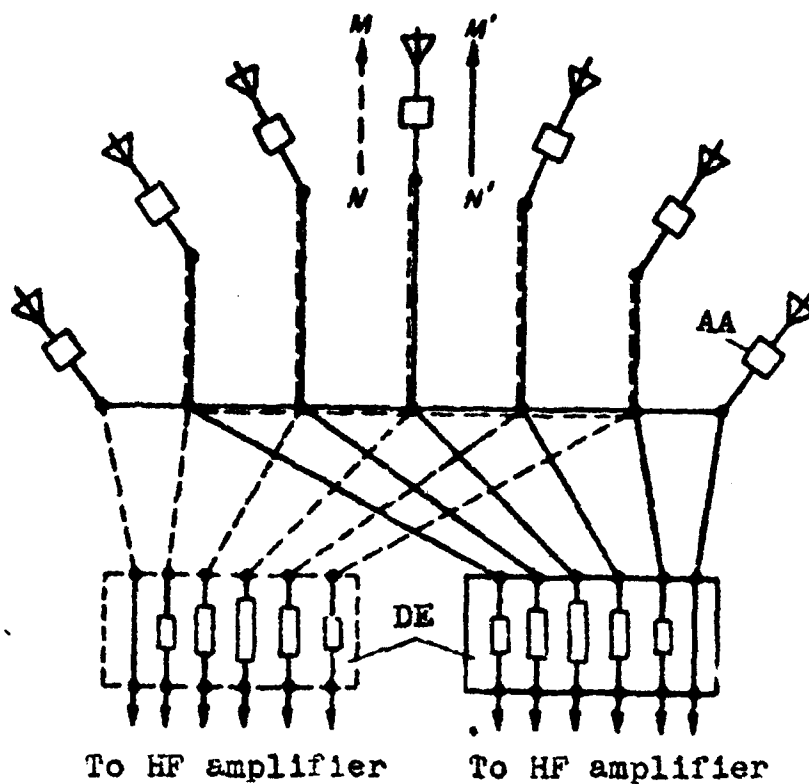


Fig. 1.12. Arrangement of phasing of antennas in two groups in one direction.

AA — antenna amplifier, DE — delay elements, MN — electrical axis of the first group of antennas, M'N' — electrical axis of the second group of antennas.

The antenna system of a long-base radio direction finder usually consists of a definite number of individual antennas, located along a circle of selected radius. For example, in the Wallenwever direction finder, there are forty antennas arranged in a circle 60 meters in radius.

Each group usually consists of four antennas. To form a group of antennas, as can be readily seen in the diagram of Fig. 1.12, it is necessary to connect delay elements between the antennas, and these can be made in the form of artificial lines or cable sections. To be able to switch the sectors, the delay elements are placed in the receiving-indicating unit. The delay elements can be connected as shown in Fig. 1.13 in each antenna, and with this the wave resistance of the common feeder should decrease, depending on the number of antennas in the group.

The delay elements can be connected also between antennas, as shown in Fig. 1.14. In this case there should be connected to the end of the feeder of each antenna a resistance equal to the wave resistance of the antenna feeder. The antenna feeder should be connected to the delay line through a decoupling element (usually an active resistance).

Naturally, the decoupling element will not make it possible to transfer the energy completely from the antenna to the common feeder. The gain of the antenna system, when such a connection diagram is used for the delay lines, is reduced. The

The voltage transferred from one antenna to the common feeder through the decoupling element is

$$u_{out} = u_{in} \frac{R_f}{R_f + |Z_d|}, \quad (1.19)$$

where Z_d is the impedance of the decoupling element.

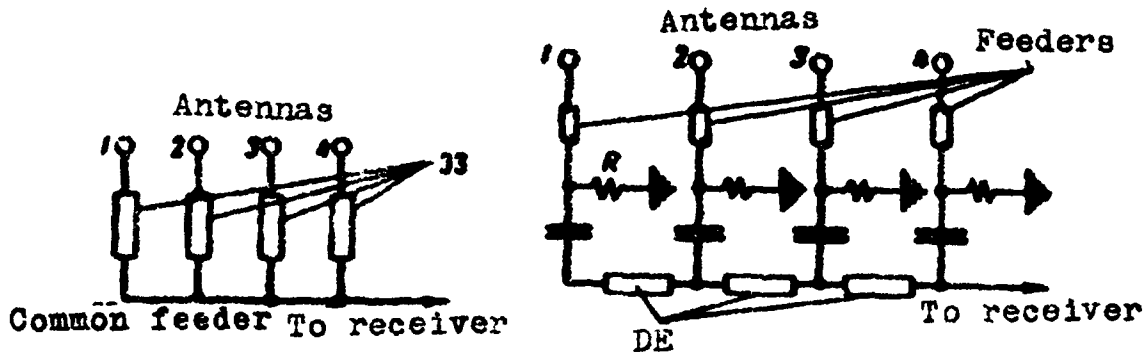


Fig. 1.13. Connection diagram for the delay elements in each antenna.

DE — delay elements.

Fig. 1.14. Connection diagram of delay elements between antennas.

DE — delay elements.

Practice has shown that the resistance of the decoupling element should be four or five times greater than the wave resistance of the feeder, and this will cause the field distortion in the common feeder to be small.

The signal transmitted by one antenna into the input of the receiver will be attenuated by a factor of four or five. This leads to a reduction in the signal to noise ratio at the input

of the receiver. Since several antennas are connected to the common group feeder (for example four or five), it is found that the signal voltage at the receiver input from the antenna group will be the same as the voltage from the signal antenna. Thus, the method of connecting the delay elements shown in Fig. 1.14 is less convenient from the energy point of view. However, in the circuit shown in Fig. 1.13 it is difficult to make use of the signal power gain, since the wave impedance of the final feeder may be very small and difficulties may arise in transforming the voltages in the input circuits of the radio direction finder.

The connection of the delay elements is called phasing of the antennas in the group. When phasing in accordance with the circuit shown in Fig. 1.13, it is quite difficult in ~~practice~~ practice to obtain a smooth displacement of the directivity pattern. The sectors can be switched only discretely. The sector switch is shown in Fig. 1.15 in the form of contacts in the circuit of each antenna. In the case of phasing in accordance with the circuit shown in Fig. 1.14, it is easier to effect a smooth rotation of the sector. However, it was perhaps necessary to take energy considerations into account primarily, since a smooth rotation of the sector is not an essential requirement in all cases.

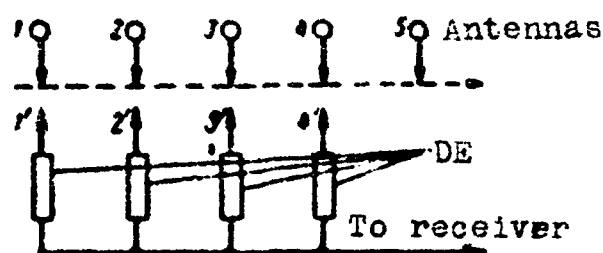


Fig. 1.15. Connection diagram for sector switch.

1, 2, 3, 4, and 5 — antennas, 1', 2', 3', and 4' — switch contacts, DE — delay elements.

Improvement of the parameters of the antenna system and of the stability of the directivity pattern can be obtained by using grounding. Usually it is effected by means of radial wires connected to concentric ones. A grounding grid is obtained, which is buried at small depth (approximately 0.5 meters) in the earth. The grounding grid is located approximately at a distance of one wavelength from the antenna circle and on one side or another. The principle of the grounding device does not differ in this case at all from the principle of the grounding device used for antennas for main line radio communication at short waves [2].

6. METHODS OF MEASURING PHASE DIFFERENCES

The block diagram of the receiving-indicating unit of a phase radio direction finder represents essentially a high frequency phase meter. The circuits solve the problem of amplifying the ~~ring~~ signals and measuring the phase differences. Depending on the method ~~of~~ used to measure the phase differences, the suitable circuit is chosen for signal amplification.

Sometimes, for convenience in the analysis, it is possible to ~~separate~~ segregate those blocks of the radio direction finder, in which the phase difference is measured, and other blocks, in which the signals are amplified. Since the methods of signal amplification in sector radio direction finders are determined essentially by the methods used to measure the phase difference, we shall start the analysis of the block diagrams with a study of methods of measuring phase differences.

Methods of Direct Measurement of Phase Differences

In the direct measurement of phase differences between ~~the~~ two voltages, one fixes definite instants of instantaneous voltages in the channels. The phase difference is determined from the difference in time for these instants.

The fixation of the definite instants of time leads to the need for using pulses. Assume that there are two voltages in two channels (fig. 1.16). When the voltage in each of the channels passes through zero and starts rising, the phase meter generates narrow pulses. The pulses obtained from the voltage in one channel are used to trigger a sweep stage, the voltage from which is applied to the horizontal ~~mix~~ deflecting plates of a cathode-ray tube.

The pulses generated by the voltage of the second channel, are applied to the vertical deflecting plates of the cathode ray tube. As a result two pulses will be seen on the oscillograph screen,

and the distance between these two will indicate the phase difference.

The advantage of this method is that the compared phases may belong to voltages that consist of a very small number of complete cycles. One can hardly expect here good interference immunity. This method is good in laboratory practice, when the voltages in the channels are free of noise. In practice, naturally, the devices that generate the pulses operate at a fixed level of input voltage. It is therefore advantageous to amplify the voltages in the channels in such a way, so that amplitude limitations can be practiced. This will make it possible to exclude the dependence of the phase-difference measurements on the amplitudes of the input voltages.

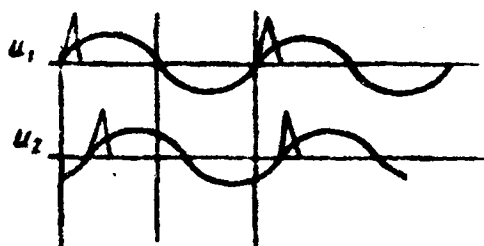


Fig. 1.16

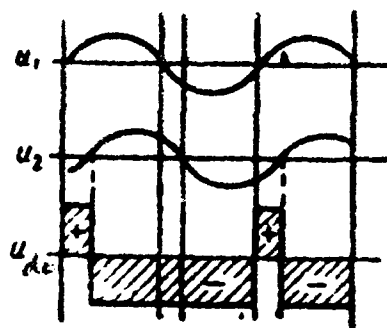


Fig. 1.17

Fig. 1.16. Voltage diagrams in two channels, showing the instants when pulses are formed for the measurement of the phase differences.

u_1 —voltage in the first channel, u_2 — voltage in the second channel.

Fig. 1.17. Voltage diagrams at the output of dc generators.

u_1 — voltage in the first channel, u_2 — voltage in the

second channel, u_{gc} -- voltage at the output of the dc generator.

It is possible to modify somewhat the pulse method of phase-difference measurement, and to increase its interference ^{rejection} immunity, by employing integration. In this case, as previously, one obtains first two series of pulses. These pulses are then used to trigger two dc voltage generators, with different polarities. The pulse of each series starts one generator, and shuts off the other. The voltage diagrams at the output of these two generators are shown in Fig.

1.17. If ~~whenever~~ we now connect to the output of the generator circuit an averaging network, then the polarity in the magnitude of the voltage at the output of this network will determine the phase difference. The phase difference of the input voltages can be measured here within $\pm 180^\circ$. A pulsed-integral method of phase difference measurement has great ^{av} interference ^{rejection} immunity, although it does require that the input voltages contain several dozens of cycles of oscillations. Different trigger circuits can be used as generators.

Compensation Methods of Measuring Phase Differences

The idea of all the compensation methods is based on connecting into one of the channels a phase shifter, which compensates for the phase shift between the voltages in the channels. Versions of this method differ by the methods of compensation. The compensation can

realized either automatically or manually. In addition, provision can be made for different indicators, which fix the instant of elimination of the original phase shift. The phase difference is read directly on a scale that indicates the position of the handle of the phase shifter.

In the non-automatic versions of compensation, visual or auditory indication is used. A typical method is that of combining the signals. An example of this method is shown in the block diagram of Fig. 1.18.

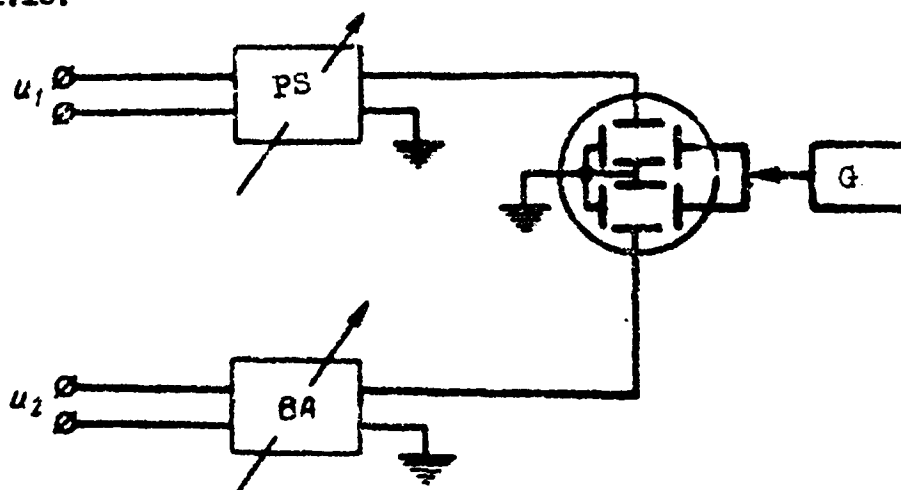


Fig. 1.18. Diagram of phase-different measurement by the method of combining of the signals.

u_1 -- voltage from the output of the first channel, u_2 -- voltage from the output of the second channel, BA -- block for amplitude balance, PS -- phase shifter, G -- sweep generator.

Assume we have a two-beam oscillograph with a common sweep for both beams. The direction from the first channel is applied to the

vertical deflecting plates through a phase shifter. The voltage from the second channel is applied to the vertical deflecting phase of the second electron gun through an amplitude-balancing stage. Two sine waves will be seen on the screen, one under the other. Here, naturally, it is necessary to synchronize the frequency of the sweep generator with that of the signal. By changing the position of the phase-shifter knob it is possible to place the sine waves exactly one under the other. It is now possible to shift one of the beams vertically and to equalize the sine waves amplitudes in such a way that one sine wave merges with the other, by means of exact setting of the phase shifter knob. The phase difference is determined from the position of the phase shifter knob. The merging of the sine wave gives a very high accuracy of phase difference measurements, approximately to 1° .

A shortcoming of this version of signal combination is the low operating efficiency, for much time is consumed in performance of each measurement.

Another method of realizing the method of compensation is shown in the block diagram (Fig. 1.19) where a voltage-summation stage (summing unit) is used. Here, too, one voltage is applied through the phase shifter and then to the summing unit, and the other to the summing unit through a network that balances the signal amplitudes.

It is quite obvious that if the phase shift between the

voltages and the antennas is zero, the amplitudes are identical, and the phase shifter produces a phase shift of 180° , then the voltage at the output of the summing stage will be zero.

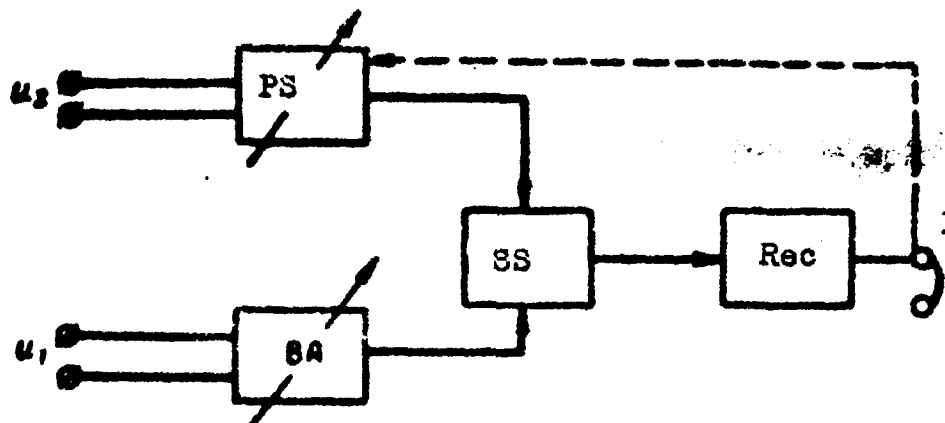


Fig. 1.19. Scheme for measuring the phase difference by the method of compensation, using a voltage summing stage.

u_1 -- voltage from the output of the first channel, u_2 -- voltage from the output of the second channel, BA -- amplitude balancing block, SS -- summing stage, Rec -- receiver, I -- indicator.

The operator listens to the signal at the output of the receiver. When the signal at the output is detected, the operator turns the knob of the phase shifter until a minimum signal is produced. He then balances the amplitudes of the voltages in the antennas, attaining a sharper minimum. The phase shift between the voltages and the antennas can be read on the knob of the phase shifter.

In the diagram (see Fig. 1.19) the dotted line shows the connection between the indicator and the phase shifter, produced

by the operator.

It is naturally possible to use instead of a summing stage a voltage difference stage. This does not change the method at all, but now an original phase difference of 0° will correspond to a zero shift in the phase shifter.

An important factor is that when using a summing stage it is possible to obtain amplification in one channel and to increase the sensitivity of the setup. The accuracy of the phase-difference measurements is not worse here than in the case of combination of sine waves, and the operating efficiency is also low.

If the phase difference of the initial voltages changes rapidly, then an automatic measurement of the bearing becomes practically impossible. An automatic rotation of the knob of the phase shifter is however impossible to realize in a circuit with a summing stage, since, in addition to rotating the knob of the phase shifter, it is necessary to balance the amplitudes. A system is obtained with two interrelated controlled elements.

Instead of combining sine waves, it is possible to use the method of combining pulses.

Let us imagine two sinusoidal voltages, the same as in the pulse methods of measuring phase shifts. If one of the voltages is used to obtain a circular sweep on the cathode ray tube, and the pulse from the second voltage is applied to the central electrode, then a circle with a ~~pulse~~ pulse will be produced on the screen of

the cathode ray tube. As seen on the block diagram (Fig. 1.20) the pulse from the second voltage is obtained in stages which are connected past the phase shifter.

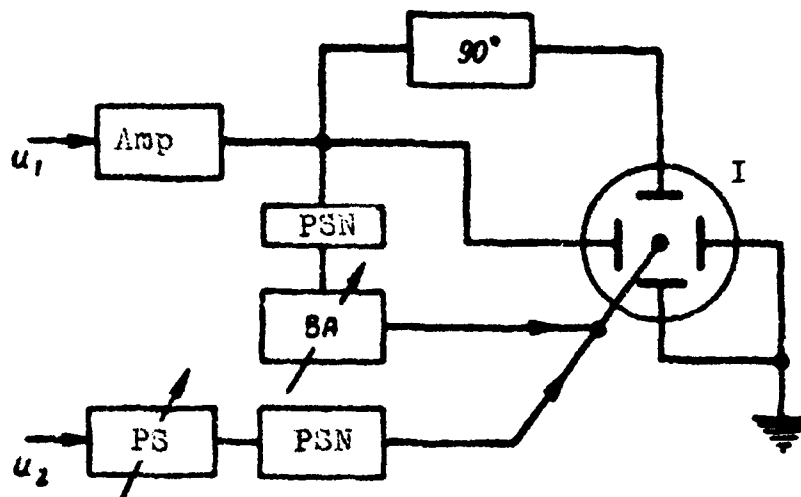


Fig. 1.20. Diagram for measuring the phase differences by the method of compensation and combination of pulses.

u_1 -- voltage from the output of the first channel, u_2 -- voltage from the output of the second channel, BA -- amplitude balancing block, PS -- phase shifter, PSN -- pulse shaping network, 90° -- phase shifting network producing a 90° phase shift. I -- indicator, Amp -- amplifier.

Also applied to the central electrode of the tube is a pulse from the voltage of the first channel. In this case two pulses will be seen on the screen, directed away from the center of the circular sweep to the periphery (Fig. 1.21, left). If we now

rotate the knob of the phase shifter, then the second pulse will be shifted along the circular sweep and finally will merge with the marker pulse.

The method of combining pulses has low operating efficiency,

but is in many cases more convenient. For example, if a pulse radio navigation range finder is on hand, then the pulses discussed above are always obtained in the range-finder equipment. These are the interrogation and the response pulses. Consequently it is possible to measure very well the phase differences at the pulse repetition frequency, in spite of the fact that the second voltage is non-sinusoidal.

Let us indicate that the instrumental accuracy of any phase meter can be increased in principle by an unlimited number of times by multiplying the frequency. In the example given above it is possible to multiply the pulse repetition frequency and to measure the phase difference with greater accuracy. However, by increasing the sweep frequency in the pulse method of measuring phase differences, it becomes unavoidably necessary to reduce the lengths of the pulses, or else they may occupy the entire circle on the screen and the measurement loses its meaning.

Multiplication of the pulse repetition frequency and use of the phase measurement method undoubtedly contribute to greater accuracy of reading. However, this accuracy still remains considerably lower than the accuracy obtained when measuring phase differences at the

pulse filling frequency.

In the case of a continuous signal, there are no principal limitations on the increase of the instrumental accuracy of phase difference readings, for example, by frequency multiplication. In practice, however, the possible instrumental accuracy of phase-difference measurements is always limited and is determined by the stability of the apparatus and by the conditions of propagation of radio waves. In addition, in frequency multiplication the reading becomes ambiguous, and this will require a subsequent performance of several rough and accurate measurements.

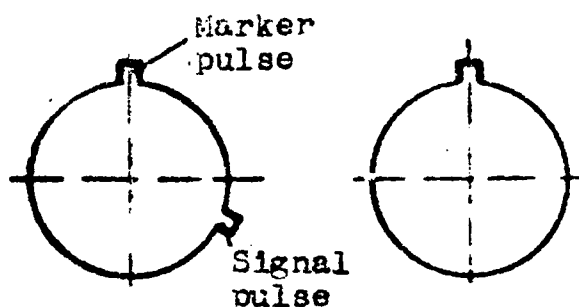


Fig. 1.21. Display of pulses on a screen with circle sweep when measuring phase differences by the compensation method (left — prior to merging of the pulses, right — after merging).

Practice has shown that the best accuracy of phase-difference measurements in various direction finders usually amounts to 0.1° . In many cases accuracy up to 1° is quite adequate. It must not be forgotten here that the measurement of phase differences is usually carried out in a range of 360° .

Finally, methods exist for automatic compensation of phase differences. The use of an automatic compensation scheme for phase differences is possible when exact balancing of the voltage amplitudes in the channels is unnecessary. As is known, the use of a summing voltage stage calls for amplitude balancing. Consequently, it is necessary to replace this stage first of all by some other stage which would respond only to phase differences and which would yield, regardless of the voltage ratio, a zero voltage at the output for a given phase difference. Such a stage is a phase detector.

The block diagram of an automatic compensation scheme for phase differences, using a phase detector, is shown in Fig. 1.22. The principal elements of the network are a phase shifter and a phase detector. The phase detector produces at the output a dc voltage, proportional to the product of the input voltages and the sine of the phase shift between them. Consequently, independent of the amplitudes of the input voltages, if the phase shift is fully compensated by the phase shifter, the voltage at the output of the phase detector is zero.

The voltage from the output of the phase detector is applied to the motor control circuit, which rotates the knob of the phase shifter. After the initial phase shift between the input voltages has been compensated for, the motor stops. This scheme has now a higher operating efficiency than those considered above. Naturally, if the measured phase shift varies rapidly, a dynamic measurement

error appears. The method of measuring phase differences with automatic compensation has a certain time lag built in, owing to the use of a follow-up drive. This time lag ~~may be increased by the choice of the parameters of the control circuit and of the filters connected past the phase detector.~~ may be increased by the choice of the parameters of the control circuit and of the filters connected past the phase detector.

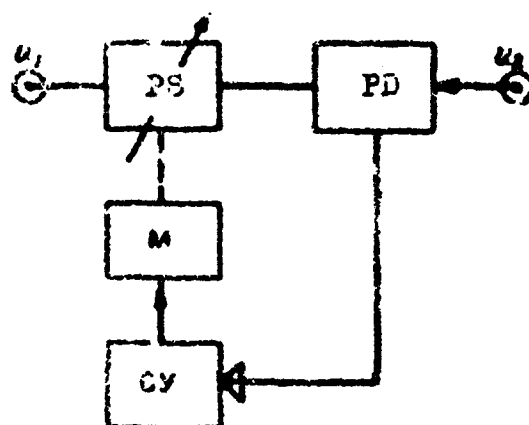


Fig. 1.22. Block diagram for the measurement of the phase difference by the method of automatic compensation.

u_1 — voltage from the output of the first channel, u_2 — voltage from the output of the second channel, PS — phase shifter, PD — phase detector, M — motor, CS — control system.

The automatic compensation scheme has high interference immunity and should be used whenever a low rate of variation of the phase differences of the input voltages is expected. The accuracy

of the measurement of the phase difference by the compensation method amounts to approximately 1° .

The automatic compensation scheme for the phase differences loses the advantage of the possibility of employing a single channel, since it is necessary to apply to the phase detector voltages which are already quite highly amplified. It is impossible to connect the phase detector in the input side of the block diagram of the radio direction finder, for it is possible to obtain sufficient gain at dc, and dc is necessary for operating of the control circuit. It is probably simpler technically to construct two identical receiving devices, instead of a stable amplifier operating with a dc gain on the order of several millions.

Indirect Method of Measuring Phase Differences

Numerous methods of measuring phase differences are based on the transformation of the signal phase differences in such a way, as to be able to use the amplitude ratios to determine the unknown difference, or else to replace the measurement of phase differences at high frequency by measurement of phase differences at low frequency, or else to use some method of indirect measurement. The easiest way to make such a measurement is with the aid of a phase meter with a phase detector, the block diagram of which is shown in Fig. 1.23. It is seen from the diagram that the two voltages are applied to the two phase detectors, and one of the voltages is

shifted in phase by 90° . As a result, two dc voltages are produced at the output of the phase detectors, and these voltages are proportional to the product of the amplitudes of the input voltages and the sine and the cosine of the phase shift angles respectively. It now remains only to compare these output voltages in magnitude and to take their ratio. This voltage ratio is determined in an indicator, which is essentially a dc ratio meter.:

Depending on the indicator, different versions of the scheme can be used. The indicator may be a magnetic needle placed in the field of two mutually-perpendicular coils, fed from the outputs of the phase detectors (see Fig. 1.23). Usually the needle of the phase meter is placed on a magnetic ring which rotates inside the coils. The coils are fed from the outputs of the phase detectors through direct current amplifiers. Such an indicator scheme has a certain time lag.

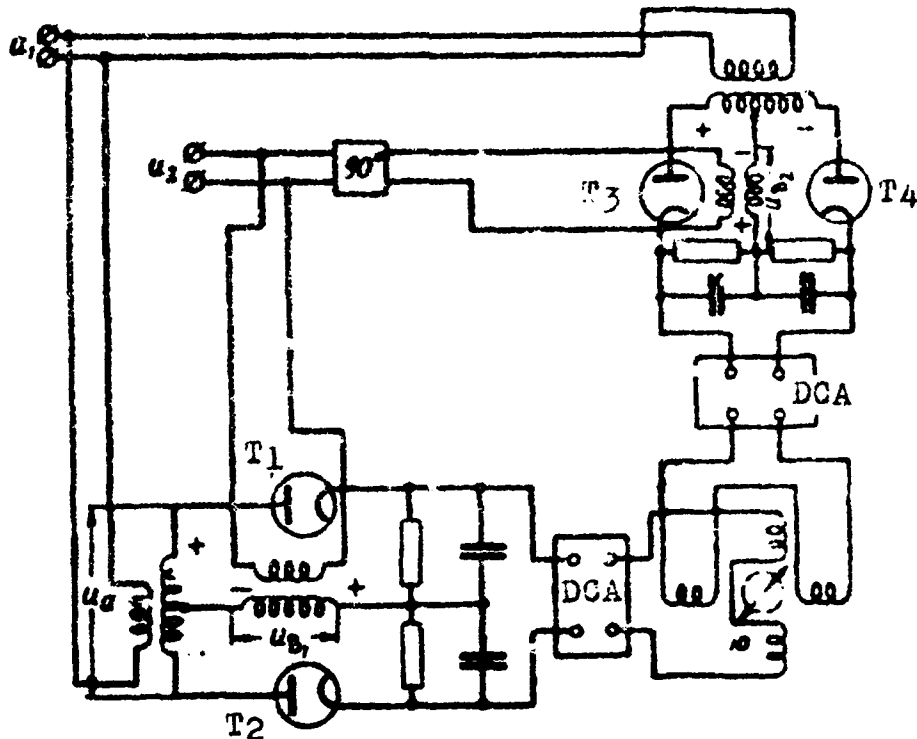


Fig. 1.23. Block diagram of phase meter with phase detectors.

u_1 -- voltage from the output of the first channel, u_2 -- voltage from the output of the second channel, 90° -- network which shifts the voltage phase by 90° . DCA -- dc amplifier, T_1, T_2 -- first phase detector, T_3, T_4 -- second phase detector.

In sector radio direction finders, operating under conditions of strong interference from neighboring stations, it is important to take the bearing at that instant, when there is no signal from the interfering station (when operating by telegraph). In this case the large time delay of the pointer indicator may be harmful. Therefore in short-wave sector radio direction finders, which have phase meters with phase detectors, it is sometimes better to use a cathode ray tube as a ratio detector. A block diagram of the indicator is shown in Fig. 1.24.

As can be seen from the diagram, the dc voltages from the outputs of the phase detectors are commutated, in order to obtain on the tube a line (instead of a spot) directed away from the center. The sawtooth voltages obtained after commutation, the amplitudes of which are proportional to the voltages from the output of the

phase detectors, are applied to the deflecting plates of the tube. The phase difference is determined from the slope of the line on the tube.

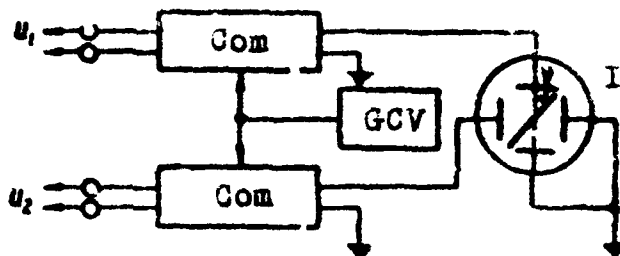


Fig. 1.24. Block diagram of an indicator of a phase meter with phase detectors using a cathode-ray tube.

u_1 — voltage from the output of the first phase detector, u_2 — voltage from the output of the second phase detector, Com — commutator, GCV — generator of commutating voltage, I — indicator, γ — reading of the phase meter.

The scheme with the phase detectors is particularly convenient when the phase difference is measured at a low difference frequency. In this case it is possible to ensure good stability of the phase meter parameters, to decrease the influence of the variation of capacitances in the circuit, and to obtain greater interference rejection, by taking one of the voltages to be greater than the other. A more detailed analysis of the operation of a phase meter with phase detectors and ~~and~~ a cathode ray as indicator is given in Chapter VI.

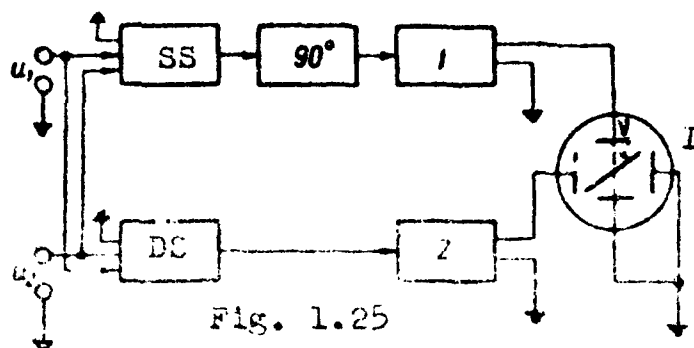


Fig. 1.25

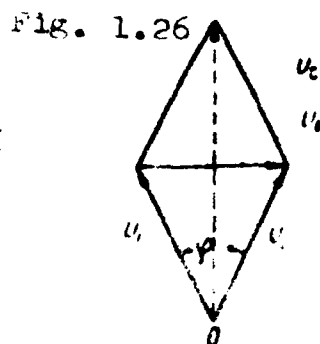


Fig. 1.26

Fig. 1.25. Block diagram of a "sum -- difference" phase meter.

u_1 -- voltage from the first group of antennas, u_2 -- voltage from the second group of antennas, SS -- summing stage (sum stage), DS -- voltage difference stage, 90° -- phase shifting stage (90° phase shift), 1 -- first amplifying channel, 2 -- second amplifying channel, I -- indicator, φ -- reading of phase meter.

Fig. 1.26. Vector diagram of the sum and difference of two voltages, of equal amplitude.

A rather simple method of converting a phase difference into a voltage amplitude ratio is the "sum -- difference" method. A block diagram of a phase meter operating on the "sum -- difference" principle is shown in Fig. 1.25. In this circuit there are two voltages with phase shifts $-\varphi/2$ and $+\varphi/2$. When the amplitudes of these voltage are equal, as can be seen from the diagram (Fig. 1.26), the sum of the voltages is

$$u_s = 2U \sin \omega t \cos \frac{\varphi}{2}; \quad (1.20)$$

and the difference of the voltages is

$$u_d = 2U \cos \omega t \sin \frac{\varphi}{2}. \quad (1.21)$$

If one of the voltages is rotated by 90° , say the sum voltage, two in-phase voltages are obtained, the amplitudes of which are proportional to the sine and the cosine of half the angle of the original phase shift. If these voltages are now applied to a two-channel amplifier with equal phase shifts and with equal gains, then the ratio of the voltage amplitudes will remain the same at the outputs of the channels. After applying the voltages from the output of the amplifying channels to the deflecting plates of the cathode ray tube, we shall obtain on the screen a diametral line, the slope of which indicates an angle equal to half the angle of the phase shift.

$$\operatorname{tg} \nu = \frac{u_d}{u_s} = \operatorname{tg} \frac{\varphi}{2}, \quad (1.22)$$

ν is the angle made by the line on the indicator.

Hence

$$\nu = \frac{\varphi}{2}. \quad (1.23)$$

As can be seen, the circuit based on the use of the "sum — difference" stage has no time lag, but requires a two-channel amplifier. When the gains of the channels or the phase shifts are not the same, the slope of the line changes or else its presentation on the screen turns into an ellipse. Any detuning of the channels also can lead to apparatus errors. The apparatus errors of such networks are considered in greater detail in subsequent chapters.

The reading scale when using the "sum -- difference" method is reduced to one half. In addition, only half of the tube screen is used. In panoramic radio direction finders, the second non-working half of the tube screen is best used for reading the frequency of the direction-finding radio stations, for example, by measuring the lengths of the lines.

7. AMPLIFICATION CIRCUITS FOR SIGNALS IN LONG-BASE SHORT-WAVE RADIO DIRECTION FINDERS

In various receiving-indicating radio direction finding schemes it is necessary to amplify the signals. Depending on the method chosen to measure the phase differences, different amplification circuits can be used for the signals. It must be taken into account, however, that two signals arrive from the antenna groups.

Consequently, if no signal conversion is made at the input for the purpose of measuring the phase differences, it becomes necessary to employ various two-channel amplifying circuits, the principal problems in which is the amplification of the signal with retention of the amplitude and phase or only the phase relations.

If signal conversion is practiced, the principal application can be in one channel, most frequently in an intermediate-frequency amplifier of a superheterodyne receiver.

Thus, the amplification circuit may be single-channel and two-channel.

Pure Single-Channel Amplification

The term "pure single-channel amplification" will denote here circuits in which the two signals are amplified in one and the same receiver. If the signals are separated in time (pulse), they can be displayed separately on the indicator screen. The distance between pulses on the sweep line will obviously determine the difference in phases of the pulse repetition frequency.

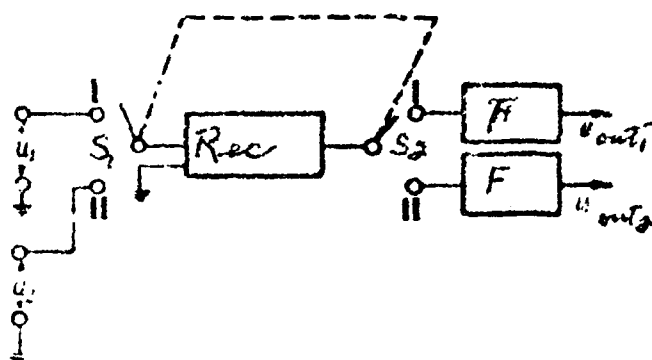


Fig. 1.27. Diagram of single-channel amplifier with switching.

u_1 — voltage from the first group of antennas, u_2 — voltage from the second group of antennas, S_1 and S_2 — synchronous switches at the input and output, Rec — receiver, F — filter.

Pure single-channel amplification is usually not employed in radio direction finders with long base, since it is necessary that the direction finder measure a high frequency phase difference, and

not the phase difference of the pulse repetition frequency, and it is furthermore necessary that the radio direction finder be able to operate with a continuous signal.

Pure single-channel amplification is used in various radio navigation pulse systems.

When operating with a continuous signal, it is possible to effect artificially time separation of the signals received by the antennas. For this purpose it is necessary to use a circuit incorporating switching of the output and input (Fig. 1.27). As can be seen from the diagram, the signals from the antennas are amplified alternately in time in one and the same direct amplification receiver. Naturally, in this case the question arises of remembering the phase of one of the signals at the output in the absence of this signal from the input. The phase must be memorized at that instant, when the switch applies to the receiver the signal from a second antenna group. The memorization of the signal phase can be realized in first approximation by means of filters with narrow bandwidths.

For direction finders with long base at short waves, such a scheme cannot be recommended, because the switching produces additional cross talk, since not only the main signal is transformed into pulses at the input, but also the signals from neighboring radio stations. The width of the spectrum from each input signal is determined by the switching frequency.

The spectrum of the output signal will consist of discrete

bands, the spacing between which, in the frequency scale, is equal to the switching frequency. With this, the components of the spectrum of a strong radio station of neighboring frequency may enter the receiver, and produce cross talk. No such cross talk is produced if the pulse signals are received from the ether. This deterioration in the interference rejection may be reduced somewhat by changing the switching frequency. Then the signals of the neighboring radio stations will shift in the passband of the receiver, and the signal of the station to which the receiver is tuned will remain stationary on the frequency scale. However, an arrangement for changing the switching frequency makes the radio direction finder more complicated. Thus, the scheme of single-channel amplification with switching of the input and output can hardly be recommended for use in sector short-wave radio direction finders. Finally, there are such single-channel amplification circuits, in which it is necessary to amplify only one signal, once the input signals from the two antennas are converted. Such a case occurs when measuring phase differences by the compensation principle using a stage for summing or subtracting voltages.

A radio direction finder operating with such a circuit has low operating efficiency. It must be noted that this amplification circuit cannot be considered as pure single-channel. Versions of this circuit will be given below.

Amplification with Frequency Separation

Another type of circuit, based on the amplification of a signal in a single channel, are circuits with two voltages of slightly differing frequencies.

Since the difference in the frequencies of the two signals is small, the amplifier will not produce any substantial phase in amplitude distortions.

Let us consider a method for a single-channel amplification with separation of frequencies and double conversion.

The task of the circuit is to amplify two signals and maintain their phase relations. A simplified block diagram of the first frequency conversion is shown in Fig. 1.26. As can be seen, we have here a low frequency and a high frequency heterodyne. After the mixer M-3, the difference and the sum of the frequencies are separated by filters. The voltages, which differ somewhat from each other in frequency, are applied to ordinary mixers of receiving channels M-1 and M-2. The voltages produced at the outputs of the mixers are somewhat different in frequency, and can therefore be amplified in a single channel.

It is technically difficult to realize the first conversion network, owing to the complexity of the problem of separating two nearly equal voltages past the mixer M-3. The difference frequency usually reaches several hundred cycles, and the hetero-

dyne frequency is several megacycles. A solution of this problem of separation of signals of such close high frequencies is possible in practice through the use of quartz filters.

It is quite clear, however, that it is necessary to retune the receiver, and consequently also the quartz filters. Obviously, in the case of smooth tuning of the receiver it is hardly possible to realize the first-conversion scheme.

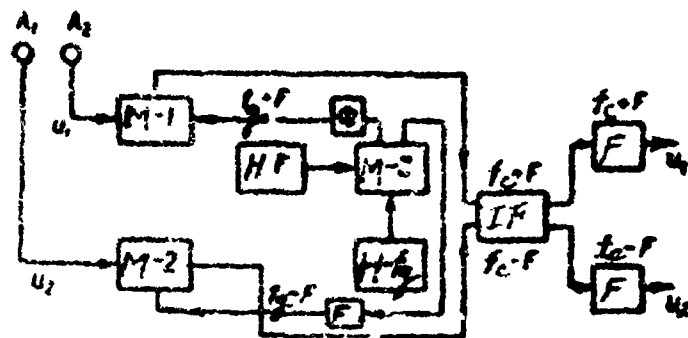


Fig. 1.28. First conversion circuit for production of two signals which differ slightly in frequency.

A_1 and A_2 — antennas, M-1, M-2, and M-3 — mixers, F — filters, IF — intermediate frequency amplifier, H-F — low frequency heterodyne of frequency F , H- f_g — heterodyne of high frequency f_g .

The second conversion makes it possible to obtain voltages of constant frequency at the output and to carry out the measurement at low frequency. The second conversion circuit is shown in Fig. 1.29, and the stages that enter into the block diagram of the radio

direction finder, which are used prior to the input of the common intermediate frequency amplifier are the same as in the circuit of Fig. 1.28.

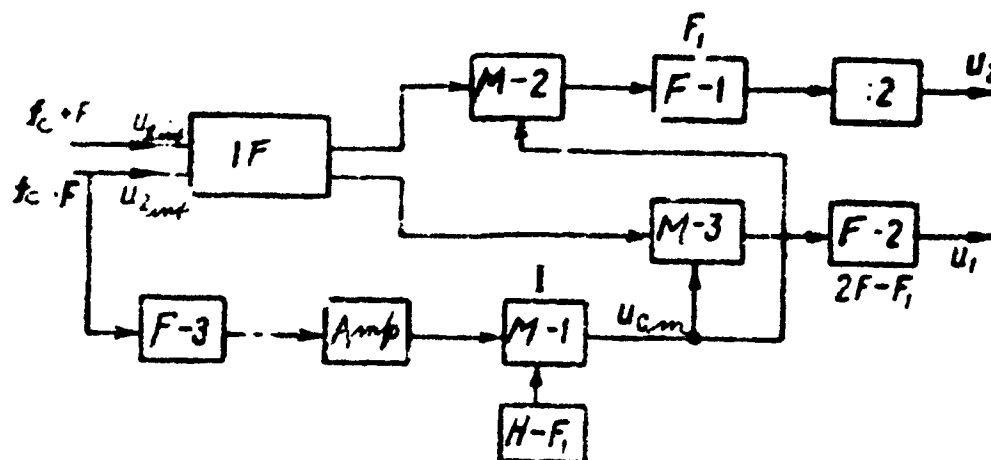


Fig. 1.29. Circuit for second conversion to obtain two low-frequency signals, which retain the phase differences of the high frequency signals.

IF — common intermediate frequency amplifier, M-1, M-2, and M-3 — mixers, AMP — amplifier, F-1, F-2 and F-3 — filters; :2 — frequency divider with coefficient 2, u_1 and u_2 — input voltages, $H - F_1$ — heterodyne of low frequency F_1 , u_m — voltage at the output of the mixer.

The limits of variations of signal frequency in the intermediate frequency amplifier are limited by the bandwidth of the input filters (see Fig. 1.28). By choosing the bandwidth of the intermediate frequency amplifier several times larger than the

frequency F , it is possible to obtain satisfactory equality of gain of both signals in the intermediate frequency amplifier.

A broadening of the bandwidth of the intermediate frequency amplifier may lead to the appearance of interference from neighboring radio stations.

Let us trace the variation of the phase differences of the voltages from the two antennas in the circuits shown in Figs. 1.28 and 1.29.

Let one of the voltages at the input has the phase shift $+\varphi_s$, and the other a phase shift $-\varphi_s$.

After the first conversion, the phase of the voltages will be respectively

$$\varphi_s - \varphi_g + \varphi_F \quad (1.24)$$

and

$$-\varphi_s - \varphi_g - \varphi_F.$$

where φ_g and φ_F are the phases of the heterodynes of the high and low frequency (see Fig. 1.28). These voltage phases will be retained at the output of the intermediate frequency amplifier after amplification.

The phase of the voltage from the output of the mixer M-1 will obviously be

$$-\varphi_s - \varphi_g - \varphi_F + \varphi_{F_1}, \quad (1.25)$$

where φ_{F_1} is the phase of the voltage of the heterodyne of frequency F_1 (see Fig. 1.29). Consequently, after the second con-

version of the signals in the mixers M-2 and M-3, the phase of the first voltage, of frequency $2F - F_1$, will be

$$2\varphi_F + 2\varphi_S - \varphi_{F_1} \quad (1.26)$$

and the phase of the second voltage, of frequency F_1 will be (after conversion)

$$\varphi_{F_1} \quad (1.27)$$

Finally, the frequency and the phase of the latter voltage is divided in two and then the phase of the voltage u_2 at the output will be

$$\frac{\varphi_{F_1}}{2} \quad (1.28)$$

The difference in the phases of the output voltages u_1 and u_2 will be

$$2\varphi_F + 2\varphi_S - \varphi_{F_1} - \frac{\varphi_{F_1}}{2}, \quad (1.29)$$

from which it is clear that if the low frequency heterodynes remain coherent, and if furthermore the following relation holds

$$F_1 = \frac{4}{3} F, \quad (1.30)$$

then the additional phase difference, which is produced by single conversion, will be zero. The coherence of both low frequency heterodyne can be ensured by obtaining a voltage of frequency F_1 from the heterodyne of frequency F . From the circuits shown in Figs. 1.28 and 1.29 it is clear that the conversion of the signals complicates

simplify the receiving apparatus. The idea of simplifying the conversion network lies in utilizing methods of additional signal modulation or using heterodyning of signals. This makes it possible to measure the phase differences at low frequencies and simplifies substantially the receiving devices.

Single-Channel Amplification with Conversion of Signals by Additional Modulation

The block diagram of the radio direction finder is shown in Fig. 1.30. Here the ratio of the phases of the input signals, of high frequency, is converted first in a "sum — difference" stage into an amplitude ratio. The amplitude ratio is then converted, by means of additional modulation, into a phase of an envelope. The phase meter measures the phase difference between the voltage at the output of the receiver and a reference voltage of a low frequency heterodyne, which produces forced modulation of the signals.

The magnitudes of the voltages at the output of the "sum — difference" stage are determined by formulas (1.20) and (1.21). After the phase of one of the voltages is rotated by 90° , we obtain the following voltages of the balanced modulators:

$$\left. \begin{aligned} u_{1m} &= 2U \sin \omega t \cos \frac{\varphi}{2} ; \\ u_{2m} &= 2U \sin \omega t \sin \frac{\varphi}{2} ; \end{aligned} \right\} \quad (1.31)$$

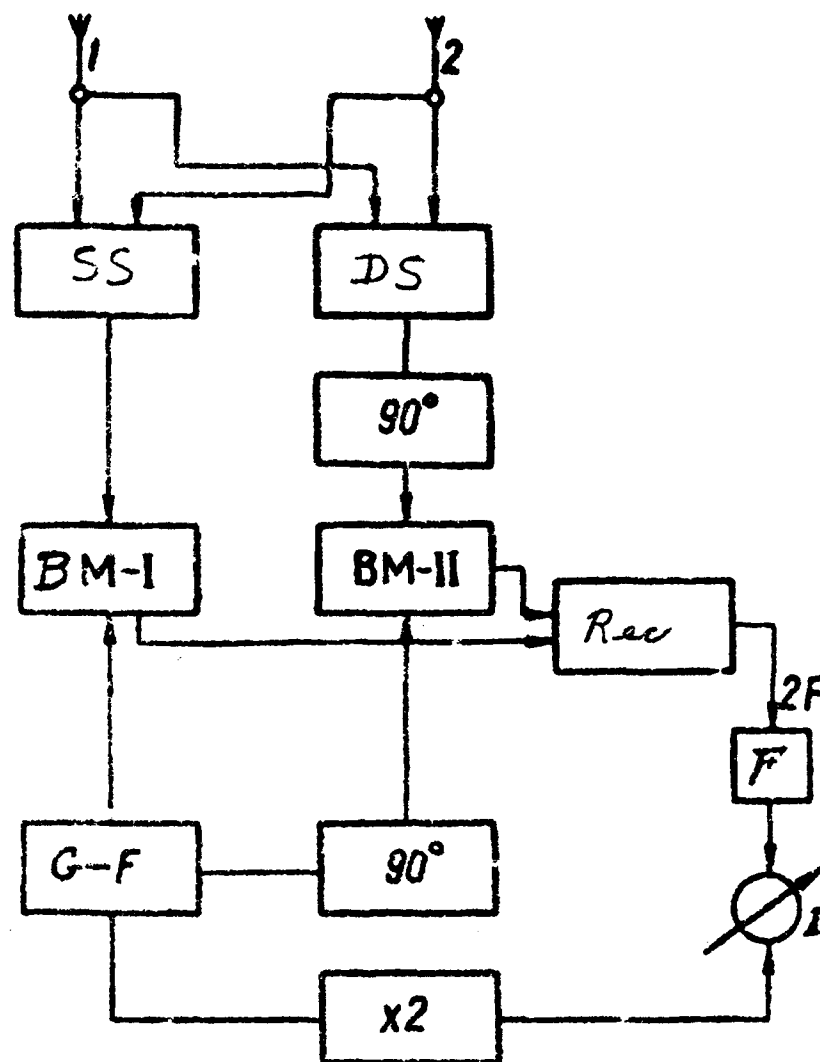


Fig. 1.30. Amplification with signal conversion by additional modulation.

1 and 2 -- antennas, SS -- sum stage, DS -- difference stage, BM-I and BM-II -- balanced modulators, Rec -- receiver, G-F -- generator of frequency F, x2 -- frequency doubler, I -- indicator, F -- filter, 90° -- stage shifting the voltage phase by 90° .

The spectrum of the voltages at the output of the balanced modulators obviously consists of sideband frequencies. The values of these voltages are

$$\left. \begin{aligned} u_1 &= 2UK \sin \omega t \sin \Omega t \cos \frac{\varphi}{2}; \\ u_2 &= 2UK \sin \omega t \cos \Omega t \sin \frac{\varphi}{2}; \end{aligned} \right\} \quad (1.32)$$

The total voltage, if the gains of the balanced modulators (k) are identical, will be

$$u_{\Sigma} = 2UK \sin \omega t \sin \left(\Omega t + \frac{\varphi}{2} \right). \quad (1.33)$$

After detection, the voltage at the output of the receiver is

$$u_{out} = UK \sin (2\Omega t + \varphi). \quad (1.34)$$

The voltage of the low frequency heterodyne is

$$u_0 = U_0 \sin \Omega t. \quad (1.35)$$

Inasmuch as the voltage on the receiver output does not contain the first harmonic of the modulation-frequency voltage, it is necessary to double the frequency of the reference voltage, before it is applied to the phase meter. The phase meter measures a phase difference, equal to the difference in phases of the initial high frequency voltages.

This signal conversion is considerably simpler. Each balanced modulator is made with two tubes. The phase-shifting networks can

be made either with tubes or with resistances and capacitances.

A high frequency phase shifting stage obviously employs a tube. The "sum — difference" stage can be sufficiently broadband and employ high frequency transformers.

A shortcoming of the circuit with signal conversion by forced modulation is the possibility of occurrence of additional apparatus errors. The inequality of the gains of the two modulators, inaccuracy in the setting of the phase shift at 90° in the low and high frequency networks may lead to apparatus errors, which must be taken into account by plotting a calibration curve for the conversion of the phase meter readings into bearing. Naturally, one should strive to make the apparatus errors stable. This makes it unnecessary to employ frequent calibration.

If the ratio of the amplitudes of the input signals changes, a direction finder operating with a single-channel amplification scheme and with conversion by additional modulation produces erroneous readings, and this is another shortcoming of this method.

Radio direction finding with short waves is accompanied by fading of the signal. It is therefore more advantageous to develop a phase-type radio direction finder, in which the change in the ratio of the signal amplitudes at the input does not produce errors in the reading of the phase difference. One such conversion scheme will be considered below.

Single-Channel Amplification with Signal Conversion by the Heterodyne

Method

A block diagram of the single-channel amplifier with signal conversion by the heterodyne method is shown in Fig. 1.31. The voltages at the output of the radio direction finder antennas are

$$u_1 = U_1 \sin \omega t; \quad (1.36)$$

$$u_2 = U_2 \sin (\omega t + \varphi), \quad (1.37)$$

where φ is the phase shift, determined by the direction of the incoming signal and by the length of the base.

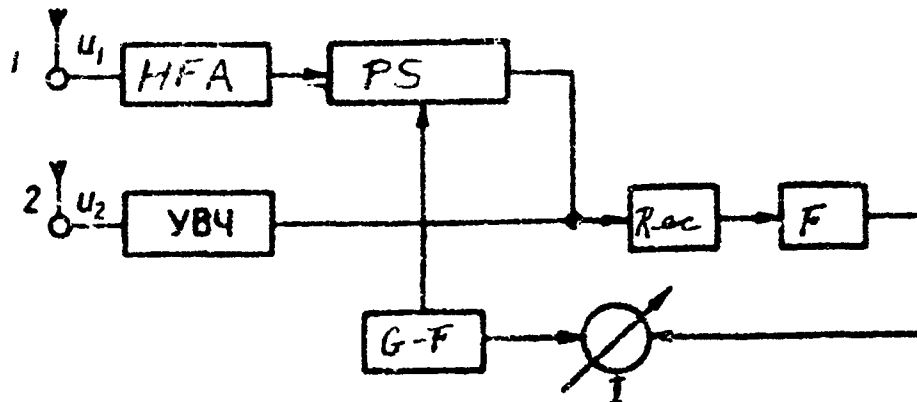


Fig. 1.31. Circuit for signal conversion by the heterodyne method.

HFA — high frequency amplifier, 1 and 2 — input voltages, PS — phase shifter, Rec — receiver, F — filter, I — indicator, G-F — generator of frequency F.

An electronic phase shifter, which operates from a low frequency reference generator, is connected in the receiving channel

associated with one antenna.

The voltage at the generator output is

$$v_g = U_0 \sin(\Omega t + \varphi_g), \quad (1.38)$$

where φ_g — initial phase.

The voltage at the output of the phase shifter is

$$u_{in} = U_1 K \sin(\omega t + \Omega t + \varphi_p). \quad (1.39)$$

It is clear from (1.37) and (1.39) that the input to the receiver will be two voltages, which differ slightly in frequency. After amplification and detection, the beat frequency voltage is separated.

The voltage at the receiver output is

$$u_{out} = U_1 U_2 K \cos(\Omega t - \varphi + \varphi_p). \quad (1.40)$$

If we now place a phase meter, which measures the phase difference between the reference voltage and the voltage from the output of the receiver (after first shifting the reference voltage 90° in phase), then the reading of the phase meter will equal the initial phase shift between the voltages and the antennas. The phase meter will indicate a phase difference

$$\nu = \varphi. \quad (1.41)$$

where ν is the reading of the phase meter.

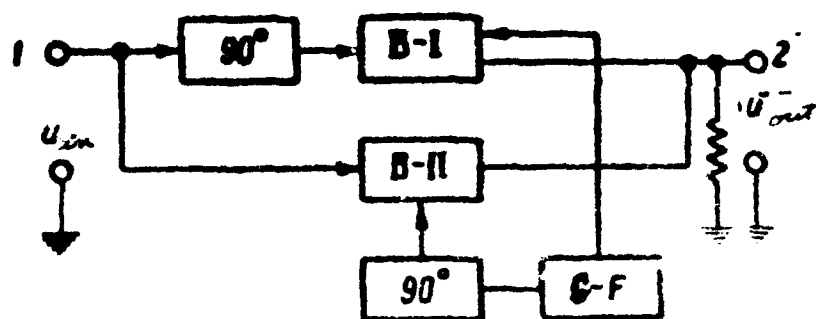


Fig. 1.32. Block diagram of electronic phase shifter.

1 — input voltage, 2 — output voltage, 90° — phase shift stage producing a 90° shift, B-I, B-II — balanced modulators, G-F — generator of frequency F.

The change in the ratio of the voltage amplitudes in the antennas leads to a change in the amplitude of the output voltage, but the readings of the phase meter remain unchanged.

In order to insure good operation of the phase meter upon change in the ratio of the input-voltage amplitudes, it is necessary to install, in addition to the ordinary automatic gain control circuit, also a circuit of automatic control for the signal strength at the receiver output (low frequency). In this amplification scheme it is possible to employ an electronic phase shifter.

The electronic phase-shifter circuit (Fig. 1.32) is known as the circuit used for separating a single sideband frequency in radio transmitting devices [10]. The phase shifter consists of balanced modulators and phase-shifting networks.

If the amplitudes of the voltages at the inputs of the balanced modulators are equal and if the gains are equal, then the voltages at the outputs of the balanced modulators are:

$$u_i = U_i K \sin \omega t \cos \Omega t; \quad (1.42)$$

$$u_{ii} = U_i K \cos \omega t \sin \Omega t, \quad (1.43)$$

where K is the gain of the balanced modulator.

The summary voltage

$$u_{\Sigma i} = K U_i \sin (\omega t + \Omega t), \quad (1.44)$$

evidently contains only one sideband frequency.

It is of interest to analyze in greater detail the circuit obtained when the gains of the balanced modulators are not the same, and to clarify the character of the receiver output voltage for this case.

The voltage at the antenna outputs can be determined from formulas (1.36) and (1.37). Let us denote by a the ratio of the gains of the balanced modulators:

$$a = \frac{K_2}{K_1}, \quad (1.45)$$

and by k the ratio of the amplitudes of the input voltages at the antennas

$$k = \frac{U_1}{U_2}. \quad (1.46)$$

Then the voltages at the output of the balanced modulators are

$$u_i = U_i K_i \sin \omega t \cos \Omega t; \quad (1.47)$$

$$u_{ii} = U_i a K_i \cos \omega t \sin \Omega t. \quad (1.48)$$

Formula (1.37) can be represented in a different form

$$u_2 = U_2 \sin \omega t \cos \varphi + U_2 \cos \omega t \sin \varphi. \quad (1.49)$$

The total voltage at the receiver input is

$$u_{in} = U_2 [(\cos \varphi + kK_1 \cos \Omega t) \sin \omega t + (\sin \varphi + kK_1 \sin \Omega t) \cos \omega t]. \quad (1.50)$$

If we denote

$$A = \cos \varphi + kK_1 \cos \Omega t; \quad (1.51)$$

and

$$B = \sin \varphi + kK_1 \sin \Omega t, \quad (1.52)$$

then the voltage at the receiver input can be represented in the form

$$u_{in} = U_2 (A \sin \omega t + B \cos \omega t) \quad (1.53)$$

or

$$u_{in} = U_{in} \sin (\omega t + \varphi_1), \quad (1.54)$$

where U_{in} is the envelope of the high frequency voltage

$$U_{in} = U_2 \sqrt{A^2 + B^2}; \quad (1.55)$$

φ_1 is the phase angle, on the high frequency side, the tangent of which is

$$\operatorname{tg} \varphi_1 = B/A. \quad (1.56)$$

The phase angle φ_1 is of no significance to the further analysis.

It is now necessary to determine the voltage at the output

after detection. The amplitude of the envelope and the phase are functions of time. The frequency of variation of the amplitude and of the phase angle of the envelope are determined by the frequency of the reference generator.

To analyze the detection products, we shall consider the characteristic of the detector to be quadratic (for the sake of simplicity):

$$i_d = \beta u_d^2 \quad (1.57)$$

Then the voltage at the output of the receiver will be

$$U_{out} = \beta K (A^2 + B^2), \quad (1.58)$$

where K is a coefficient that is determined by the gain of the receiver.

It is of interest to know the voltage of the first and second harmonics. Leaving out the constant component, we obtain for the first harmonic voltage

$$2U_1 U_2 \beta K_1 \sqrt{\cos^2 \varphi + a^2 \sin^2 \varphi} \cos [\Omega t + \arctg (a \operatorname{tg} \varphi)]; \quad (1.59)$$

and for the second harmonic voltage

$$\frac{\beta U_1^2 U_2^2 K_1^2}{2} (1 - a^2) \cos 2\Omega t. \quad (1.60)$$

If the reference voltage is shifted ahead in phase by 90° , before it is applied to the phase meter, then the latter will show the phase shift in accordance with formula (1.59)

$$\nu = \arctg (a \operatorname{tg} \varphi). \quad (1.61)$$

It follows therefore that if the gains of the balanced modulators are not equal, the circuit will introduce an error $\Delta \varphi$ in the measurements of the output phase difference

$$\Delta \varphi = \arctg(a \operatorname{tg} \varphi) - \varphi. \quad (1.62)$$

The apparatus error $\Delta \varphi$ can be taken into account in calibrating the radio direction finder, and it is important here that it be stable. If small phase differences are measured, for example, on the longer-wave portion of the band, then by increasing the coefficient a it is possible to obtain an artificial increase in the scale. Since the scale of the radio direction finder, i.e., the number of degrees of phase shift between voltages in the antenna per degree of bearing of the signal, depends on the frequency, then by changing the coefficient a in accordance with the frequency it is possible to equalize the scale of the radio direction finder.

In the calculation of bearing, it is more convenient to have a scale for the phase radio direction finder, which is linear. However, it must be borne in mind that as the coefficient a deviates from unity, the voltage of the second harmonic at the input of the receiver increases, as follows from formula (1.60), and the amplitude of the first harmonic becomes dependent on the measured phase shift angle. Therefore, if one is concerned with high stability and good waveform of the output voltage, the coefficient

a must be chosen to be equal to unity.

An advantage of the phase-type radio direction finder is that it employs the principle of separating the beat frequency for the conversion of the signals, rather than modulation of the signals. In this connection, a signal of only two frequencies is amplified in the receiving channel, and not of three frequencies (carrier and two sidebands), as occurs in the case of signal conversion by additional modulation.

One other remark must be made. In the block diagram (see Fig. 1.31) there are shown ahead of the phase shifter two high frequency amplifiers. It is essential to have the two high-frequency amplifiers at the input tuned by a single knob for two reasons.

First, the phase shifter may attenuate the signal, and the absence of preamplification in high frequency may deteriorate the signal to noise ratio at the receiver input. This pertains in particular to a mechanical phase shifter.

Secondly, the phase shifter may be essentially a nonlinear element, for example, when an electronic phase shifter is used. The presence of a nonlinear element at the input of the receiver may lead to the appearance of cross-modulation distortions and to a deterioration in the interference immunity of the radio direction finder.

One must not think, however, that the presence of two high-frequency amplification stages at the input of the receiver eliminates the basic advantages of single-channel amplification scheme. The principal is still in a standard single-channel receiver. In addition, it is easy to make identical two relatively broadband amplifiers at high frequency. The principal difficulties in the two-channel systems arise when the intermediate frequency amplifiers are to be balanced in phase. Therefore the use of high frequency amplifiers in the phase-type radio direction finder circuit, although it does complicate the circuit somewhat, it does increase substantially the actual sensitivity of the radio direction finder.

Simple Two-Channel Amplification

Simple two-channel amplification is essential in realization of the method of phase-difference measurement by the "sum -- difference" method with a cathode ray tube as an indicator (see Fig. 1.25). Both amplifying channels must satisfy the requirement of equality of the gains and of the phase shifts. This equality must be attained not only for a single point of the resonance characteristic but within the bandwidth of the transmitted frequencies for all points, or else instrumental errors will appear. In various schemes used to measure phase differences, these errors will vary.

A detailed analysis of the instrumental errors in the case of a two-channel scheme is given in later chapters. It was previously assumed that when the signal is received in the form of a single carrier frequency, the requirements imposed on the channels can be relaxed, compared with reception of a pulse signal. It has now been proved, however, that the magnitude of the instrumental errors remains approximately the same in either case.

Amplification with Use of Driver-Frequency Voltage

A two-channel amplification scheme employing a driver-frequency voltage, applied to the intermediate-frequency amplifier, is shown in Fig. 1.33. One applies here to the inputs of both intermediate-frequency amplification channels a driver-frequency voltage, which differs insignificantly from the signal frequency.

The voltage appearing at the output of the channels will have a frequency

$$f_c = f_{oi} + F, \quad (1.63)$$

where f_i -- value of the intermediate frequency during detuning;

f_{oi} -- the same during exact tuning of the receiver to the radio station.

When the receiver is exactly tuned to the received radio station, then the frequency of the signal in the intermediate frequency channels will be f_{oi} . The frequency of the voltage

appearing at the output channels will be F .

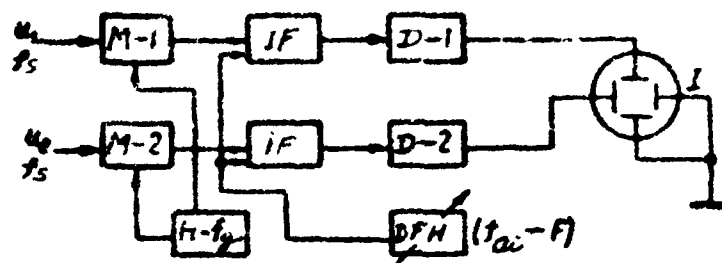


Fig. 1.33. Amplification with use of driver-frequency voltage, applied to the intermediate frequency amplifier.

$M-1$ and $M-2$ — mixers, $H-f_g$ — receiver heterodyne.
 DFH — driver-frequency heterodyne, IF — intermediate frequency amplifier, $D-1$ and $D-2$ — detectors, I — indicator.

There exists several versions of amplification with driver frequency. One can apply the driver frequency voltage not to the intermediate frequency amplifier, as in the preceding case, but to the inputs of the receivers (Fig. 1.34) and to use automatic frequency control such that the frequency of the output voltage remains unchanged. Here one tunes the driver-frequency heterodyne.

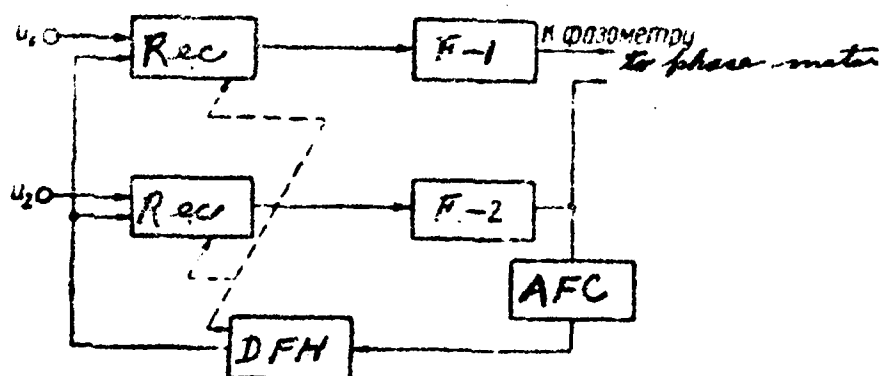


Fig. 1.34. Two-channel amplification of signals using driver-frequency voltage applied to the receiver inputs.

u_1 and u_2 — input voltages, Rec — receiver, F-1 and F-2 — filters, AFC — automatic frequency control, DFH — driver frequency heterodyne.

A plot of the signals on phase-frequency characteristics of the IF channels is shown in Fig. 1.35. Denoting the phase of heterodyne of the ~~and~~ driver frequency by φ_{hd} and the phase shifts of the signal in the first and second channels respectively by φ'_s and φ''_s , we obtain the additional phase shift which the signals experience after amplification. Assume that two signals are fed to the input of the intermediate frequency amplifier with a phase shift between them of ~~two~~ $2\varphi_s$. In the receiver, the ~~next~~ driver frequency voltage will experience a phase shift $\varphi'_d + \varphi_{hd}$ in the first channel and $\varphi''_d + \varphi_{hd}$ in the second channel.

Then the phase shifts of the signal and of the driver frequency will be: for the voltages at the output of the intermediate frequency amplifier of the first channel

$$\left. \begin{array}{l} +\varphi_s + \varphi'_s \\ \varphi'_d + \varphi_{hd} \end{array} \right\} \quad (1.64)$$

and for the voltages at the output of the intermediate frequency of the second channel

$$\left. \begin{array}{l} -\varphi_s + \varphi'_s \\ \varphi'_d + \varphi_{hd} \end{array} \right\} \quad (1.65)$$



1 — phase characteristic of the first channel, 2 — phase characteristic of the second channel.

The phase difference at the output of the receivers, based on the beat frequency, can be represented in the form

Thus, in a circuit with a driver frequency, the additional phase shift in the amplification is due only to the inequality of the relative phase shifts in the channel between the driver frequency and the signal frequency, and not to the absolute phase shifts. In

other words, the resultant phase shift in the amplification will depend only on the differences in the slopes of the phase characteristics of the channels, i.e., on the equivalent Q of the channels, will be independent of the detuning. This result can be seen from the phase characteristics of two channels (see Fig. 1.35).

Formula (1.66) can be rewritten

$$2\varphi + \Delta\varphi_1 - \Delta\varphi_2$$

where

$$\begin{aligned} \Delta\varphi_1 &= \varphi'_s - \varphi'_d; \\ \Delta\varphi_2 &= \varphi''_s - \varphi''_d. \end{aligned} \quad (1.67)$$

(1.67)

In many radio direction finders the scheme used to amplify the signals with a driver frequency was realized successfully. The change in the phase shift of the signal during the tuning of the receiver, even without special trimming of the channels, is reduced by a factor of many times in the presence of a driver frequency. Thus, for example, in one of the experiments without a driver frequency two ordinary receivers produced a 180° phase shift, and with a driver frequency merely 18° , within the intermediate frequency bandwidth.

However, independent of the version of the driver-frequency scheme, the following singularities of this scheme should be indicated.

The stability of the frequency at which the phase difference is measured, is determined by the stability of the driver-frequency

heterodyne. In addition, when tuning the receiver by the scheme shown in Fig. 1.33, the output frequency will change all the time, and this may unfavorably affect the operation of the phase meter. Therefore, schemes are necessary for automatic regulation of the driver frequency. The principal value in schemes with driver-frequency voltages is the use of detectors in the channels. This reduces the ^{interference} ~~interference~~ ^{rejection} ~~rejection~~, since the detectors can produce cross talk.

Finally, the driver-frequency voltage cannot be used when using direction finding by means of pulses, which require the measurement of the phase difference at high frequency. Consequently, schemes with driver frequency can be used successfully only for direction finding by means of a telegraph signal. However, for these cases, it is frequently more advantageous to employ the conversion scheme indicated above, which are simpler to realize technically. Therefore schemes with driver frequency have a limited application.

In schemes with driver frequency it is essential to use automatic frequency control. Instead of an automatic frequency control circuit it is possible to use a two-channel amplification scheme, in which the signal frequency in the intermediate frequency amplifier will be unchanged during the tuning of the receiver. Such a scheme is called a two-channel amplification scheme with driver heterodyne.

Amplification With Driver Heterodyne

A block diagram of the amplification version with a driver heterodyne is shown in Fig. 1.36.

As can be seen, in this two-channel scheme of amplification there is a double frequency conversion. After the first conversion, the signal taken from one of the intermediate frequency amplifier channels is amplified and is then mixed with the signal from an additional heterodyne. The resultant signal is used as a heterodyne voltage for the second conversion in mixers M-3 and M-4.

After determining the change in the signal phase in the same sequence as in the amplification scheme with driver frequency, it is possible to note that the phase difference between the signals at the input remains completely the same also for the output voltages. The frequency of the output voltages remains unchanged when the receiver is tuned or when the signal frequency is changed, and it always remains equal to the frequency of the additional heterodyne.

When realizing an amplification scheme with driver heterodyns, it is necessary to take steps to prevent the voltage from the additional heterodyne from entering the input of the intermediate frequency amplifiers, since the tuning frequency of the intermediate frequency amplifiers coincide with the frequency of the additional heterodyne.

In direction finding with a signal that consists only of

one carrier frequency, it is enough in a two-channel amplification scheme with driver heterodyne to equalize the parameters of the intermediate frequency amplifiers in both channels only for one point of the resonance curve.

In direction finding with pulsed radio signals, an amplification scheme with driver heterodyne does not give any substantial advantages over simple two-channel amplification, since it is no longer necessary to have identical channels within the frequency band.

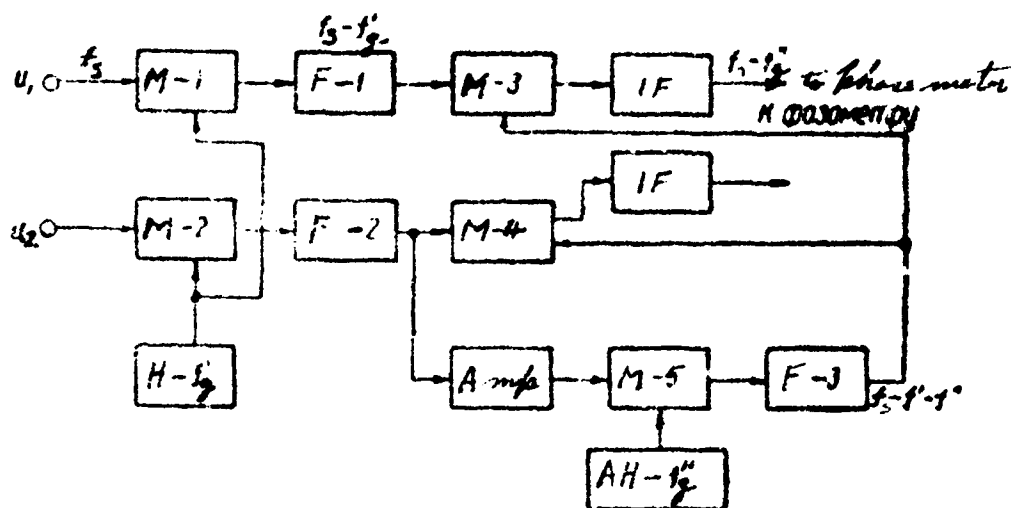


Fig. 1.36. Block diagram for the amplification of signals with a driver heterodyne. M-1, M-2, M-3, M-4, and M-5 -- mixers, IF -- intermediate-frequency amplifier, F-1, F-2, and F-3 -- filters, H -- f'_g -- receiver heterodyne, AH -- f''_g -- additional heterodyne of frequency f''_g , Amp -- amplifier.

When direction finding with continuous signals, single-

channel amplification schemes compete successfully with this scheme, based on signal conversion. It must be noted, however, that for single-channel amplification one must have a detector to generate out the envelope, whereas for amplification with a driver heterodyne no detector is needed and this possibly reduces somewhat the sensitivity of the circuit to noise.

Analysis of systems for amplification and measurement of phase differences shows that for direction finding with pulse signals it is advantageous to choose two-channel simple systems, but for direction finding for telegraph signals it is necessary to give preference to single-channel amplification systems with signal conversion and with measurement of phase difference on the low frequency side.

CHAPTER II

ERRORS OF SHORT-WAVE RADIO DIRECTION FINDERS, DUE TO CONDITIONS OF RADIO WAVE PROPAGATION

1. INFLUENCE OF THE IONOSPHERE ON THE PROPAGATION OF RADIO WAVES

Any investigation of short-wave direction finders must be connected in some form or another with a study of the singularities of propagation of short waves.

The most important circumstance is that the radio communication between the transmitter and the direction finder is realized at short waves by means of a "sky ray," i.e., with the aid of radio waves which are reflected from the ionosphere. Therefore the quality of the operation of the direction finder depends substantially on the state of the ionosphere.

It is known that processes in the ionosphere are not stable. The degree of ionization varies continuously depending on the solar activity. Regular variations are observed in the density of the ionization and the height of the layers during the day, the year, etc. In addition, irregular changes occur also in the ionosphere, sometimes very radical (ionospheric storms), which may completely interrupt the radio communication. Even in the normal state of the ionosphere, there

are irregularities in it in the form of condensations of ionization - "ion clouds," which move relatively rapidly both in a horizontal and in a vertical direction. In short-wave radio lines of the communication type, the effect of ionospheric irregularities manifest itself in the well known fadings of the signal. The effect of the characteristics of the ionosphere on navigational radio lines is more complicated and has been less studied.

Among the singularities in direction finding at short waves one must also include the substantial influence of local objects, the sizes of which are comparable with the wavelength. This circumstance must be taken into account when choosing the location for the direction-finding stations.

We consider below the characteristic errors that arise when measuring bearings at short waves, and also certain methods, aimed at increasing the accuracy of the direction finding.

The analysis is carried out essentially as applied to long-base direction finders, although many of the conclusions remain in force also for other types of direction finders.

2. BEARING ERRORS, DUE TO SINGULARITIES IN THE PROPAGATION OF SHORT WAVES

In considering the ionosphere as a homogeneous ionized region in a horizontal plane, it is possible to analyze questions of short-wave radio communication. However, such an analysis cannot

contribute to an explanation of many phenomena which arise in direction finding at short waves.

It was shown in many investigations that the ionosphere contains local condensations of ionization [3, 15, 16], and that the ionosphere is inhomogeneous not only in a vertical plane, but also in the horizontal plane. The variation of the ionization

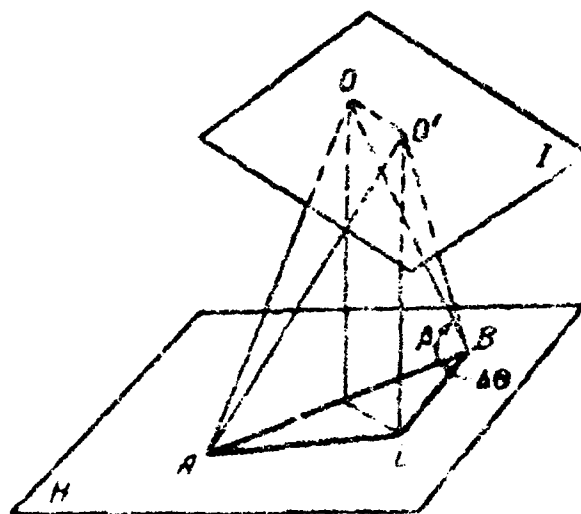


Fig. 2.1 Trajectory of propagation of a radio beam when the reflecting layer of the ionosphere is inclined.

H -- plane of the earth, I -- plane of the reflecting layer of the ionosphere, A -- transmitter, B -- direction finder, O -- point of reflection at a horizontal reflecting layer, O' -- point of reflection at an inclined layer, $\Delta \theta$ -- error in the determination of the bearing -- "error due to lateral deflection."

density in the horizontal direction leads to the curving of the equal ionization density surfaces, i.e., to a curving or to an inclination of the surface of the reflecting layer. This causes the propagation of the reflected radio waves to deviate from a great-circle arc. In this case the conditions of reflections recall in general "mirror reflection," and the plane of the "mirror" is so to speak inclined to the earth's surface (Fig. 2.1).

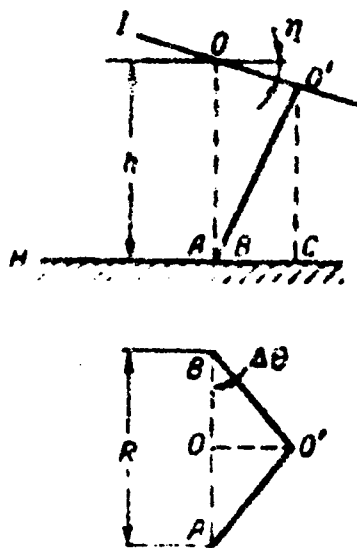


Fig. 2.2. Projection of the trajectory of the radio beam on the vertical and horizontal planes.

η — angle of inclination of the reflecting layer of the ionosphere, R — distance between the direction finder and the trans-

mitter, h -- effective height of the reflecting layer.

When the reflecting layer occupies a horizontal position, the radio beam propagates along the path AOB. The horizontal projection AB gives the correct direction to the transmitter. If the reflecting layer is inclined, the point of reflection is shifted and the radio beam propagates along the path AC'E. The horizontal projection of the beam at the point of reception B does not show the true direction to the transmitter A. An error $\Delta\theta$ appears in the measurement of the bearing.

The bearing errors which are due to the inclination of the reflecting layer, are frequently called errors due to lateral inclination.

Fig. 2.2 shows projections of the path of beam propagation on vertical and horizontal planes. From the diagram one can find an approximate relation between the inclination of the layer in the bearing error $\Delta\theta$, assuming that the angle η is small.

From elementary relations we have

$$\Delta\theta \approx \frac{2h}{R} \eta, \quad (2.1)$$

where R -- distance to the radio direction finding station;

h -- effective height of the reflecting layer.

As follows from geometric considerations, the magnitude of the lateral deflection errors decreases with increasing distance *as long as* almost hyperbolically ~~until~~ a once-reflected beam is received. As the

multiplicity of reflection increases, the errors due to lateral inclination increase [16]. Thus, in the case of double reflection from the ionosphere, the error in the measurement of the bearing is given by the formula

$$\Delta\theta \approx \frac{2h}{R} (\eta_1 + 3\eta_2), \quad (2.2)$$

where η_1 and η_2 — angles of transverse inclination of the ionosphere in the first and second reflection points, measuring from the transmitter;

h — altitude of the layer at the points of reflections.

In the derivation of Eqs. (2.1) and (2.2), the earth and the ionosphere are considered arbitrarily as planes. This approximation is valid, naturally, at small distances, but the principal relations remain correct also in the general case. The inclination of the layer at the second point of reflection affects the error of the bearing more strongly than the inclination of the layer at the first point. Naturally, at equal inclinations of the layer, the direction finding of a singly-reflected beam can insure greater accuracy than direction finding with the aid of doubly, triply, etc. or multiply reflected beams at equal distance.

The errors due to lateral inclination are particularly substantial at small distances, comparable with the height of the layer. At distances on the order of 300 kilometers, the errors due to lateral inclination reach tens of degrees in bearing (when operating with the F layer under normal conditions)

and exceed considerably all the remaining error of the radio direction finder/16/. This circumstance makes it possible to investigate the "lateral inclinations" of the ionosphere with the aid of radio direction finders, mounted at small distances from the transmitter.

As a result of experimental investigations, it was established that the inclination of the reflecting layer is a random quantity with zero average value and with a mean squared value of approximately 1° . The average period of variation of the inclinations is 20 to 40 minutes.

Measurements of the bearing of reflected waves have made it possible to detect also another type of ionospheric inclinations with a daily period. Their appearance is connected with periodic variations of the ionization under the influence of solar radiation. These inclinations are particularly noticeable on routes in a meridional direction in morning and evening hours.

Experiments have confirmed the reduction in errors due to lateral inclination with increasing distance, and the independence of the values of the errors on the parameters of the measuring apparatus/3, 16/. Many investigators believe that the error due to lateral inclination limit the maximum accuracy of short-wave direction finders. Errors due to lateral inclination are not the only type of errors in direction finders which are connected with the influence of the ionosphere. The whole series of other types of

errors, both systematic and random, arising during work with reflected radio waves, have been investigated.

A systematic bearing error may ~~xxxxx~~ be caused by a curving of the trajectory of the radio beam under the influence of the earth's magnetic field/4/. However, these errors can be noticeable only at small distances between transmitter and receiver and have no great significance on long lines.

Short-wave direction finders are characterized by a polarization error, which appears when the horizontal component of the field acts on the feeder system of the direction finder.

The polarization errors arise because of the presence of a horizontal component of the electric field, which appears upon reflection from the ionosphere. It must be emphasized, however, that the reception of the horizontal component of the field by the antenna of the direction finder itself not only does not lead to the appearance of an error, but, to the contrary, may be useful. The arises is due exclusively to reception by the feeder system

As a result of the reception by the feeder, two electro-motive forces will act at the input of each of the channels of the radio direction finders. One of these will be induced in the antenna, and the other in the feeder. The phase shift between these voltages is random and varies relatively rapidly with time. This causes the bearing indicator to start fluctuating, i.e., an error appears in the measurement of the bearing.

The signal reflected from the ionosphere arrives at the direction finder making a certain angle β with a horizontal plane (see Fig. 2.1). This circumstance may cause the so-called altitude error. The readings of the phase direction finder are connected with the direction of arrival of the signal by means of formula (1.14), which determines the phase difference between the signals in the antennas. The dependence of the altitude error on the azimuth and elevation angle is determined by formula (1.18).

We see that the angle Θ can be determined exactly if we know the angle β . In the contrary case, the angle β is assumed to be constant and equal to a ~~zack~~ certain average value, which is characteristic of the given radio line. Here obviously, an altitude error is introduced, depending on the difference between the assumed and actual values of the angle β .

If β does not exceed 20° -- 30° and the measurements are carried out in a narrow sector near the perpendicular direction to the base of the direction finder, the altitude error can be neglected.

If it is necessary to eliminate completely the altitude error, additional measurements of the phase difference can be made with a direction finder, whose base is perpendicular to the direction MW (Fig. 2.3).

In this case the phase difference is given by the formula

$$\varphi_1 = \frac{2\pi d}{\lambda} \cos \beta \cos \Theta. \quad (2.3)$$

Solving Eqs. (1.14) and (2.3) simultaneously, it is possible to eliminate the angle β and to determine the bearing accurately.

At short waves there are always received at the ~~range~~ reception point several radio beams, reflected from different regions of the ionosphere. The bearings and elevation angles of the different beams will also be different. A short-wave direction finder always operates in a "complex" field, which consists of many "simple" plane waves.

The analysis of the operation of a phase direction finder in the field of a complex signal shows that the position of the bearing indicator will be determined at each instant by the directions of arrival of the individual beams, their relative power, and the phase shifts between the voltages due to different beams.

The phase shifts vary quite rapidly with time. This causes rapid fluctuations in the bearing indicator. The rapid fluctuations are carried out about a certain average position, which can be determined by time averaging.

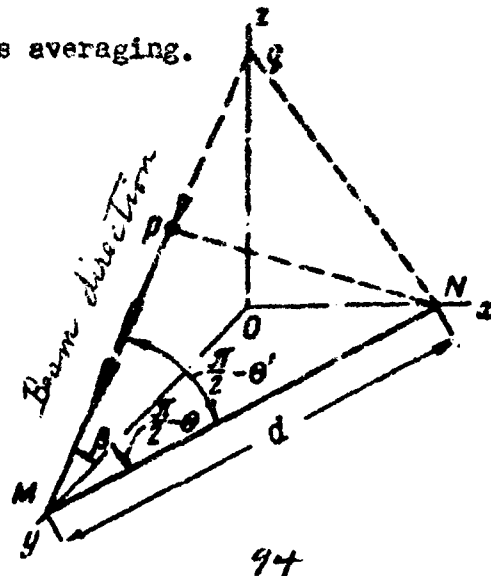


Fig. 2.3. Determination of altitude error of a direction finder.

M and N — direction finder antennas, d — direction finder base, β — elevation angle of radio beam, θ — bearing of radio beam, measured from the direction of the perpendicular to the direction-finder base. θ' — bearing in the inclined plane.

The simultaneous action of many beams causes the appearance of interference errors in short-wave direction finders. The appearance of interference errors is frequently accompanied by changes in the amplitude of the signal in the antennas (fading).

There are many reasons for the arrival of beams with different directions at the reception point. The five most characteristic cases are illustrated in Fig. 2.4.

At large distances to the transmitter, the propagation of radio waves may proceed over different paths. There may arrive at the point of reception singly, doubly, and multiply reflected beams from the ionosphere, (see Fig. 2.4a). The points of reflection of the different beams will be apart by many hundreds of kilometers in a horizontal direction. Naturally, the inclinations of the layer at different of the reflection are different in magnitude and their relative values vary independently.

Consequently, the inclinations of the singly, doubly, and multiply reflected beams will be different and independent of each other. Measurements have shown [14, 15] that the difference in bearings of rays of different multiplicity of reflection is characterized by a mean-squared value of 2 — 4 degrees at distances of approximately 100 kilometers.

Beams reflected from different layers of the ionosphere (see Fig. 2.4b) may arrive from different directions. The lateral inclinations upon reflection from the F layer, are as a rule larger than upon reflection from the E layer or from the sporadic E_s layer.

It is known that upon reflection from the ionosphere the beam breaks up into an ordinary component o and extraordinary component x. The directions of arrival of the two magneto-ionic components of the signal (o and x) may be different, as a result of the difference in the horizontal gradients of ionization in the region of reflection of the ordinary and extraordinary beam (see Fig. 2.4c).

The presence of local irregularities in the ionization leads to the appearance of scattered reflections (see Fig. 2.4d) which shows a projection perpendicular to the direction of propagation).

The scattered reflections may arrive at a considerable angle to the direction of the principal signal. Inclinations up to 30 — 50° in azimuth have been observed [4, 6]. The mean-squared inclination can be estimated to be 5 — 7°. Scattered reflections are characterized by a signal power which is one or two orders of magnitude less than the power of the main signal under normal conditions.

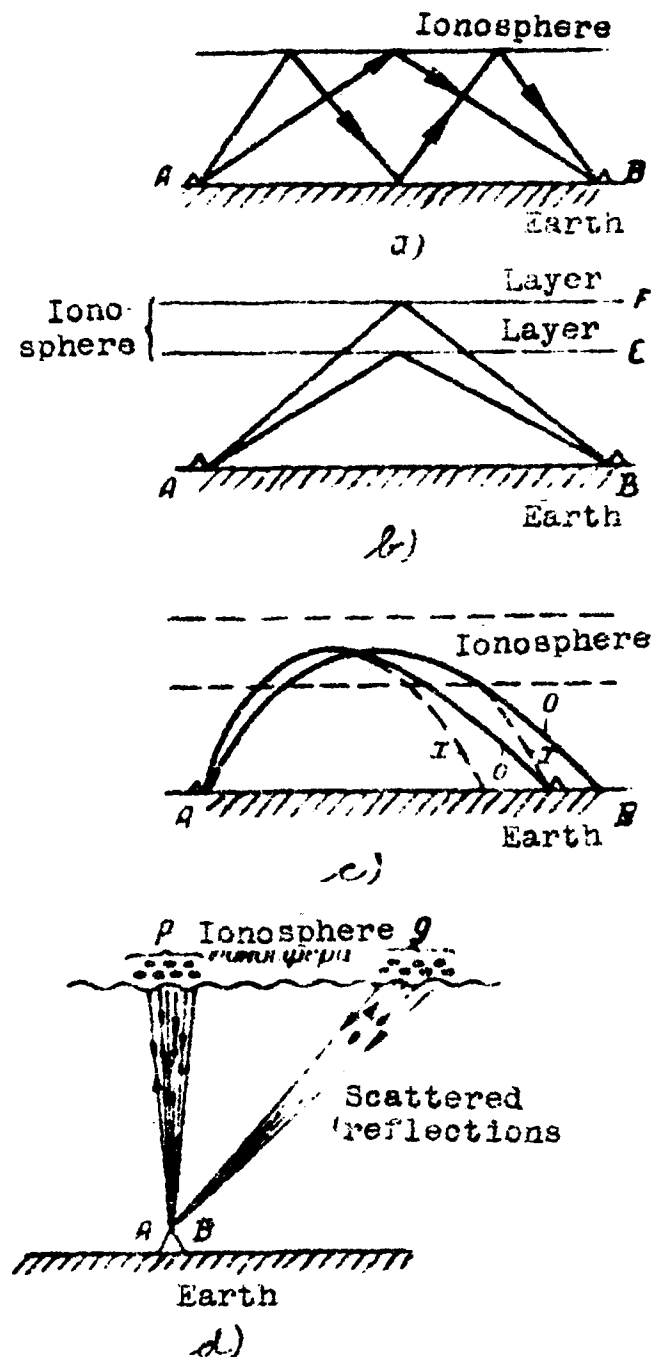


Fig. 2.4. Causes of formation of a complex field at short waves.

a — multiple scatterings, b — scatterings from different layers of the ionosphere, located at different altitudes, c — magnetic splitting of the beams, d — reflections from small irregularities and scattered reflections of radio waves.

The reflected signal, even when the ionosphere is in quiet state, consists actually of a bundle of rays, which are reflected as to speak from a rough surface (see region p of Fig. 2.4d). In this case the deviations in the direction of arrival of the waves reach considerable magnitudes. Certain measurements of the width of the bundle of reflected rays give values of $3 - 5^\circ$ (measured at the half-power point). More rarely one observes even greater numbers -- up to $10^\circ/3$.

A source of strongly deviating beams may be local objects, which re-radiate the radio waves incident on them. Even with a correct choice of the location of the direction finders it is impossible to get rid completely of the influence of local objects. The reason is that the direction finder is sensitive to re-radiated waves from local objects, which are up to several kilometers away.

As a result, errors arise in the direction finder which, however, are difficult to take into account in view of their dependence on the frequency, the influence of the weather, etc.

Many local objects have a clearly pronounced polarization characteristic and consequently, upon variation of the signal polarization, they change the intensity of re-radiation. Thus the changes in the polarization may cause corresponding fluctuations in a bearing indicator which is free of polarization errors proper.

3. METHODS OF REDUCING INTERFERENCE ERRORS

In view of the fact that the errors due to peculiarities in the propagation of short waves determine to a considerable extent the overall accuracy of the direction finder, the interest that attaches to possible methods of reducing these errors is quite understandable.

We have already indicated above that the errors due to lateral inclination limit the maximum accuracy of the direction finders. This is due to the fact that up to now no satisfactory method has been found for reducing errors due to lateral inclination. It must be emphasized, however, that at large distances the relative share of errors due to lateral inclination decreases. Therefore the reduction in errors of other types may also give noticeable results.

Many investigations devoted to a reduction in polarization errors have been reported. In view of this, we shall not dwell on this matter in detail. We shall merely indicate that a reduction in polarization error is attained essentially by thorough shielding of the finders, or else by using a symmetrically balanced feeder system.

Methods of reducing the altitude errors are relatively well known. As indicated in the preceding section, the altitude errors decrease considerably upon going to sector direction finder or

else can be eliminated in direction finding by means of two mutually-perpendicular bases.

The accuracy of direction finders may be increased considerably by reducing interference errors. Interference errors

arise because the direction finder receives a large number of beams from different directions. Therefore, in order to reduce the errors it is necessary to separate by some means or other a portion of the beams that arrive at the direction finder along the shortest path. On the other side, the interference of many beams results in rapid fluctuations in the bearing indicator. Investigations have shown, that if the bearing readings are averaged over a certain time, the accuracy of direction finding also increases.

Let us consider in greater detail certain methods used to reduce interference errors of short-wave direction finders.

Spatial selection of the signal is realized by choosing a corresponding directivity pattern for the antenna system of the direction finder. The directivity pattern of the antennas is best chosen in a vertical plane in such a manner as to increase the intensity of reception of beams that arrive at small angles to the horizontal.

It is easy to note that at a given distance, the beams arriving at small angles will be those that experienced the smallest number of reflections. The direction of arrival of these beams is closer to the true direction.

Experiments show that re-radiation from local objects, scattered over a large area at distances up to several kilometers from the direction finder, cause an error of approximately 0.25° in the bearing measurement at a frequency of 10 Mcs and 0.5° at 5 Mcs at small values of elevation angle and when the signal direction coincides approximately with the symmetry axis of the direction finder. These measurements were carried out with a direction finder having an 80-meter base with non-directional antennas [17]. If the directivity of the antennas is increased in the horizontal plane, the errors may be reduced considerably. In this case the direction finder becomes the sector finder. The working sector of the direction finder can be shifted as convenient, if necessary for normal operation. As the directivity is increased, bearing errors due to scattered reflections also diminish.

The extent to which the directivity pattern can be narrowed down is limited by requirements of a normal servicing of the working sector of the direction finder and by the permissible dimensions of the antenna system. Therefore, the influence of rays which deviate less than 10 or 15° from the principal direction, can hardly be reduced substantially by this method.

The signal arrives at the direction finder from the radio station along different paths, and consequently, with different time delays. If the transmitter operates in pulses, it is possible to separate in the direction finder that portion of the signal, which arrives first.

In this case the bearing measurement accuracy increases, since the first pulse has experienced less reflections or was reflected from lower layers. This results in a time selection, which eliminates completely the influence of multiple scattering of rays. The influence of rays that are scattered by ionospheric irregularities or which are re-radiated by local objects is ^{not} attenuated thereby, since they arrive practically simultaneously with the main signal. The effect due to the introduction of time selection will vary, depending on the presence of delayed rays and on their relative power. In general it can be assumed that on ^{routes} ~~ways~~ of ^{great} ~~long~~ length, in evening and in night time, the gain in accuracy due to the introduction of time selection will be more considerable than at short routes and in the day time.

Narrowing down the bandwidth of the receiving apparatus of the direction finder on the high frequency or on the intermediate-frequency side will naturally reduce the influence of many kinds of interferences. However, the narrower the receiver bandwidth, the more significant are the apparatus errors due to instability in the system parameters. Thus, the possibility of narrowing down the receiver bandwidth in the direction finder is quite limited. The bandwidth of the system can be narrowed down in the indicating apparatus which measures the phase difference. If the direction finder operates with a continuous signal or if the method of accumu-

lation of pulsed signals is used, then the bandwidth of the phase meter can be made quite narrow. It is obvious that narrowing down the bandwidth of the phase meter is equivalent to increasing its time lag.

The greater the time lag of the phase meter, the smaller will be the intensities of fluctuations of the bearing indicator. For effective response to rapid fluctuations of the bearing indicator, it is necessary to reduce the bandwidth to hundredths of a cycle.

A reduction in the intensity of the rapid fluctuations may also be obtained in a practically inertialess indicator as a result of numerical averaging of the instantaneous readings. Such an averaging over four or five minutes can insure the reduction in the mean squared error of bearing by approximately a factor of 1.5.

The increase in the accuracy obtained by averaging the reading over five minutes is illustrated by the results of the measurement of the bearing by telegraph stations, as listed on the following table/16/.

Расстояние до передатчика км 1)	2) Частота МГц	Средняя квадратическая ошибка пеленга по мгновенным отсчетам град. 3)	Средняя квадратическая ошибка пеленга по отсчетам, усредненным за 5 мин. град. 4)	Месяц, время суток 5)
1250	10,0	1,44	1,19	6) Январь — август, день
1910	12,0	1,09	0,88	
2050	14,0	1,31	1,05	
5500	15,0	1,40	1,11	
5500	15,0	0,82	0,59	7) Июнь — июль, день*
7000	15,0	1,22	0,65	
8500	15,5	1,32	1,10	

Table

1) Distance to transmitter, kilometers.

2) Frequency, megacycles.

3) Mean-squared bearing error as given by the instantaneous readings, degrees.

4) Mean-squared bearing error as given by readings averaged over five minutes, degrees.

5) Month and time of the day.

6) January -- August, day time.

7) June -- July, day time.*

* The measurements were carried out under particularly favorable conditions.

Approximately similar results can be obtained when using phase meters with large time lag^s. In either case the increase in the accuracy is gained at the expense of the increased time consumed in the reading.

Among the many radio beams that arrive at the direction finder, there frequently exists one specularly reflected beam, the power of which constitutes a considerable fraction of the total power of the received signal. Thus frequently the direction of arrival of the specularly reflected beam is closer to the true direction to the radio transmitter. Therefore a direction finder which separates out the strongest beam has the greater accuracy.

Such a separation takes place in any phase direction finder to one degree or another, if readings of the direction finder,

in the presence of several beams, approach the direction of the beam of maximum power. However, the degree of this approximation ~~depends~~ depends substantially on the parameters of the direction finder. The longer the base of the direction finder (more accurately, the greater the ratio d/λ), the closer the bearing reading is to the direction of the strongest beam.

The foregoing can be verified by means of the following argument.

Assume that the radio direction finder is acted upon by two beams: the first is a beam of large power, arriving from a direction $\Theta_1 = 0$, and the second is a beam arriving from the direction Θ_2 .

Let us assume also that the elevation angles of both beams are small, so that

$$\cos \beta_1 \approx \cos \beta_2 \approx 1. \quad (2.4)$$

The first beam induces in the antennas M and N of the direction finder (see Fig. 2.3) voltages which are of equal phase. The second beam will also induce voltages in the antennas M and N, but these will be separated by a phase

$$\varphi_2 = \frac{2\pi d}{\lambda} \sin \Theta_2. \quad (2.5)$$

The phase shift ψ between two voltages in the antenna M

is a quantity that varies with time in a random manner and depends on the difference in the paths of propagation of the first and second beam.

The vector diagrams of this case are shown in Fig. 2.5 for three different instants of time.

The indicating device of the direction finder measures the phase shift φ between the resultant voltages at the outputs of the two antennas.

It is seen from the vector diagrams that the measured value of φ changes with time as a result of variations of the phase shift ψ . Let us assume that the first beam is the principal one, and the second one is the interfering beam. Then, obviously, the correct measurement in the absence of an interfering beam should be equal to zero.

There are possible cases of correct measurement in spite of the presence of an interfering beam (instant t_3).

In the other instants of time, however, an error in the measurement is unavoidable. The bearing indicator will fluctuate, and it is easy to see that the maximum deviation from the correct position corresponds to the instant $t_3(\varphi = \varphi_{\max})$. Let us find the corresponding error in the determination of the bearing. For this purpose we make use of formula (1.15), assuming that the direction

finding takes place in a narrow sector (Θ is small). Assume that a certain reading φ is read on the scale of the direction finder. Then, by formula (1.15), the bearing of the beam is

$$\Theta = \frac{1}{2\pi d/\lambda} \varphi. \quad (2.6)$$

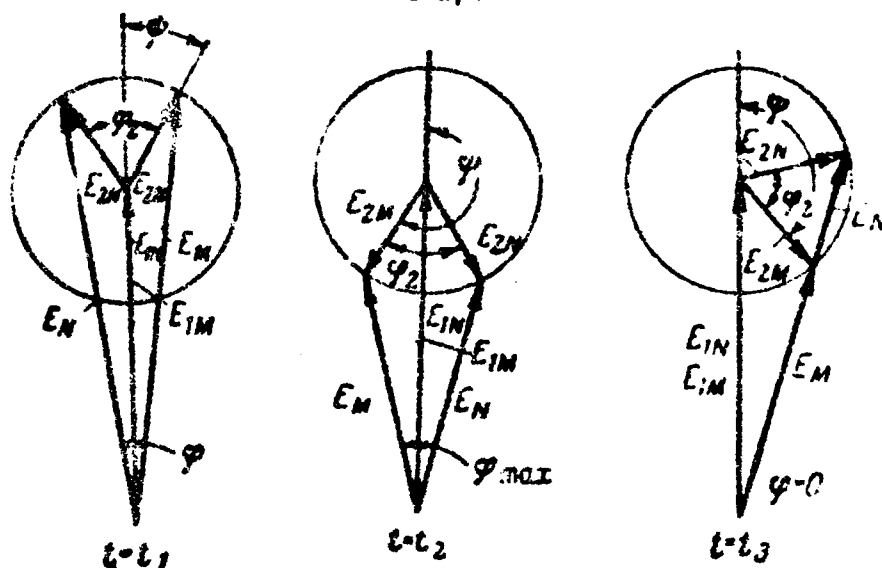


Fig. 2.5. Vector diagrams of the voltages in the direction finder antennas.

Applying formula (2.6) to this case, we note that the maximum error in the determination of the bearing (instant t_2) is

$$\Delta\Theta_{\max} = \frac{1}{2\pi d/\lambda} \varphi_{\max}. \quad (2.7)$$

Let us investigate the variation of the quantity $\Delta\Theta_{\max}$ upon increase in the direction finder base. For this purpose we return to the vector diagram at $t = t_2$. Considering that the diagram

is symmetrical with respect to the vertical axis, we can write down the following equations for the projections of the vectors on the vertical and horizontal axes.

$$\left. \begin{aligned} E_M \cos \frac{\tilde{\gamma}_{\max}}{2} + E_{2M} \cos \frac{\tilde{\gamma}_2}{2} &= E_{1M} \\ E_M \sin \frac{\tilde{\gamma}_{\max}}{2} - E_{2M} \sin \frac{\tilde{\gamma}_2}{2} &= 0. \end{aligned} \right\} \quad (2.8)$$

After finding from the second equation the value of E_M and substituting it in the first equation, we obtain, after a few transformations

$$\tilde{\gamma}_{\max} = 2 \operatorname{arctg} \frac{K \sin \left(\frac{\tilde{\gamma}_2}{2} \right)}{1 - K \cos \left(\frac{\tilde{\gamma}_2}{2} \right)}, \quad (2.9)$$

where $K = E_{2M}/E_{1M}$ is the ratio of the amplitudes of the voltages due to the second and to the first beams. Now, using formulas (2.7) and (2.9), we can obtain the value of the maximum error in the determination of the bearing:

$$\Delta \theta_{\max} = \frac{\lambda}{\pi d} \operatorname{arctg} \frac{K \sin \left(\frac{\pi d}{\lambda} \sin \theta_2 \right)}{1 - K \cos \left(\frac{\pi d}{\lambda} \sin \theta_2 \right)}. \quad (2.10)$$

Let us investigate the dependence of $\Delta \theta_{\max}$ on the ratio d/λ for the case $K \ll 1$. From formula (2.10) we obtain in first approximation

$$\Delta \theta_{\max} \approx K \frac{\sin \left(\frac{\pi d}{\lambda} \sin \theta_2 \right)}{\pi d/\lambda}. \quad (2.11)$$

It is seen from formula (2.11) that an increase in the direction finder base (more accurately, an increase in the ratio of the length of the base to the wavelength) reduces the maximum bearing error.

Thus, an increase in the direction finder base can reduce the interference errors of the direction finder, which arise as a ~~primary~~ result of strongly deflected rays (scattered by ionospheric irregularities or re-radiated by local objects).

The most substantial increase in the direction finding errors occurs when the base is increased to several wavelengths. A further increase in the ratio d/λ hardly increases the accuracy. At the same time, at long bases the reading becomes more difficult, since the fluctuations of the bearing indicator become more intense. It is seen from formulas (2.9) and (1.14) that φ_{\max} increases with increasing d/λ .

It is practically impossible to use a base six times the wavelength or longer, for in this case it is impossible to resolve the ~~phase direction finding~~ resultant ambiguities in the determination of the bearing.

The phase direction finders employed at the present time for short waves have bases of approximately 2 to 4 wavelengths.

In the practice of short-wave direction finders there exists a rule, according to which one must not take a bearing reading at those instants, when the fading signal passes through a minimum.

This decreases the errors due to a relative increase in the level of the noise during fading. In addition, this rule is confirmed also by the character of the connection between the amplitude and the phase of the signal. Even in the examination of the simplest case -- fading due to the interference of two beams -- it is seen that the maximum error at $t = t_2$ (see Fig. 2.5) coincides in time with a small amplitude of the resultant voltage (E_M and E_N).

In the case of simultaneous reception of many beams, a statistical connection is retained between the variation in the amplitude and the variation in the phase. The character of this connection is such, that a small amplitude corresponds on the average to large phase deviations. Consequently, by excluding readings with small signal amplitude, one discards readings with the maximum errors. This increases the measurement accuracy. However, such an increase in the accuracy is attained at the expense of increasing the time necessary to take the reading, during a certain portion of the time it is impossible to make the reading because of the small signal amplitude.

In conclusion, let us consider still another type of selection, which is practiced in short-wave direction finders. This is the so-called mental selection.

are
By mental selection are meant peculiarities in the bearing measurements, when this measurement is carried out by the operator, unlike the purely automatic measurement without human participation.

In observing the direction finder screen and simultaneously controlling the signal by ear, the operator establishes a connection between the readings of the indicator and the sound signals. Thus, when observing the screen the operator is capable of segregating the sharp deviations of the reader, due to atmospheric interference, since they are accompanied by characteristic crackling in the ear-phones.

When neighboring telegraph stations produce the interference, the operator can catch the instants that are most favorable for reading, when the signal of the interfering station fades. And since the telegraph signals of two different stations sometimes differ in tone, an experienced operator frequently can determine what reading on the screen corresponds to the necessary station, and which is due to the interfering station. Here the operator makes use of the fact that a bearing indication appears on the direction finder screen with a cathode ray tube only during the instant when the telegraph key is pressed down, and that the indication vanishes during the time of the pause. This makes it easier for the operator to establish a connection between the sound and the visual observations.

Thus, in mental selection use is made of the high selectivity of the ear to refine the visual reading.

Another feature of the operator's work is the time delay of the reading, due to memory. Even when observing the screen of a

practically inertialess direction finder, the operator actually carries out an averaging of rapidly fluctuating readings. The fluctuation of the indicator, due to the interference of many rays, is usually not so fast as to make use of persistence of vision. However, by observing the consecutive changes in the positions of the indicator, the operator can retain them in his memory for a relatively long time, and thus carry out a mental averaging.

The capabilities of mental selection are essentially connected with the time delay of the indicator used for the reading. Actually mental selection can be used completely only in practically inertialess indication. A phase meter with time delay responds slowly to the changes in the bearings of the signal. This rids the operator of the possibility of taking the reading at the instant when the interference disappears for a short time, for the indicator cannot change substantially then. It also becomes quite difficult to establish a connection between the visual and auditory observations.

The experimental data show that mental selection makes it frequently much more advantageous to use inertialess indicators and ensures high accuracy.

Conditions are encountered, however, when the best results are produced with a time-delay indicator (the presence of ^{white} noise, and strong scattering of the main signal). In this connection it is better to have apparently two indicators for the direction

finder, one with high inertia and the other one with low inertia,
so as to make use of either depending on the actual reception conditions.

Chapter III

EFFECT OF CHANNEL UNBALANCE ON THE APPARATUS ERRORS OF TWO- CHANNEL RADIO DIRECTION FINDERS

1. Two Versions of Two Channel Amplification Schemes

The direction finding of pulsed radio signals is best carried out with low-inertia radio direction finders, particularly if the number of radiated pulses is counted in units. The observation of passive instantaneous targets, particularly meteorites, ~~is possible~~ is possible in this case by radio direction finders in conjunction with a pulse range finder using a wavelength on the order of ten meters.

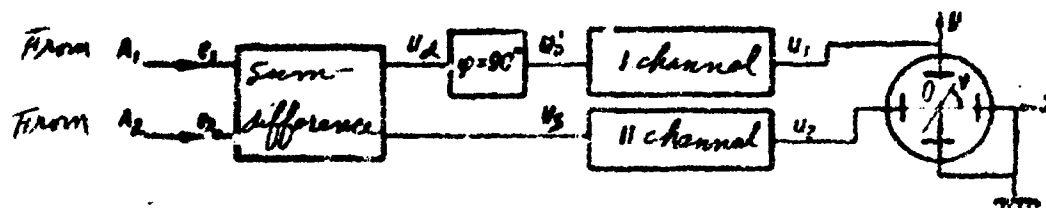


Fig. 3.1. Diagram of two-channel receiving-indicating apparatus with post amplification of the signals.

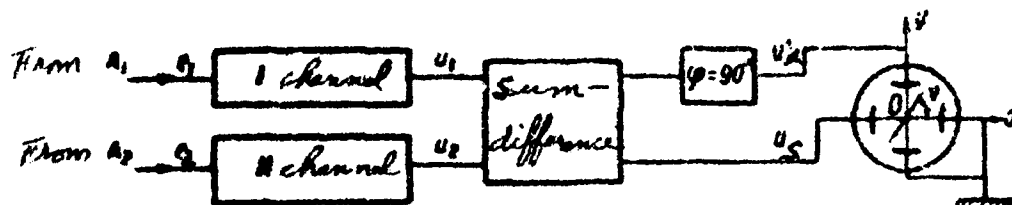


Fig. 3.2. Diagram of two-channel receiving-indicating apparatus with preamplification of the signals.

In the preceding chapter we have shown the advantages of using low-inertia direction finders for longer signals, since these radio direction finders make it possible to carry out mental selections which increases the accuracy of direction finding.

Low inertia direction finders are two-channel radio direction finders with cathode ray tubes [12, 19]. Figs. 3.1 and 3.2 show the diagrams of two-channel receiving-indicating apparatus used in short-wave direction finders with long base.* Such devices solve two problems: amplification of the signals with the necessary selectivity, and measurement of the phase difference. In both circuits, the phase differences are measured by the "sum -- difference" method (see Chapter I). The difference between the circuits shown in Figs. 3.1 and 3.2 lies in the fact that in the first one the amplifying channels are connected after the "sum -- difference" device, and in the second they are connected ahead of it. We shall therefore call arbitrarily the first circuit (Fig. 3.1) a post-amplification circuit, and the second one (Fig. 3.2) a pre-amplification circuit.

* The operating principle of the phase direction finder is treated in Chapter I).

For normal operation, the amplification channels should be absolutely identical. If the channels have non-identical parameters, apparatus errors arise.

The only channel differences tolerated in well-designed equipment are those at which apparatus errors do not limit the direction-finding accuracy. Thus, at short waves, the mean-squared direction-finding error over long distances amounts to approximately 1° , owing to the influence of radio wave propagation conditions. The apparatus errors in the determination of bearing must therefore be considerably less than the indicated value.

In phase direction finders, one degree of bearing corresponds to several degrees of phase difference, so that the tolerances can be relaxed somewhat as regards phase-difference measurements. The apparatus errors, nevertheless, still amount to a considerable fraction of the bearing error, for it is technically quite difficult to ensure perfect identity of the channels.

Let us examine the apparatus errors due to non-identity of the channels of the receiving-indicating devices of radio direction finders. For the analysis we choose circuits with post amplification (see Fig. 3.1) and with preamplification (see Fig. 3.2).

If the input to the amplifier in the stationary mode is

$$e(t) = E \sin \omega_0 t,$$

then the output voltage is $u(t) = KE \sin(\omega_0 t + \Phi)$,

where

K — modulus of the gain coefficient;

Φ -- phase angle of the gain or phase shift.

For a sinusoidal signal of fixed frequency ω , it is best to describe the differences between amplification channels by means of the ratio of the moduli of the gain:

$$\alpha = \frac{K_1}{K_2} \quad (3.1)$$

and the difference in phase shifts

$$\varphi = \Phi_1 - \Phi_2, \quad (3.2)$$

where K_1 and K_2 -- moduli of the gains of the first and second amplification channels;

Φ_1 and Φ_2 -- the phase shifts of the same channels.

Thus the quantity α characterizes the amplitude unbalance of the channels, and φ characterizes the phase unbalance.

We shall carry out the analysis of the apparatus errors as functions of these non-identity parameters (α and φ) of the amplifying channels.

2. ERRORS IN THE POST-AMPLIFICATION CIRCUIT

The voltages reach the amplification channels after passing through the "sum -- difference" device and the phase-shifting stage. The amplitudes of these voltages are proportional

to the sine and cosine of half of the angle of measured phase difference

$$u'_p = E_0 \sin \frac{\varphi}{2} \sin \omega_0 t; \quad (3.3)$$

$$u_c = E_0 \cos \frac{\varphi}{2} \sin \omega_0 t. \quad (3.4)$$

where u'_d -- voltage at the input of channel I.

u_c -- voltage at the input of channel II.

φ -- measured phase difference.

The voltages on the deflecting plates of the tube (past the amplifying channel) will be

$$u_1 = K_1 E_0 \sin \frac{\varphi}{2} \sin (\omega_0 t + \Phi_1); \quad (3.5)$$

$$u_2 = K_2 E_0 \cos \frac{\varphi}{2} \sin (\omega_0 t + \Phi_2), \quad (3.6)$$

or, taking into account the differences in the phase shifts

$$u_1 = K_1 E_0 \sin \frac{\varphi}{2} \sin \omega_0 t; \quad (3.7)$$

$$u_2 = K_2 E_0 \cos \frac{\varphi}{2} \sin (\omega_0 t - \psi). \quad (3.8)$$

Since the inclination of the beam is proportional to the applied voltage,

$$y = K_1 \sin \frac{\varphi}{2} \sin \omega_0 t; \quad (3.9)$$

$$x = K_2 \cos \frac{\varphi}{2} \sin (\omega_0 t - \psi), \quad (3.10)$$

where x -- horizontal deflection, y -- vertical deflection.

Assume that the sensitivity of the deflecting plates is the same in the horizontal and vertical direction, and the proper-

tionality coefficient is arbitrarily set at $1/E_0(\text{mm/v})$.

The Eqs. (3.9) and (3.10) can be represented in the form of an equation for the figure on the cathode ray tube

$$y^2 - 2 \frac{K_1}{K_2} \operatorname{tg} \frac{\varphi}{2} \cos \psi xy + \left(\frac{K_1}{K_2} \right)^2 \operatorname{tg}^2 \frac{\varphi}{2} = K_1^2 \sin^2 \frac{\varphi}{2} \sin^2 \psi. \quad (3.11)$$

From analytic geometry we note that such an equation is the equation of an ellipse, the axes of which are inclined by a certain angle ν relative to the axes of the tube (Fig. 3.3), with

$$\operatorname{tg} 2\nu = \frac{2a \operatorname{tg} \frac{\varphi}{2} \cos \psi}{1 - a^2 \operatorname{tg}^2 \frac{\varphi}{2}}. \quad (3.12)$$

The error in the determination of $\varphi/2$ is given by the difference

$$\nu - \frac{\varphi}{2},$$

and the ~~max~~ error in φ will be twice as large

$$\Delta = 2 \left(\nu - \frac{\varphi}{2} \right).$$

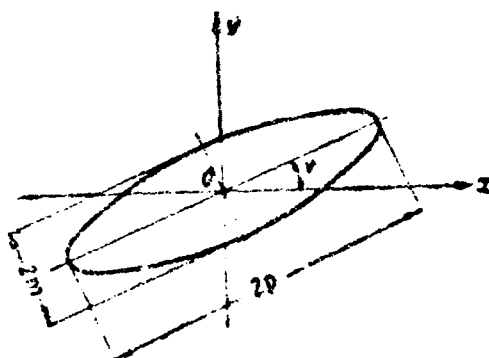


Fig. 3.3. Pattern on the tube of the screen.

Therefore, the overall expression for the error in the measurement of the phase difference is

$$\Delta = \arctg \frac{(a^2 - 1) \sin \varphi - (a^2 + 1 - 2a \cos \psi) \sin \varphi \cos \varphi}{2a \cos \psi - (a^2 - 1) \cos \varphi + (a^2 + 1 - 2a \cos \psi) \cos^2 \varphi}. \quad (3.13)$$

To determine the extremal values of the error it is necessary to find the derivative $\partial\Delta/\partial\varphi$, set it equal to zero, and to determine from this equation the value of φ at which the error has a maximum value. As a result we obtain

$$\varphi_{\max} = \arccos \left\{ \frac{(a^2 - 1)(a^2 + 1 - a \cos \psi)}{(a^2 + 1)^2 - 4a^2 \cos^2 \psi} \right\} \pm \frac{\sqrt{(a^2 - 1)^2(a^2 + 1 - a \cos \psi)^2 - [(a^2 + 1)^2 - 4a^2 \cos^2 \psi][(a^2 - 1)^2 - 4a^2 \cos^2 \psi]}}{(a^2 + 1)^2 - 4a^2 \cos^2 \psi} \quad (3.14)$$

Analysis shows that to determine φ_{\max} , corresponding to the maximum value of the maximum error, it is necessary to take in (3.14) a plus sign in front of the radical for $a < 1$ and a minus sign for $a > 1$. This must be taken into account, for in general when $a \neq 1$ and $\psi \neq 0$ the extrema of the error are not of the same magnitude.

To find the value of the maximum error it is necessary to insert in formula (3.13) the value φ_{\max} from formula (3.14).

From formulas (3.13) and (3.14) we can obtain two particular cases under the following conditions

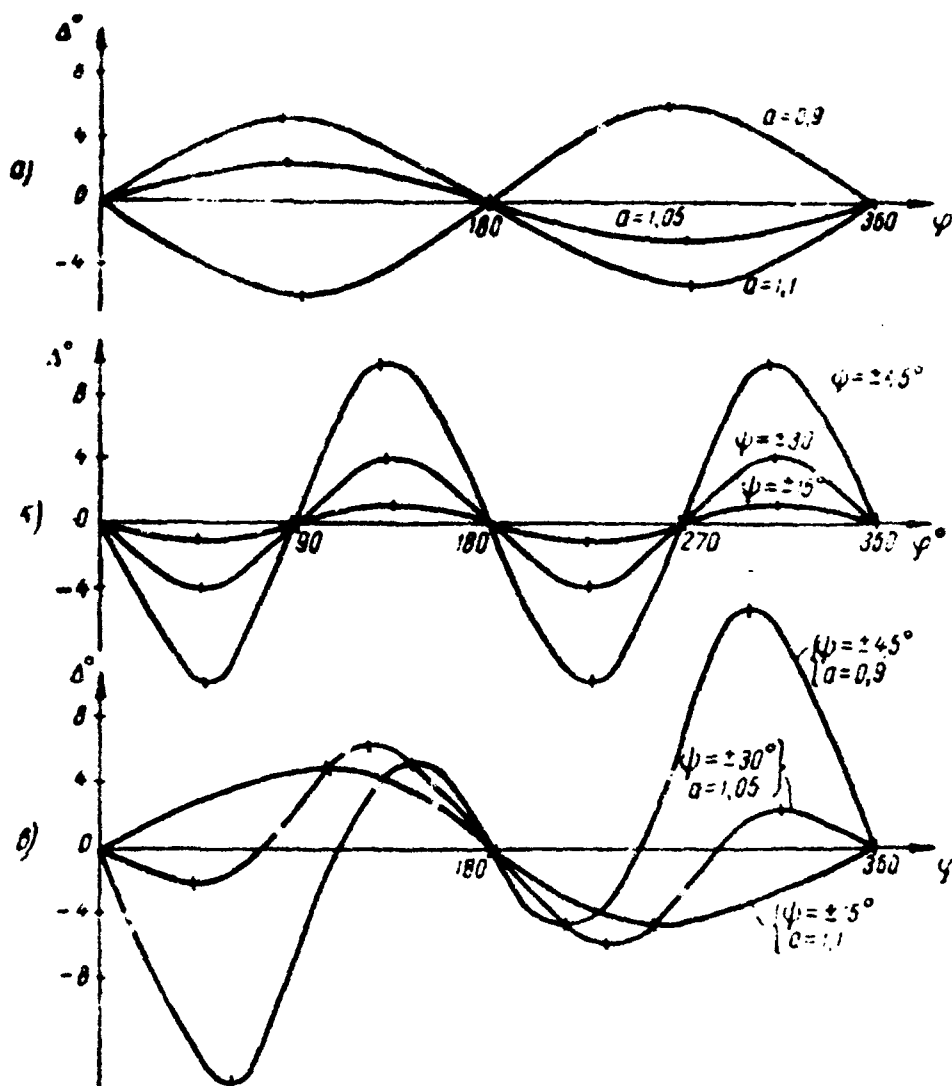


Fig. 3.4. Plot of the error vs. the magnitude of the measured phase difference.

In the first case, when $\psi = 0$, the pattern on the screen will be in the form of a line, and the formulas become

$$\Delta = 2 \operatorname{arc} \operatorname{tg} \frac{\frac{a-1}{a+1} \sin \varphi}{1 - \frac{a-1}{a+1} \cos \varphi}; \quad (3.15)$$

$$\varphi_{\max} = \operatorname{arc} \cos \frac{a-1}{a+1}; \quad (3.16)$$

$$\Delta_{\max} = 2 \operatorname{arc} \operatorname{tg} \frac{a-1}{2\sqrt{a}}. \quad (3.17)$$

Fig. 3.4a shows a plot of the error based on formula (3.15).

For the second particular case, when $a = 1.0$, we obtain

$$\Delta = \operatorname{arc} \operatorname{tg} \frac{\frac{\cos \psi - 1}{\cos \psi + 1} \sin 2\varphi}{1 - \frac{\cos \psi - 1}{\cos \psi + 1} \cos 2\varphi}; \quad (3.18)$$

$$\varphi_{\max} = \frac{1}{2} \operatorname{arc} \cos \frac{\cos \psi - 1}{\cos \psi + 1}; \quad (3.19)$$

$$\Delta_{\max} = \operatorname{arc} \operatorname{tg} \frac{\cos \psi - 1}{2\sqrt{\cos \psi}}. \quad (3.20)$$

Fig. 3.4b shows a plot of the error based on formula (3.18) while Fig. 3.4c shows the error based on (3.13). The graph corresponding to (3.13) corresponds also to the general case, when $a \neq 1$ and $\psi \neq 0$.

We see that, depending on the amplitude and phase unbalances, the shape of the error curve varies, and in addition the curve has different absolute extremal values. We note also that the errors vanishes, no matter how non-identical the channels are, when the measured phase difference is equal to zero or 180° .

It was indicated above that in the general case the pattern on the screen is an ellipse. Let us find the ratio of the minor to the major semi-axis (see Fig. 3.3).

If the equation of the ellipse is represented in the form

$$Ax^2 + 2Bxy + Cy^2 + F = 0,$$

then the ratio of the axes is given by

$$\left(\frac{2m}{2p}\right)^2 = \frac{A + C - \sqrt{(A - C)^2 + 4B^2}}{A + C + \sqrt{(A - C)^2 + 4B^2}}.$$

Analogously we obtain from (3.11)

$$\left(\frac{m}{p}\right)^2 = \frac{a^2 \lg^2 \frac{\varphi}{2} + 1 - \sqrt{\left(1 - a^2 \lg^2 \frac{\varphi}{2}\right)^2 + 4a^2 \lg^2 \frac{\varphi}{2} \cos^2 \psi}}{a^2 \lg^2 \frac{\varphi}{2} + 1 + \sqrt{\left(1 - a^2 \lg^2 \frac{\varphi}{2}\right)^2 + 4a^2 \lg^2 \frac{\varphi}{2} \cos^2 \psi}}, \quad (3.21)$$

where m -- length of the minor semi-axis of the ellipse;

p -- length of the major semi-axis.

To determine the ratio m/p in the cases when the error has a maximum value, it is necessary to insert the value of φ_{\max} from (3.14) into (3.21). Figs. 3.5 and 3.6 show the graphs of the dependence of the maximum error on the amplitude and phase unbalance of the channels (a and ψ). Within the limits of the diagram, the dependence of the error on a is almost linear, while the dependence on ψ recalls a quadratic curve. As ψ varies from 0 to $\pm 10^\circ$ the maximum error increases very slowly, but upon further increase in the phase unbalance, it increases rapidly.

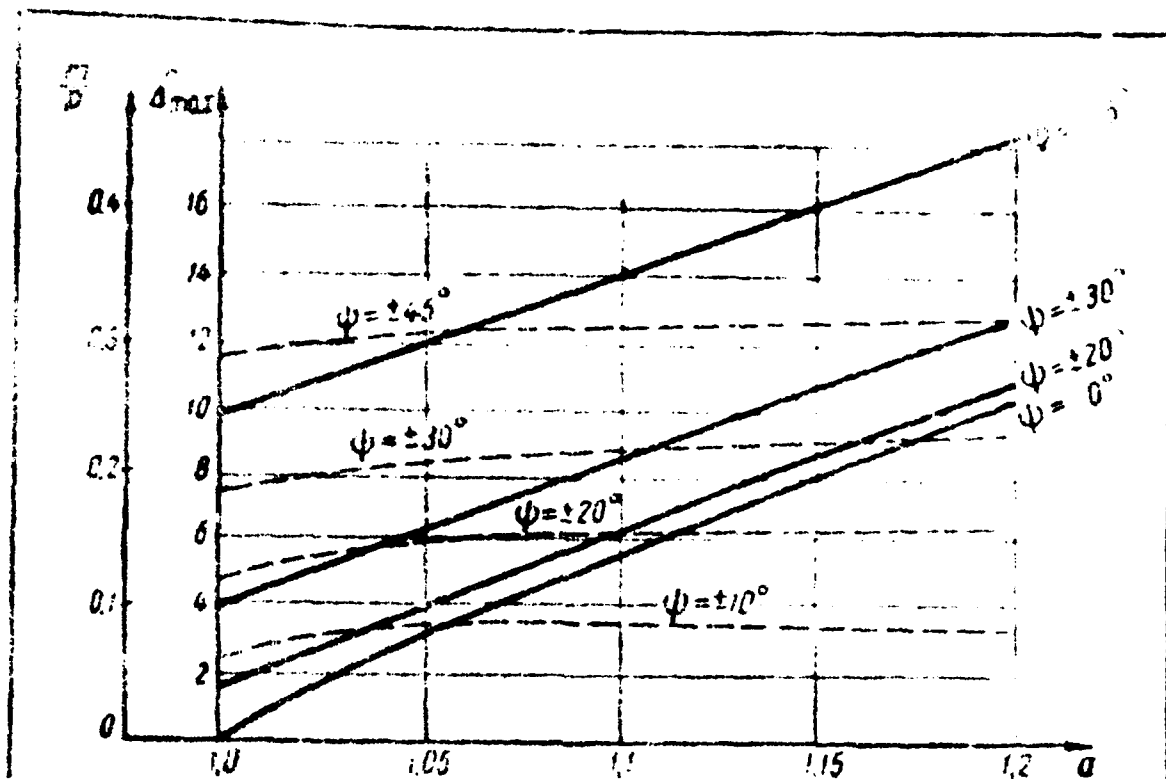


Fig. 3.5. Effect of amplitude unbalance on Δ_{\max} and m/p for different values of the phase ~~max~~ unbalance (solid lines for Δ_{\max} , dotted for m/p).

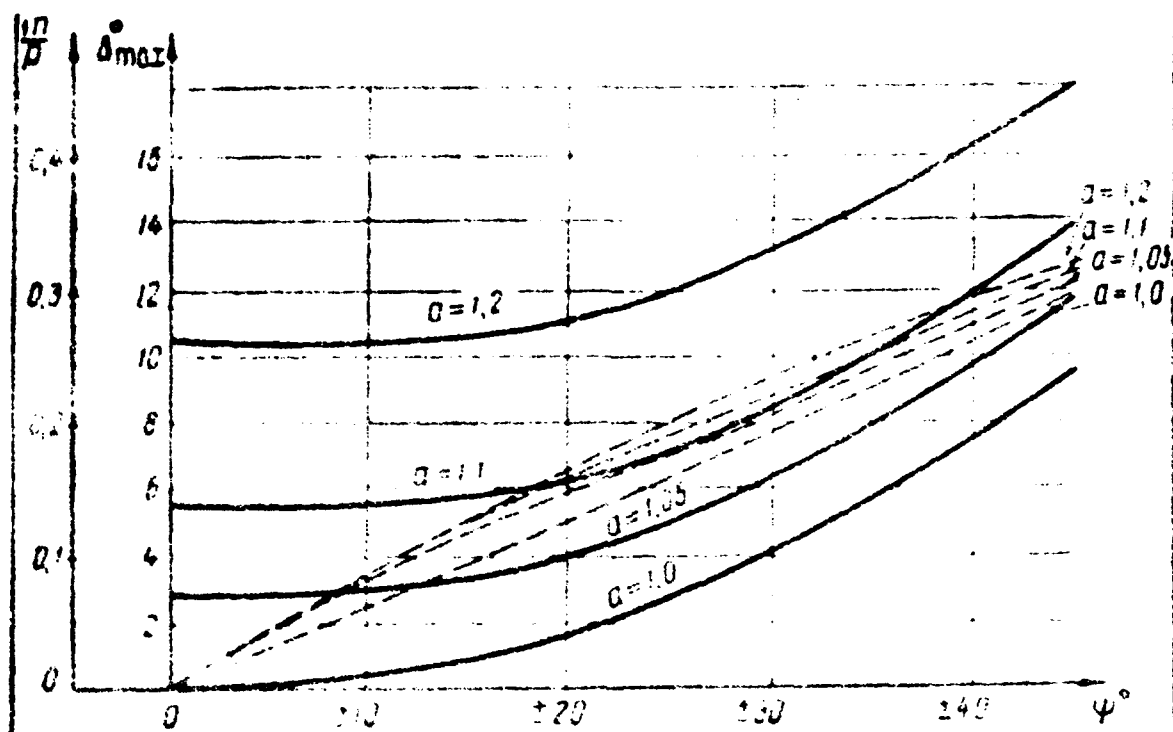


Fig. 3.6. Effect of phase unbalance on Δ_{\max} and a/p at different values of the amplitude unbalance (solid lines for Δ_{\max} , dotted for a/p).

The same figures show graphs of the ratio a/p , plotted from formula (3.21) at $\psi = \psi_{\max}$. It is seen from the graphs that the ratio a/p depends little on the parameter a .

Fig. 3.7 shows in a very convenient graph of the dependence of the absolute value of the maximum error on the parameters a and ψ . It is easy to determine from this graph the permissible unbalances of the amplification channels, such that the maximum

error does not exceed a specified limit.

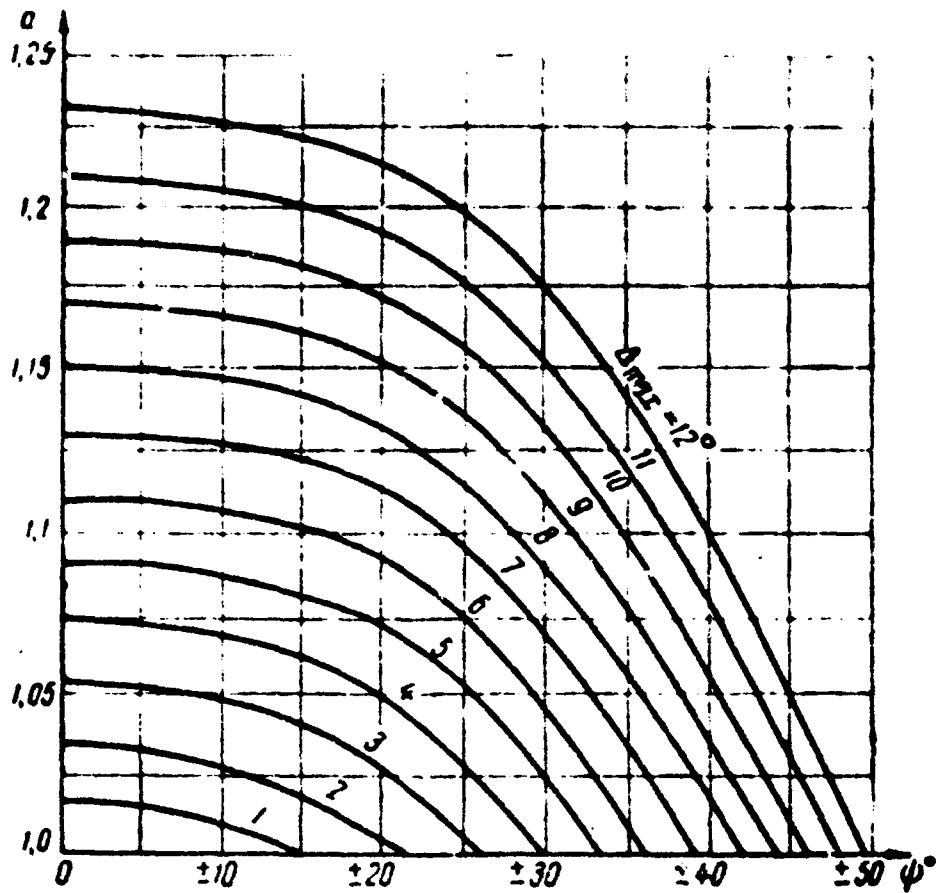


Fig. 3.7. Graph showing the dependence of the maximum error on the amplitude and phase unbalances.

3. ERRORS IN A PRE-AMPLIFICATION CIRCUIT

The voltage at the output of the amplification channels in a circuit with pre-amplification (see Fig. 3.2) are

$$e_1 = E \sin\left(\omega_0 t + \frac{\varphi}{2}\right);$$

$$e_2 = E \sin\left(\omega_0 t - \frac{\varphi}{2}\right),$$

where φ -- the phase difference, due to the difference in path,

to be measured.

The voltages at the output of the amplification channels

are

$$u_1 = K_1 E \sin \left(\omega_0 t + \frac{\pi}{2} + \Phi_1 \right);$$

$$u_2 = K_2 E \sin \left(\omega_0 t - \frac{\pi}{2} + \Phi_2 \right).$$

or, taking into account the differences in the phase shifts

$$u_1 = K_1 E \sin \omega_0 t; \quad (3.22)$$

$$u_2 = K_2 E \sin (\omega_0 t - \varphi - \phi) = K_2 E \sin (\omega_0 t - \Psi), \quad (3.23)$$

where

$$\Psi = \varphi + \phi.$$

Thus, when $K_1 \neq K_2$ and $\Psi \neq 0$, the voltages at the input of the amplification channels will have unequal amplitudes, and the phase difference changes by the value of the phase unbalance of the channels.

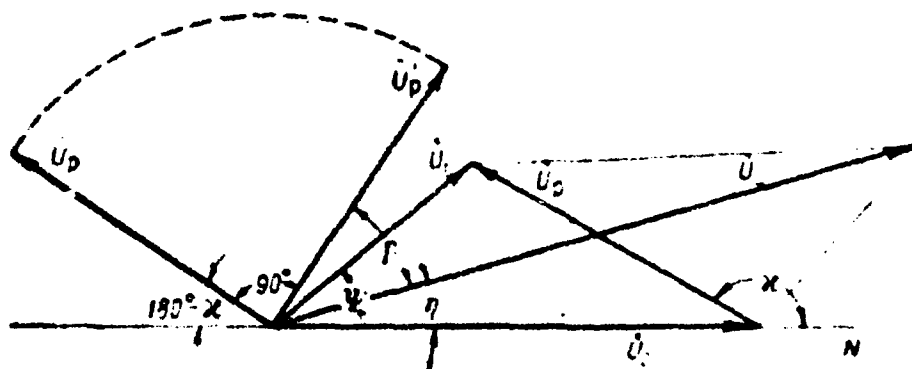


Fig. 3.8. Vector diagram for the general case.

\dot{U}_1 — voltage at the output of channel I, \dot{U}_2 — voltage at the output of channel II, \dot{U}_Σ — sum voltage, \dot{U}_Δ — difference voltage, \dot{U}'_Δ — voltage of difference with phase changed by 90° ,

η — phase difference between voltage \dot{U}_0 and \dot{U}_2 , κ — phase difference between voltages \dot{U}_0 and \dot{U}_2 .

The voltages from the output of the amplifying channels proceed next to the "sum — difference" device. *

Let us consider the general case, when the amplitudes are not equal [17]. Fig. 3.8 shows the vector diagram for the general case.

From the geometrical construction of the vector diagram we have

$$\begin{aligned} U_S^2 &= U_1^2 + U_2^2 + 2U_1U_2 \cos \Psi; \\ U_A^2 &= U_1^2 + U_2^2 - 2U_1U_2 \cos \Psi; \\ \operatorname{tg} \eta &= \frac{U_1 \sin \Psi}{U_2 + U_1 \cos \Psi}; \quad \operatorname{tg} \kappa = \frac{-U_1 \sin \Psi}{U_2 - U_1 \cos \Psi}. \end{aligned}$$

Considering that $U_1 = K_1 E$ and $U_2 = K_2 E$, we get

$$\begin{aligned} U_S &= EK_2(1 + a^2 + 2a \cos \Psi)^{1/2} = E_0 S; \\ U_A &= EK_2(1 + a^2 - 2a \cos \Psi)^{1/2} = E_0 D; \\ \operatorname{tg} \eta &= \frac{a \sin \Psi}{1 + a \cos \Psi}; \quad \operatorname{tg} \kappa = \frac{-a \sin \Psi}{1 - a \cos \Psi}. \end{aligned}$$

* The method of measuring the phase differences at equal amplitudes of output voltages is discussed in Chapter I.

where

$$S = (1 + a^2 + 2a \cos \Psi)^{1/2}; \quad (3.24)$$

$$D = (1 + a^2 - 2a \cos \Psi)^{1/2}; \quad (3.25)$$

$$E_0 = EK_s.$$

The phase difference between the voltages u'_d and u_s (from Fig. 3.8) will be

$$\gamma = \alpha - 90^\circ,$$

hence

$$\operatorname{tg} \gamma = \operatorname{tg} (\alpha - 90^\circ) = -\operatorname{ctg} \alpha = -\frac{1}{\operatorname{tg} \alpha} = \frac{1 - a \cos \Psi}{a \sin \Psi}.$$

The voltages applied to the deflecting plates of the tube are u'_d and u_s , and the phase difference between them is

$$\Gamma = \gamma - \eta,$$

hence

$$\operatorname{tg} \Gamma = \operatorname{tg} (\gamma - \eta) = \frac{\operatorname{tg} \gamma - \operatorname{tg} \eta}{1 + \operatorname{tg} \gamma \operatorname{tg} \eta} = \frac{1 - a^2}{2a \sin \Psi}.$$

The voltages on the plates of the tubes can be represented in the form

$$u'_d = E_0 D \sin \omega_0 t; \quad (3.26)$$

$$u_s = E_0 S \sin (\omega_0 t - \Gamma). \quad (3.27)$$

Accordingly we obtain for the deflection of the beam in the vertical and horizontal directions, assuming the sensitivity of the plates to be equal

$$y = D \sin \omega_0 t; \quad (3.28)$$

$$x = S \sin (\omega_0 t - \Gamma). \quad (3.29)$$

Eqs. (3.28) and (3.29) can be reduced to the equation

$$y^2 - 2 \frac{D}{S} \cos \Gamma xy + \left(\frac{D}{S} \right)^2 x^2 = D^2 \sin^2 \Gamma. \quad (3.30)$$

Thus, according to (3.30), the pattern on the screen is an ellipse, the axes of which are turned at an angle ν , with

$$\operatorname{tg} 2\nu = \frac{2 \frac{D}{S} \cos \Gamma}{1 - \left(\frac{D}{S}\right)^2}; \quad (3.31)$$

$$\cos \Gamma = \frac{1}{\sqrt{\operatorname{tg}^2 \Gamma + 1}} = \frac{2a \sin \Psi}{\sqrt{(1-a^2)^2 + 4a^2 \sin^2 \Psi}}. \quad (3.32)$$

Inserting in (3.31) the values of S , D , and $\cos \Gamma$ from (3.24), (3.25) and (3.32), we get

$$\operatorname{tg} 2\nu = \frac{2 \frac{\sqrt{1+a^2-2a \cos \Psi}}{\sqrt{1+a^2+2a \cos \Psi}}}{1 - \frac{1+a^2-2a \cos \Psi}{1+a^2+2a \cos \Psi}} \frac{2a \sin \Psi}{\sqrt{(1-a^2)^2 + 4a^2 \sin^2 \Psi}} = \operatorname{tg} \Psi,$$

hence

$$\nu = \frac{\Psi}{2}. \quad (3.33)$$

Thus, if the voltages have unequal amplitudes ahead of the "sum — difference" device, in accordance with (3.22) and (3.23), the slope of the major axis of the ellipse on the tube screen will still correspond to ^{half} ~~area~~ the phase difference of the input voltages. However, when the amplitudes are equal, the ellipse degenerates into a line, and this is much more convenient for ease in reading.

The ratio of the minor axis of the ellipse to the major one can be determined, according to (3.30), from the expression

$$\left(\frac{m}{p}\right)^2 = \frac{\frac{D^2}{S^2} + 1 - \sqrt{\left(1 - \frac{D^2}{S^2}\right)^2 + 4 \frac{D^2}{S^2} \cos^2 \Gamma}}{\frac{D^2}{S^2} + 1 + \sqrt{\left(1 - \frac{D^2}{S^2}\right)^2 + 4 \frac{D^2}{S^2} \cos^2 \Gamma}}. \quad (3.34)$$

Inserting into this expression the values of S , D and $\cos \Gamma$ from (3.24), (3.25) and (3.32), we get

$$\left(\frac{m}{p}\right)^2 = \frac{(1-a)^2}{(1+a)^2},$$

or finally

$$\frac{m}{p} = \frac{1-a}{1+a}, \quad (3.35)$$

where a is the ratio of the voltage amplitudes ahead of the "sum -- difference" device. The ratio a in the circuit shown in Fig. 3.2 is equal to the ratio of the moduli of the gains, since it was assumed that the amplitudes are the same at the input of the amplifying channels.

Consequently, the inequality of the moduli of the gains, i.e., the presence of an amplitude unbalance, causes the image to become elliptical, but does not change the direction of the major axis of the ellipse, i.e., it does not produce a systematic apparatus error. On the other hand, the phase unbalance of the channels enters in its entirety into the error.

Thus, the error

$$\Delta = 2\psi - \varphi = \Psi - \varphi = \psi \quad (3.36)$$

is independent of the magnitude of the measured phase difference.

This analysis enables us to compare the circuits shown

in Figs. 3.1 and 3.2 as regards apparatus errors. Obviously, the circuit which permits greater differences in the amplifying channels for the same values of the error is preferred.

A circuit with pre-amplification admits of a large amplitude unbalance, but allows no phase unbalance. If it is technically easier to make the channels identical in gain but not in phase shift it is best to use a circuit with post-amplification. Nevertheless, a circuit with pre-amplification is used successfully, because the apparatus errors that it introduces can be readily calculated, since it is equal to the phase unbalance of the channels and is independent of the value of the measured phase difference. This circumstance makes this circuit in many cases preferable.

If no provision is made for the control and regulation of the identity of the channels, considerable apparatus errors in the measurement of the phase difference may enter into a circuit with pre-amplification, since it is difficult to ensure identity of phase shifts in channels, even within 10%, over a prolonged time interval.

In the circuits considered here, the non-identity of the amplifying channels, in addition to apparatus errors, may cause errors in observation, i.e., errors that arise when bearing is measured from the pattern on a cathode ray tube screen.

4. OBSERVATION ERRORS

In these circuits, the pattern on the screen of the tube is in general an ellipse, and the direction of its major axis determines the reading. The ratio of the minor axis of the ellipse to the major one, m/p , characterizes the possibility of reading. It is most convenient to make the readings when the ellipse degenerates into a line. As m/p increases, it becomes less convenient to make the readings, and when $m/p = 1$, i.e., when the ellipse becomes a circle, a reading is impossible.

Readings made by different operators with the same ellipse will be different. The reading errors in the direction of the major axis of the ellipse are of random character. It can be assumed that the law of distribution of the observation errors will be normal. To each value of the ratio m/p there will correspond a definite value of the mean squared error in reading, σ .

To obtain the dependence of σ on m/p , experiments were performed, in which several operators took readings based on the major axis of the ellipse with different values of m/p , and the major axes of the ellipse on each pattern was equal to the scale diameter, the thickness of the line of the ellipse equaled one scale division (the arc of 1°) and the time of reading was not less than three seconds. For each ellipse pattern with a corresponding ratio of axes, from 10 to 30 readings were

made and subsequently processed.

The results of the experiment confirmed the normal law of distribution of the observation errors. The dependence of σ^2 on m/p , obtained in the experiments, is shown in Fig. 3.9. The accuracy of reading, from the line, will depend to a great degree already on the thickness of the line of the pattern and on a certain parallax. Therefore in the experiments the mean squared error for $m/p = 0$ does not vanish (see Fig. 3.9). Obviously the quality of the scale and the thickness of the line determine the maximum reading accuracy.

Thus, if the amplifying channels are not identical, an error arises which consists of an apparatus error and of a random observation error. The accuracy of direction finding can in this case be estimated by the quantity

$$\Delta_I = \sqrt{\Delta^2 + \sigma^2}, \quad (3.37)$$

where Δ -- apparatus error;

σ^2 -- mean squared observation error.

The square of the quantity defined by expression (3.37), in accordance with the probability theory, is the second moment of the distribution/9/. We shall call the ~~sum~~ error Δ_{Σ} , for brevity, the general error.

In those cases when the apparatus error has a maximum, the magnitude of the total error is

$$\Delta_{I \max} = \sqrt{\Delta_{\max}^2 + \sigma^2}. \quad (3.38)$$

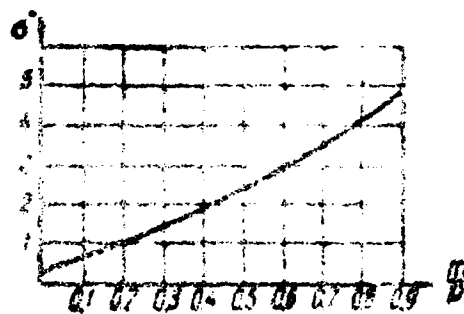


Fig. 3.9. Dependence of the mean squared observation error on the ellipticity of the pattern.

Fig. 3.10 shows curves of the errors due to non-identical channels in a circuit with post-amplification, based on Fig. 3.5 with allowance for Eq. (3.38). In calculations based on (3.38), the values of the mean squared observation error were taken from the graph shown in Fig. 3.9.

It follows from Fig. 3.10 that in a circuit with post-amplification the observation errors are not significant, since the apparatus errors predominate. The predominant role of the apparatus error is retained as the non-identity of the channels is increased. The difference between the total error and the apparatus error is seen on the graph (see Fig. 3.10) to be insignificant.

In pre-amplification circuits, the amplitude unbalance does not produce an apparatus error, but increases the observation error. However, even a 44% difference in amplitude gives a mean squared error on the order of merely 10^{-2} . It is also

known from practice that it is not too difficult to obtain channels with amplitude that is equal within 20%, and therefore we shall not consider the observation errors specially from now on.

Nevertheless, it must be borne in mind that when the apparatus error is small, the observation error influences substantially the accuracy. The observation error naturally can be reduced by using the average readings obtained by several operators, but this is not always possible, for it increases the time required to perform the readings.

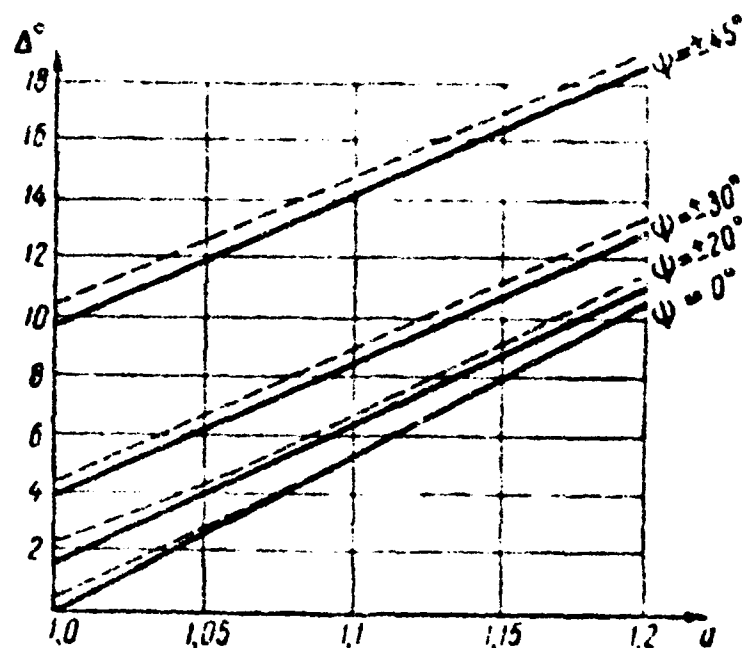


Fig. 3.10. Dependence of the errors due to the non-identity of amplifying channels (solid curve for Δ_{\max} , dashed curve for Δ_{\min}).

Chapter IV

EFFECT OF UNEQUAL CHANNEL PARAMETERS ON THE APPARATUS ERRORS OF TWO CHANNEL RADIO DIRECTION FINDERS

1. PARAMETERS OF NON-IDENTICITY

In the preceding chapter the non-identity of amplifying channels was characterized by the ratio of the moduli of the gains, a , and by the difference of the phase shifts, ψ' , of the channels at the signal frequency, without regards to what the amplifying channels comprised.

Since the amplifying channels in two-channel radio direction finders must insure the necessary selectivity, the actual channels have suitable amplitude-frequency characteristics.

Fig. 4.1 shows the characteristics of channels for the general case.

It is seen that the channels may differ in their bandwidth, in their resonant frequencies, and in their detuning relative to the signal frequency.

It is of interest to examine the errors, if the channels are detuned relative from each other and the bandwidths of the channels are not the same, while the frequency of the received

signal differs from the resonant frequencies of the channels.

The error may be specified in terms of quantities that characterize the non-identity of the channels, for example, the detuning of the channels relative to each other, $\Delta\omega$, and the ratio of the bandwidths $\frac{2\Delta\Omega_2'}{2\Delta\Omega_1'}$, and also the quantity $\Delta\omega_1$ (or $\Delta\omega_2$), in which characterizes the tuning of the receiving apparatus by the operator to the signal frequency.

Let us introduce the dimensionless relative detunings

$$\frac{\Delta\omega_1}{\Delta\Omega_1'}; \frac{\Delta\omega_2}{\Delta\Omega_2'}; \frac{\Delta\omega}{\Delta\Omega'}$$

where the arithmetic mean of the bandwidth is

$$2\Delta\Omega_{av}' = \Delta\Omega_1' + \Delta\Omega_2'. \quad (4.1)$$

and

$$\frac{\Delta\omega_1}{\Delta\Omega_{av}'} = \frac{\Delta\omega_2}{\Delta\Omega_{av}'} + \frac{\Delta\omega}{\Delta\Omega_{av}'} \quad (4.2)$$

The non-identity parameters of the amplifying channels will be taken to be the ratio of the bandwidths

$$\xi = \frac{\Delta\Omega_2'}{\Delta\Omega_1'} \quad (4.3)$$

and the relative detuning between channels

$$\frac{\Delta\omega}{\Delta\Omega_{av}'}$$

It is obvious that if the channels are completely unidentical

$$\xi = 1.0 \text{ and } \frac{\Delta\omega}{\Delta\Omega_{av}'} = 0.$$

Thus, in the analysis of the systematic error the independent variables will be

$$\xi, \frac{\Delta\omega}{\Delta\Omega_{av}'} \text{ and } \frac{\Delta\omega_1}{\Delta\Omega_{av}'}$$

It is probable that the error will also depend on the type of the

stages used in the amplifying channels (for example, tuned or broadband) and particularly, on the number of stages in each channel.

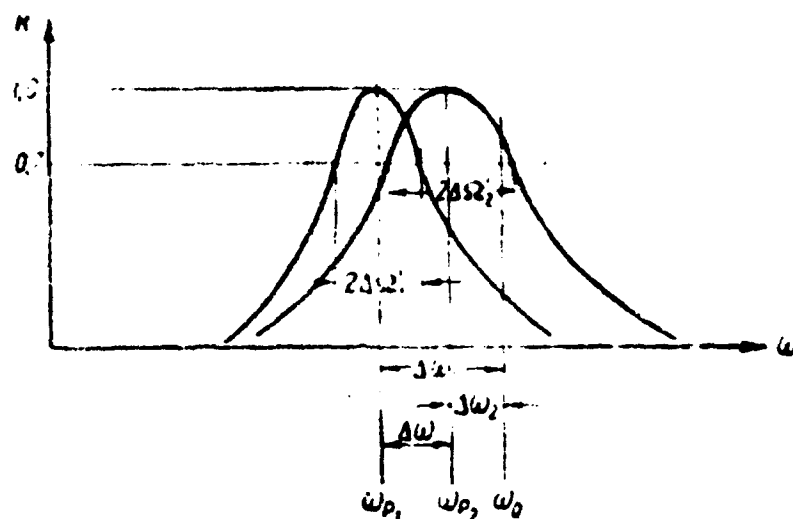


Fig. 4.1. Amplitude-frequency characteristics of amplifying channels in the general case of non-identity.

ω_{p1} -- tuning frequency (resonant frequency) of channel I, ω_{p2} -- tuning frequency of channel II, ω_0 signal frequency, $\Delta\omega_1$ -- detuning of channel I relative to the signal, $\Delta\omega_2$ -- detuning of channel II relative to the signal, $\Delta\omega$ -- detuning of the channels relative to each other, $2\Delta\omega_1'$ -- bandwidth of channel I, $2\Delta\omega_2'$ -- bandwidth of channel II.

We confine ourselves now to an analysis of channels that are resonant amplifiers. The circuit of one stage of a resonant amplifier is shown in Fig. 4.2.

As is known, the gain of a multi-stage resonant amplifier is

$$K = \left(\frac{K_r}{1 + ja} \right)^n, \quad (4.4)$$

wherein n -- number of the stages in the amplifier,

K_r -- gain of one stage in resonance.

a -- generalized detuning.

The generalized detuning is

$$a = \frac{2\Delta\omega}{\omega_r} = \frac{2\Delta\omega}{\omega_r} Q = \frac{\Delta\omega}{\Delta\Omega}, \quad (4.5)$$

where $\Delta\omega$ -- detuning ($\omega = \omega_r + \Delta\omega$);

Q -- the figure of merit of the tuned circuit,

ξ -- the damping factor of the tuned circuit;

ω_d -- resonant frequency of the tuned circuit ($\omega_d = 1/\sqrt{LC}$).

$2\Delta\Omega$ -- bandwidth of the tuned circuit ($2\Delta\Omega = \omega_d/Q$).

It can be considered that

$$K_r = SR_r,$$

where S -- static transconductance of the tube.

$R_r = L/Cr$ -- resonant resistance of the tuned circuit.

The amplitude-frequency and phase-frequency characteristics, according to formula (4.4), will have the form

$$K = \frac{1}{(1 + a^2)^{\frac{n}{2}}}; \quad (4.6)$$

$$\Phi = -n \arctg a. \quad (4.7)$$

In formula (4.6) the gain at resonance is taken to equal unity.

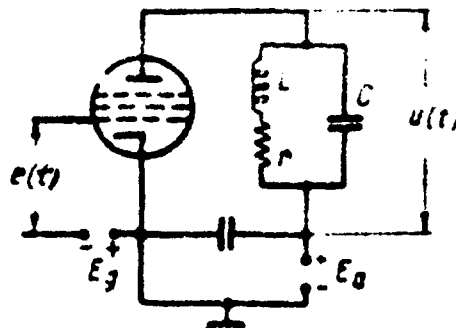


Fig. 4.2. Diagram of one stage of a tuned amplifier.

The bandwidth of the amplifier is

$$2\Delta\Omega' = 2\Delta\Omega\alpha_A,$$

where $2\Delta\Omega$ -- bandwidth of one stage of the amplifier

α_A -- a quantity which is a function of the number of stages.

The quantity α_A equals

$$\alpha_A = \left[\left(\sqrt{2} \right)^{\frac{2}{n}} - 1 \right]^{\frac{1}{2}} = \left(2^{\frac{1}{n}} - 1 \right)^{\frac{1}{2}}. \quad (4.8)$$

With increasing number of stages in the amplifier, its bandwidth will decrease. For a specified bandwidth, the damping of the tuned circuit should be greater, the greater the number of stages

$$\delta = \frac{2\Delta\Omega}{\omega_r} \frac{1}{\left(2^{\frac{1}{n}} - 1 \right)^{\frac{1}{2}}}.$$

The modulus of the gain will be represented in the form

$$K = \frac{1}{\left| 1 + \left(\frac{\Delta \omega}{\Delta \Omega'} x_1 \right)^2 \right|^{\frac{n}{2}}}. \quad (4.9)$$

The phase angle of the gain will be represented in the form

$$\Phi = -n \arctg \left(\frac{\Delta \omega}{\Delta \Omega'} x_1 \right). \quad (4.10)$$

Taking into consideration the foregoing parameters of channel non-identity, we obtain for each channel

$$K_1 = \frac{1}{\left| 1 + \left(\frac{\Delta \omega_1}{\Delta \Omega'_{av}} \frac{1+\xi}{2} x_1 \right)^2 \right|^{\frac{n}{2}}}; \quad (4.11)$$

$$\Phi_1 = -n \arctg \left(\frac{\Delta \omega_1}{\Delta \Omega'_{av}} \frac{1+\xi}{2} x_1 \right); \quad (4.12)$$

$$K_2 = \frac{1}{\left\{ 1 + \left[\left(\frac{\Delta \omega_1}{\Delta \Omega'_{av}} - \frac{\Delta \omega}{\Delta \Omega'_{av}} \right) \frac{1+\xi}{2\xi} x_1 \right]^2 \right\}^{\frac{n}{2}}}; \quad (4.13)$$

$$\Phi_2 = -n \arctg \left[\left(\frac{\Delta \omega_1}{\Delta \Omega'_{av}} - \frac{\Delta \omega}{\Delta \Omega'_{av}} \right) \frac{1+\xi}{2\xi} x_1 \right]. \quad (4.14)$$

Let us establish the connection between the parameters of non-identity, used in the preceding chapter, with the new parameters. For this purpose we substitute in Eqs. (3.1) and (3.2) the expressions for the amplitude-frequency and phase-frequency characteristics of the amplifying channels, in accordance with formulas (4.11), (4.12), (4.13), and (4.14).

We then have

$$a = \left\{ \frac{1 + \left[\left(\frac{\Delta\omega_1}{\Delta\Omega'_{av}} - \frac{\Delta\omega}{\Delta\Omega'_{av}} \right) \frac{1+\xi}{2\xi} a_d \right]^2}{1 + \left(\frac{\Delta\omega_1}{\Delta\Omega'_{av}} - \frac{1+\xi}{2} a_d \right)^2} \right\}^{\frac{n}{2}}. \quad (4.15)$$

$$\psi = n \left\{ \arctg \left[\left(\frac{\Delta\omega_1}{\Delta\Omega'_{av}} - \frac{\Delta\omega}{\Delta\Omega'_{av}} \right) \frac{1+\xi}{2\xi} a_d \right] - \arctg \left(\frac{\Delta\omega_1}{\Delta\Omega'_{av}} - \frac{1+\xi}{2} a_d \right) \right\}. \quad (4.16)$$

In the expressions for the amplitude-frequency characteristics, according to formulas (4.11) and (4.13) obtained from (4.4), the resonance coefficients of the channel gains were assumed to be identical and equal to unity.

However, when the capacitance of the resonant circuit is constant, its resonant resistance will change with the bandwidth, and consequently, the gain K_r will also change, if the transconductance of the tube is constant.

For example

$$K_r = SR_p = S \frac{L}{Cr} = \frac{S}{C2\Delta\Omega},$$

i.e., K_r is inversely proportional to the bandwidth. Then, taking this into account, we get

$$a' = \xi^n \left\{ \frac{1 + \left[\left(\frac{\Delta\omega_1}{\Delta\Omega'_{av}} - \frac{\Delta\omega}{\Delta\Omega'_{av}} \right) \frac{1+\xi}{2\xi} a_d \right]^2}{1 + \left(\frac{\Delta\omega_1}{\Delta\Omega'_{av}} - \frac{1+\xi}{2} a_d \right)^2} \right\}^{\frac{n}{2}}, \quad (4.17)$$

i.e.,

$$a' = at^n. \quad (4.18)$$

It should be noted that in the initial expression (4.4), the generalized detuning was determined by formula (4.5), according to which the amplitude-frequency and the phase-frequency characteristics will be symmetrical, this is a certain idealization of the real characteristics. Such an assumption is quite justified for narrow band amplifiers ($Q \gg 1$).

2. BANDWIDTH OF A TWO-CHANNEL RADIO DIRECTION FINDER

It is obvious that when the amplifying channels are completely identical, the bandwidth of the receiving and indicating unit of the direction finder will equal the bandwidth of any of its channels. When the frequency of the signal coincides with the resonant frequency of the channels, the length of the line on the tube screen will be a maximum. On the boundaries of the bandwidth, the lengths of the line will amount to 0.707 of the maximum length.

For radio directionfinders based on post-amplification and pre-amplification (see Figs. 3.1 and 3.2), the pattern on the screen will in general be an ellipse. Starting with this, one can take as the bandwidth of the direction finder that interval of tuning frequencies, on the boundaries of which the length of the major axis of the ellipse amounts to 0.707 of the maximum length.

Usually the operator does not take any readings outside the bandwidth, since the size of the pattern is considerably

decreased then. Therefore greatest interest attaches to the value of the error within the bandwidth of the direction finder.

To determine the bandwidth it is necessary to find the dependence of the length of the pattern on the screen of the tube on tuning frequency. For a circuit with post-amplification (see Fig. 3.2) one obtains

$$p = K_1 + K_2 = \frac{1}{\left\{1 + \left(\frac{\Delta\omega_1}{\Delta\Omega_{av}} \frac{1+\xi}{2} \cdot \frac{1}{\omega_1}\right)^2\right\}^{\frac{n}{2}}} + \frac{1}{\left\{1 + \left[\left(\frac{\Delta\omega_1}{\Delta\Omega_{av}} - \frac{\Delta\omega}{\Delta\Omega_{av}}\right) \frac{1+\xi}{2\xi} \cdot \frac{1}{\omega_1}\right]^2\right\}^{\frac{n}{2}}}. \quad (4.19)$$

It follows therefore that in this circuit the size of the major semi-axis of the ellipse is independent of the measured phase difference φ .

In general, the determination of the exact values of $\Delta\omega_1/\Delta\Omega_{av}$, corresponding to the boundaries of the passband, ~~is~~ entails serious mathematical difficulties.

The center of the passband can be determined with good approximation from the expression

$$\left(\frac{\Delta\omega_1}{\Delta\Omega_{av}}\right)_{center} = \frac{\Delta\omega}{\Delta\Omega_{av}} \frac{1}{1+\xi}. \quad (4.20)$$

The values of $\Delta\omega_1/\Delta\Omega_{av}$, corresponding to the boundaries of the passband, can be obtained with sufficient

approximation by adding ± 1 to the abscissa of the center.

$$\left(\frac{\Delta \omega_1}{\Delta \Omega'_{av}} \right)_{\text{boundary}} = \frac{\Delta \omega}{\Delta \Omega'_{av}} \cdot \frac{1}{1 + \xi} \pm 1. \quad (4.21)$$

For a circuit with post-amplification (see Fig. 3.1)

the length of the major semi-axis of the ellipse depends on φ and more weakly on φ' . Assuming $\varphi = 90^\circ$ and neglecting the influence of φ' , we get

$$p = \sqrt{\frac{K_1^2 + K_2^2}{2}} = \sqrt{\frac{1}{2 \left\{ 1 + \left(\frac{\Delta \omega_1}{\Delta \Omega'_{av}} \frac{1 + \xi}{2} \right)^2 \right\}^{\frac{n}{2}}} + \frac{1}{2 \left\{ 1 + \left[\left(\frac{\Delta \omega_1}{\Delta \Omega'_{av}} - \frac{\Delta \omega}{\Delta \Omega'_{av}} \right) \frac{1 + \xi}{2\xi} \right]^2 \right\}^{\frac{n}{2}}}}}. \quad (4.22)$$

An analysis of (4.22) gives results which are close to the case described by (4.19).

Thus, in practice, the bandwidth is the same for a circuit with pre-amplification and post-amplification.

3. ERRORS DUE TO NON-IDENTICITY OF TUNED AMPLIFIER CHANNELS

Let us consider now the apparatus errors due to the following independent variables: ξ ; $\Delta \omega / \Delta \Omega'_{av}$; $\Delta \omega_1 / \Delta \Omega'_{av}$, and n , of which the first two characterize the non-identity of the channels.

For circuits with free amplification, the system error,

according to (3.36), equals the phase unbalance of the channels. Therefore expression (4.16) is an analytic dependence of the error on these parameters.

An analysis of the errors in the circuit with pre-amplification ~~amplification~~ is given in a published article by the author, and we shall here therefore only on an analysis of the errors in a circuit with post-amplification. In this circuit the apparatus error depends also on the value of the measured phase difference φ , and we shall therefore consider the maximum error determined by the graph in Fig. 2.7.

As noted in the preceding chapter, the expression for the maximum error, as a function of the parameters a and ψ , can be obtained by substituting into (3.13) the value φ_{\max} from formula (3.14). If we then insert in the resultant expression the new parameters, in accordance with formulas (4.15) and (4.16), one should obtain analytic expressions for the maximum error

$$\Delta_{\max} = \Delta_{\max} \left(\xi, \frac{\Delta \omega}{\Delta \Omega_{ev}}, \frac{\Delta \omega_i}{\Delta \Omega_{ev}}, n \right), \quad (4.23)$$

which determines the functional dependence of the maximum apparatus error on the new non-identity parameters. It is impossible to write out (4.23) in a more developed form, since ^{both} the intermediate and the initial operations yield complicated transcendental expressions.

Since the maximum error is a function of several parameters, it is necessary to specify fixed values of the remaining parameters in order to exhibit the dependence of this function on any of the parameters.

Fig. 4.3a shows graphically the variation of the maximum error from the tuning of the direction finder by an operator, for a single-stage ($n=1$) amplifying channel, when the channels have identical bandwidths, but when the channels are not tuned to the same frequency.

Fig. 4.3b shows the variation of the error, when the detuning between channels is absent, i.e., when $\Delta\omega/\Omega'_{av} = 0$, but the channels have different bandwidths.

Figs. 4.3c and 4.3d show the variations of the maximum error for the most general case of non-identity of the channels, when

$$\Delta\omega/\Omega'_{av} \neq 0 \text{ and } \xi \neq 1.0.$$

As can be seen from Fig. (4.3), the curves have a discontinuity at the point when the parameter a , determined by formula (4.15), assumes values equal to unity. Corresponding to these points are two equal values of the error, but of opposite signs.

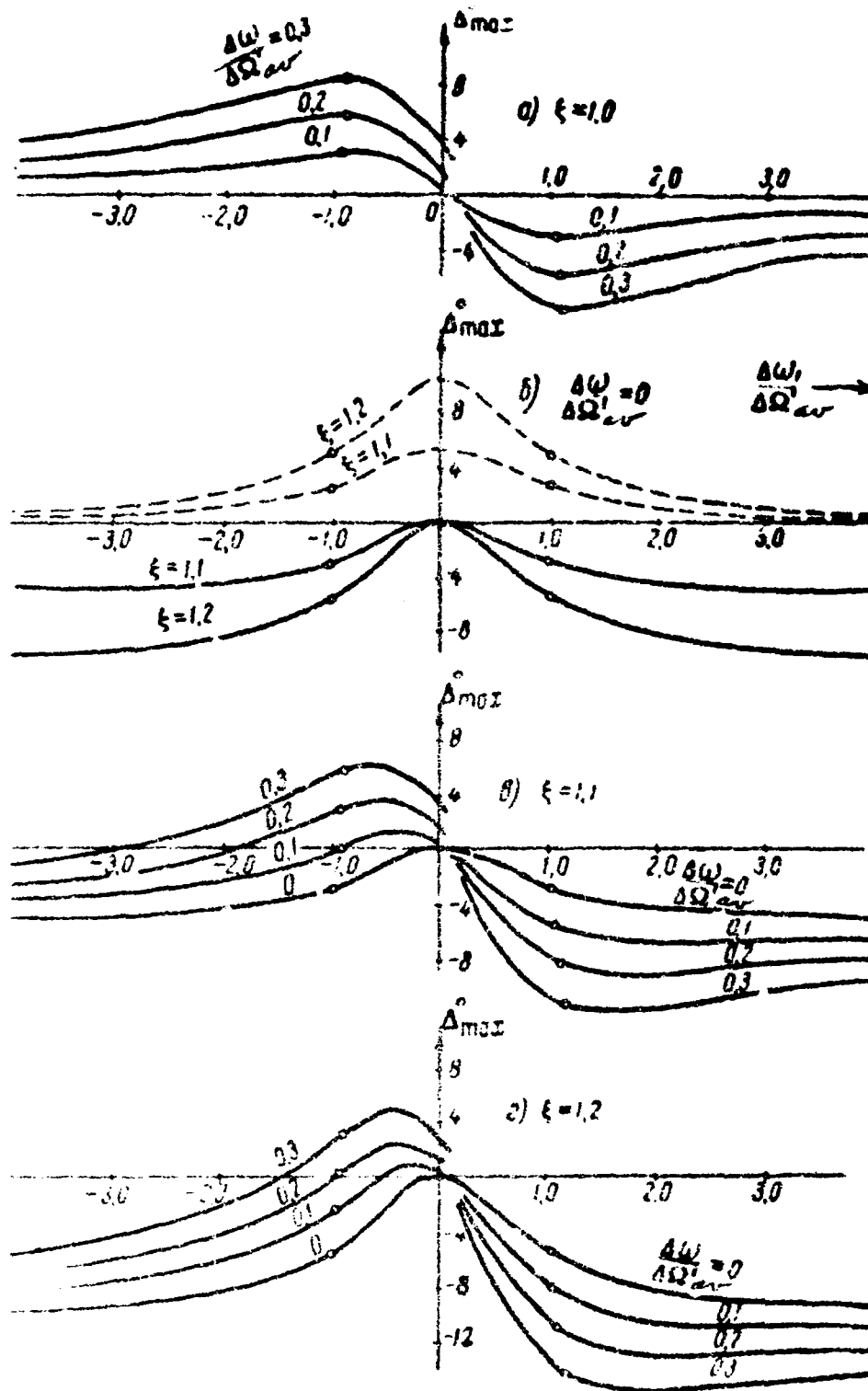


Fig. 4.3. Dependence of the maximum error on the tuning of the direction finder by the operator, at different values of the non-identity parameters of single-stage channels.

The dashed curve shown in Fig. 4.3 corresponds to the case when parameter a is determined by formula (4.17), i.e., with allowance for the correction for the variation of the resonant gain of the channels.

The curves of Fig. 4.3 show that the maximum apparatus error changes with variation of the tuning of the radio direction finder by the operator, and that at certain values of the tuning it reaches a maximum value. The curves contain the points corresponding to the boundaries of the bandwidth of the direction finder, according to formula (4.21). It can be seen that in certain cases the greatest value of the maximum error falls within the bandwidth of the direction finder, and in others the greatest value of the error is outside the limits of the bandwidth.

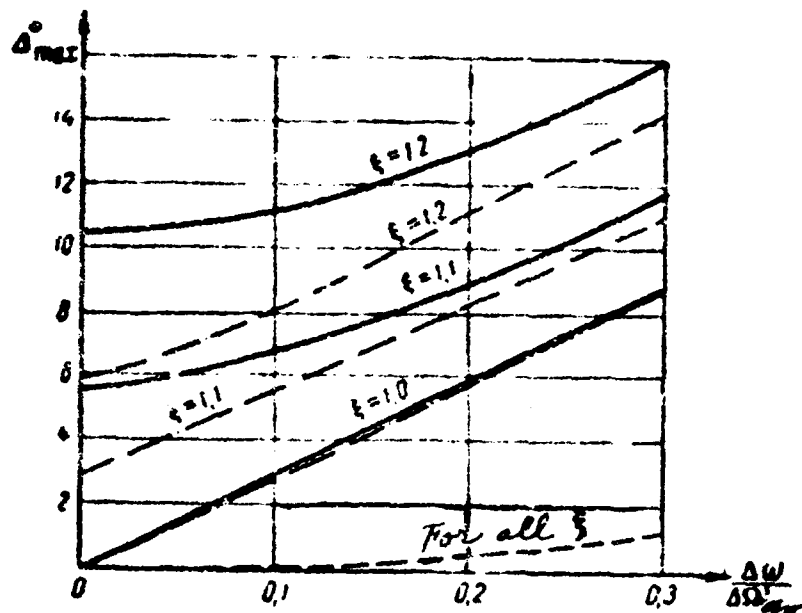


Fig. 4.4. Effect of detuning between single-stage

channels on the maximum error at different channel bandwidths (continuous line for Δ_{\max_m} , dash-dot for Δ_{\max}^* , dash-dash for Δ_{\max_c}).

Therefore, for a circuit with post-amplification, it is advantageous to introduce the following notation:

Δ_{\max_m} — maximum value of the maximum error;

Δ_{\max}^* — the maximum value of the maximum error within the bandwidth of the direction finder;

Δ_{\max_c} — value of the maximum error at the center of the passband of the direction finder.

Fig. 4.4 shows the dependence of the maximum error on the detuning between single-stage amplifying channels at three values of the ratio of channel bandwidths, ξ . When $\xi = 1.0$, the following equality holds

$$\Delta_{\max}^* = \Delta_{\max_m}.$$

As can be seen from the curve, the error has a maximum value at the center of the passband, and this value increases little with increasing detuning between channels and is independent of the difference between bandwidths.

Let us note that the numerical values for the Fig. 4.4 were taken from the corresponding points of the solid curves in Fig. 4.3.

Fig. 4.5 shows the dependence of the maximum error on

the detuning between single-stage channels for unequalized gains. Unlike Fig. 4.4, the parameter a is determined by formula (4.17). According to this formula, the inequality of the bandwidths causes the resonant gains of the channels to be unequal.

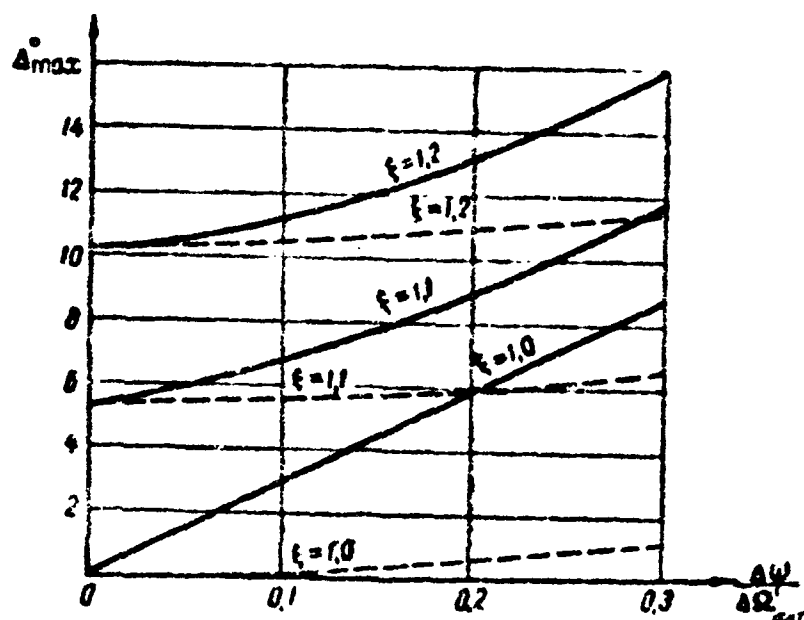


Fig. 4.5. Dependence of the maximum error on the detuning between single-channel stage channels for unequalized (owing to the inequality of the bandwidths) resonant gains of the channels (the continuous lines for Δ_{\max}^* and Δ_{\max_m} , since $\Delta_{\max}^* = \Delta_{\max_m}$, dash line -- for Δ_{\max_c}).

Thus, the curves of Fig. 4.5 correspond to unequal channel gains due to inequality of the bandwidths, while those of Fig. 4.4 correspond to those equalized, for example, by adjusting

the transconductance of the tubes or the gains.

It is seen from the curves of Fig. 4.5 that Δ_{\max_c} is less than the errors Δ_{\max_m} and Δ^*_{\max} . This difference increases with increasing detuning between channels, $\Delta\omega / \Delta\Omega'_{av}$, since Δ_{\max_c} increases more slowly than Δ_{\max_m} and Δ^*_{\max} .

Upon equalization of the gains of the channels, the curves of the errors Δ_{\max_c} for $\xi = 1.2$ and 1.1. will coincide with the line for $\xi = 1.0$. One can therefore conclude that it is necessary to equalize the gains of the channels, for in this case the error is considerably reduced.

If the equality $K_{r1} = K_{r2}$ is reached, the operator should tune the radio direction finder in such a way, that the frequency of the transmitter falls exactly at the center of the passband. In the case of inaccurate tuning, the error may reach a value Δ^*_{\max} which is considerably greater than Δ_{\max_c} .

A control over the exact tuning may be the size of the pattern on the screen of the tube. A maximum length of the major axis of the ellipse is obtained when the signal frequency is at the center of the passband of the direction finder.

In the case of two-stage ($n = 2$) tuned amplifier channels, the dependence of the maximum error on the tuning of the direction finder by the operator, at different values of the non-identity parameters, is shown in Fig. 4.6. The curve is drawn for the same values of the non-identity parameters, as were used in the case

of the single-stage channels (see Fig. 4.3), and the pass bands of the two-stage channels are assumed to be equal respectively to the passbands of the single-stage channels. As can be seen, the overall character of the dependences is analogous to the case of $n = 1$.

Thus, one can expect that for a larger number of stages in the channels the conclusions will (qualitatively) also remain valid.

For a quantitative estimate of the influence of n on the maximum systematic errors let us dwell on two cases: a) when the bandwidths of the channels are equal, and b) when there is no detuning between channels.

Fig. 4.7 shows the dependence of the maximum errors Δ_{\max_m} and Δ_{\max}^* on the number of stages for $\xi = 1.0$. It is seen from the figure that $\Delta_{\max}^* < \Delta_{\max_m}$ for all $n > 1$. This means that the greatest value of the maximum error does not fall in the passband of the radio direction finder. As n is increased the greatest value of the maximum error shifts towards the larger absolute values of detuning $|\Delta\omega / \Delta\omega_{av}'|$. The same can be seen from the graph for n equals 2 (see Fig. 4.6a), if the boundaries of the pass band are marked on the curves.

Fig. 4.8 shows, for the same conditions, a graph of the dependence of the values of the maximum error at the center of the passband, Δ_{\max_0} , on the number of stages m . This graph is

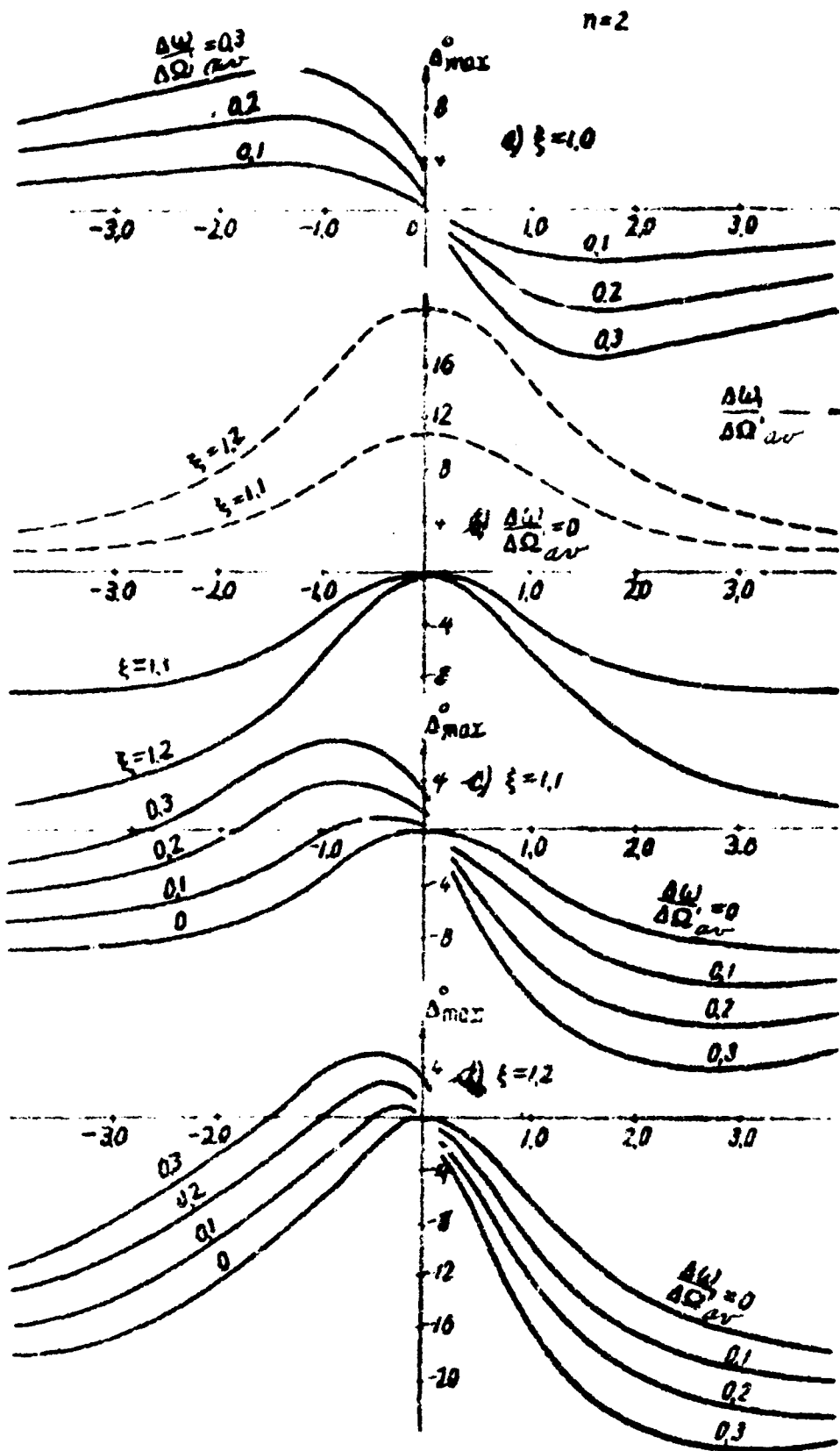


Fig. 4.6

Fig. 4.6. Dependence of the maximum error on the tuning of the radio direction finder by the operator, at different values of the non-identity parameters of two-stage channels.

shown with a larger scale for the ordinate axis.

We note that the graph of Fig. 4.8 is correct for all values of the parameter ξ , since it is assumed that the resonant gains of the channels are equalized, for example, by adjusting the operating conditions of the tubes.

Fig. 4.9 shows the dependence of the errors on the number of stages m , in the absence of detuning between the channels ($\Delta\omega/\Delta\Omega'_{av} = 0$). It is seen from the curves that the greatest maximum error, Δ_{\max_m} , increases relatively rapidly with increasing number of stages, and the greatest error in the passband, Δ^*_{\max} , increases slightly, and is substantially less, since the maximum value of the error does not enter into the passband of the radio direction finder.

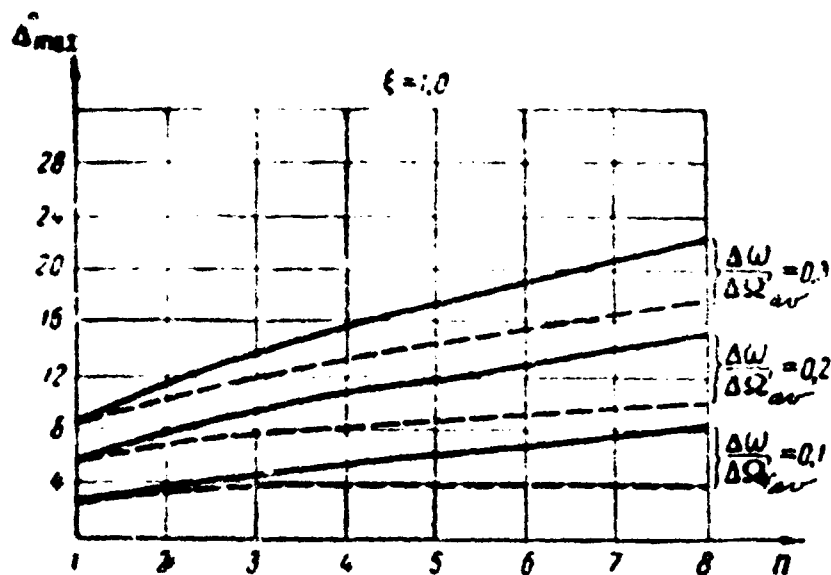


Fig. 4.7. Dependence of the maximum errors on the number of stages for identical bandwidths, but different detunings between channels (continuous lines for Δ_{max_m} , ^{dashed} -- for Δ^*_{max}).

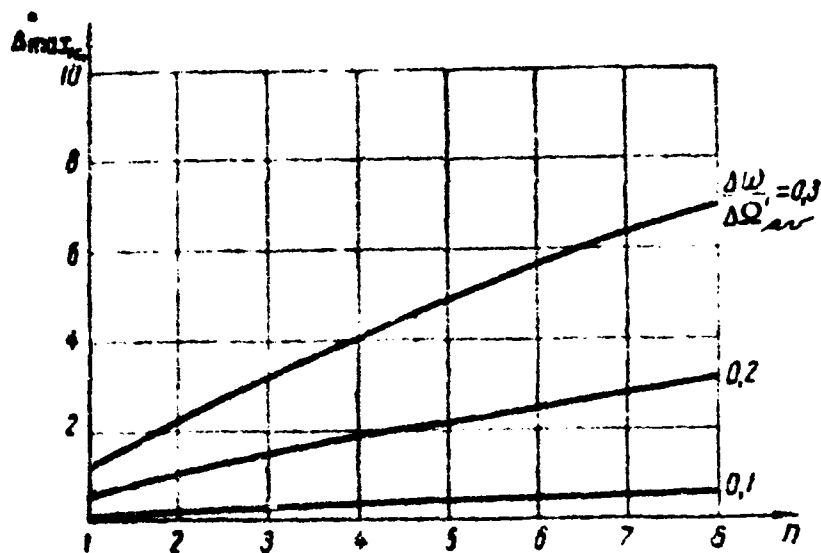


Fig. 4.8. Effect of the number of stages on the maximum error in the center of the passband for different detunings between channels.

In the absence of detuning between channels, the value of the maximum error at the center of the passband is 0, regardless

of the number of stages in each channel.

When the resonant gains of the channels are not equalized, the maximum error reaches its maximum value at $\Delta\omega_0 = \frac{\Delta\omega}{2}$, i.e., within the passband, more accurately, at the center of the band. The absolute values will remain unchanged both when the resonant gains are equal and when they are different. Thus, the solid lines of Fig. 4.9 show also the dependence of the error in the case of equalized resonant gains.

With this, the values of all three types of errors coincide.

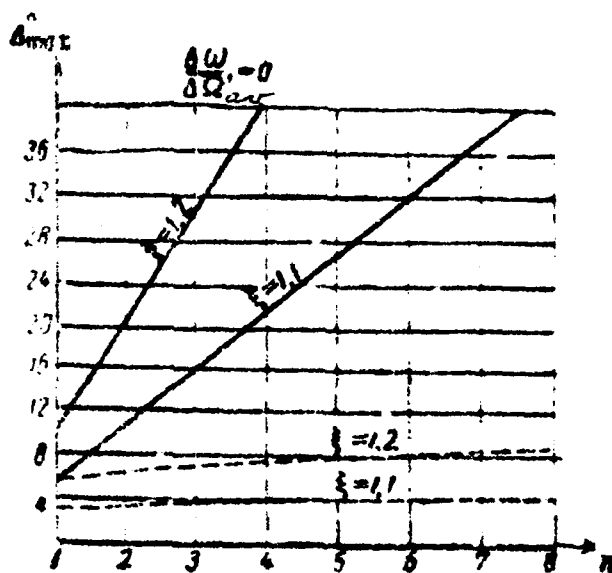


Fig. 4.9. Dependence of the maximum error on the number of stages at different bandwidths, but in the absence of detuning between the channels (continuous lines for Δ_{\max} , dashed for Δ^*_{\max}).

Chapter V

APPARATUS ERRORS OF A TWO-CHANNEL RADIO

DIRECTION FINDER FOR A PULSED RADIO SIGNAL

1. CHARACTER OF THE PATTERN ON THE TUBE SCREEN IN THE CASE OF A PULSED SIGNAL

Let us note, that the voltage of remote complicated radio signals is usually represented in the form

$$u(t) = \vec{U}(t) \sin \omega_0 t,$$

where

$$\vec{U}(t) = U(t) e^{i\Phi(t)}.$$

The quantity $\vec{U}(t)$ is the complex amplitude or the envelope, and the quantities $U(t)$ and $\Phi(t)$ are respectively the modulus and the phase of the envelope, which in general are functions of time.

For a continuous (harmonic) radio signal, the moduli and the phases of the envelopes at the output of the amplifying channels are constant, and the pattern on the screen represents an ellipse if the channels are not identical (see Chapter III).

In radio direction finding by means of pulsed radio signals

the moduli and the phases of the envelopes at the outputs of the channels will not be constant during the transient process, and if the channels are not identical the transients in them will differ somewhat, and therefore the ratio of the moduli and the phase difference of the envelopes will also vary. Consequently, the pattern on the screen will in general be an ellipse which varies during the time of the transient in size, in slope, and in ratio of the axes.

Since the amplifying channels have a limited bandwidth, the moduli and the phases of the envelopes at the outputs of the amplifying channels will be slowly varying functions of the time (compared with the period of the carrier). Then during one cycle of the carrier, the values of the envelopes can be considered constant, and to each cycle of the high frequency oscillation there will correspond a fully defined ellipse, and consequently, also a fully defined instantaneous value of the error. Thus, the error in the case of a pulsed radio signal is a function of time. To find the instantaneous values of the error it is necessary first to determine the envelopes at the output of the amplifier channels.

It is known that the transfer function $\vec{B}(t)$ determines the variation of the envelope at the output of a four-terminal network in response to a unit step of envelope voltage at the input. If a

radio pulse of rectangle form is applied to the input, then the envelope at the output can be found with the aid of the transfer function in the following manner:

$$\vec{G}(t) = \vec{B}(t + \tau) - \vec{B}(t),$$

where τ is the duration of the rectangular radio pulse at the input.

Next, the envelope at the output will be represented in exponential form

$$\vec{G}(t) = G(t) e^{j\Phi_p(t)},$$

where $G(t)$ is the modulus, and $\Phi_p(t)$ is the phase of the envelope in the case of a pulsed signal.

The expressions for the modulus and the phase of the envelope at the output of a multi-stage tuned amplifier are quite cumbersome, since the transfer function is very complicated [7]. We shall consider therefore henceforth only the cases of single-stage and two-stage amplifying channels.

If we apply to the input of the amplifier a radio pulse of such duration, that the transient has time to die out, we obtain at the output of a single-stage tuned amplifier ($n=1$), for the leading front,

$$G = \frac{k_p}{\sqrt{1+\rho^2}} \sqrt{1 - 2e^{-\pi y} \cos(\rho\pi y) + e^{-2\pi y}}; \quad (5.1)$$

$$\Phi_p = \arctg \frac{e^{-\pi y} \sin(\rho\pi y)}{1 - e^{-\pi y} \cos(\rho\pi y)} - \arctg \rho. \quad (5.2)$$

where $y = \Delta\Omega' t / \pi = 2\Delta F' t$ is the dimensionless time.

$\rho = \Delta\omega_1 / \Delta\Omega'$ -- relative detuning.

For the trailing front we obtain

$$G = \frac{K_p}{\sqrt{1+\rho^2}} e^{-\pi y}; \quad (5.3)$$

$$\Phi_p = -\pi y - \arctg \rho. \quad (5.4)$$

Fig. 5.1 shows graphs for the modulus G and for the phase Φ_p of the envelope at the output of a single-channel tuned amplifier ($n=1$) to the input of which is applied the prolonged radio pulse, such that at the beginning of the trailing front, the process of establishment of the envelope (amplitude and phase of the oscillation) has already terminated. In practice it is sufficient that the dimensionless duration of the rectangular pulse $Y = (\Delta\Omega' / \pi) \pi = 2\Delta F' \tau$ be equal to 2.

The radio pulse may have a different detuning of the carrier relative to the resonant frequency of the amplifier

$$\rho = \frac{\Delta\omega}{\Delta\Omega'} = \frac{\Delta f}{\Delta F'}.$$

The graph of Fig. 5.1 is based on formulas (5.1) and (5.2) for the leading front and on formulas (5.3) and (5.4) for the trailing front. The expression for the envelope at the output of the two-stage tuned amplifier becomes quite cumbersome, and will not be given here.

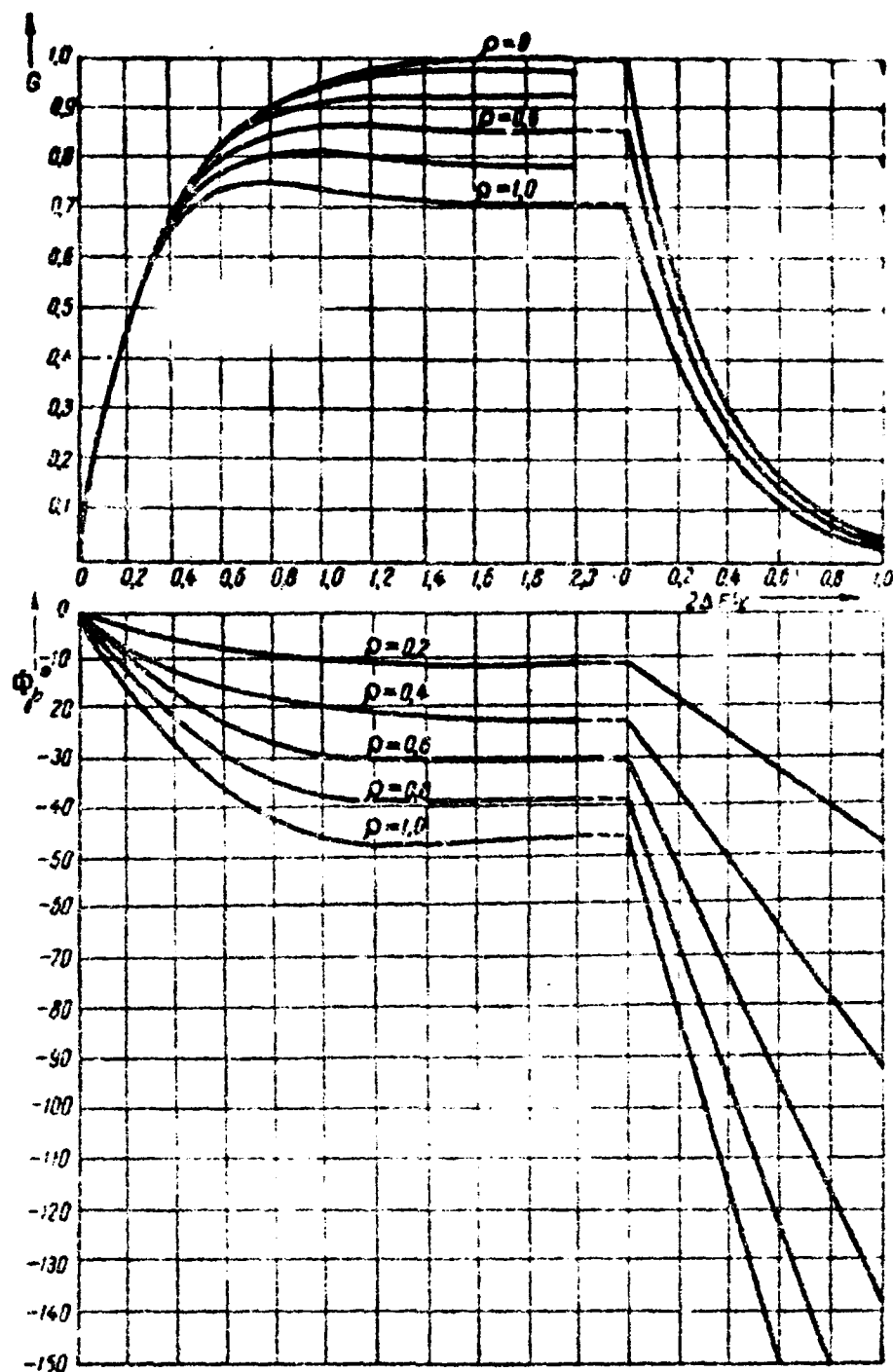


Fig. 5.1. Curves for the modulus and the phase of the envelope at the output of the single-stage tuned amplifier to whose input is applied a radio pulse with a different detuning of the carrier relative to the tuned frequency of the amplifier.

However, Fig. 5.2 shows for comparison a graph for the modulus G and the phase Φ_p of the envelope at the output of a two-stage tuned amplifier ($n=2$), which has the same bandwidth as the single-stage tuned amplifier referred to above.

It is possible to obtain from Figs. 5.1 and 5.2 the values of the modulus and of the phase of the envelope for even shorter pulses at the input of the amplifier. Analysis shows that the modulus of the envelope of the leading front of the shorter pulse coincides with the corresponding curves for a longer pulse within the range from $y = 0$ to $y = Y$, where Y is the duration of the shorter pulse. The modulus of the envelope of the trailing front of the shorter pulse can be obtained from the corresponding curves for the trailing front of the longer pulse by reducing the ordinates of a ratio

$$\frac{G_{(y=Y)}}{G_{(y=\infty)}},$$

where $G_{(y=Y)}$ and $G_{(y=\infty)}$ are the values of the moduli of the envelope of the longer pulse at the instants of time

$y = Y$ and $y = \infty$ respectively. In practice one can assume

$$G_{(y=\infty)} = G_{(y=2)}.$$

The phase of the envelope of the leading front of the shorter pulse also coincides with the corresponding curves for the longer pulse, within the range from $y = 0$ to $y = Y$. The phase of the envelope of the trailing front of the shorter pulse can be obtained by changing the ordinates of the corresponding curve of the phase of the envelope of the longer pulse by a constant quantity, equal to the difference

$$\Phi_p(y=Y) - \Phi_p(y=\infty),$$

where $\Phi_p(y=Y)$ and $\Phi_p(y=\infty)$ are the values of the phase of the envelope of the longer pulse during the corresponding instants of time.

Henceforth, after performing certain recalculations that take into account the non-identity of the channels, the curves of Figs. 5.1 and 5.2 have been used to determine the envelopes at the output of each of the amplifier channels.

It is now necessary to determine the ratio of the moduli of the envelopes

$$a_p = \frac{a_1}{a_2} \quad (5.5)$$

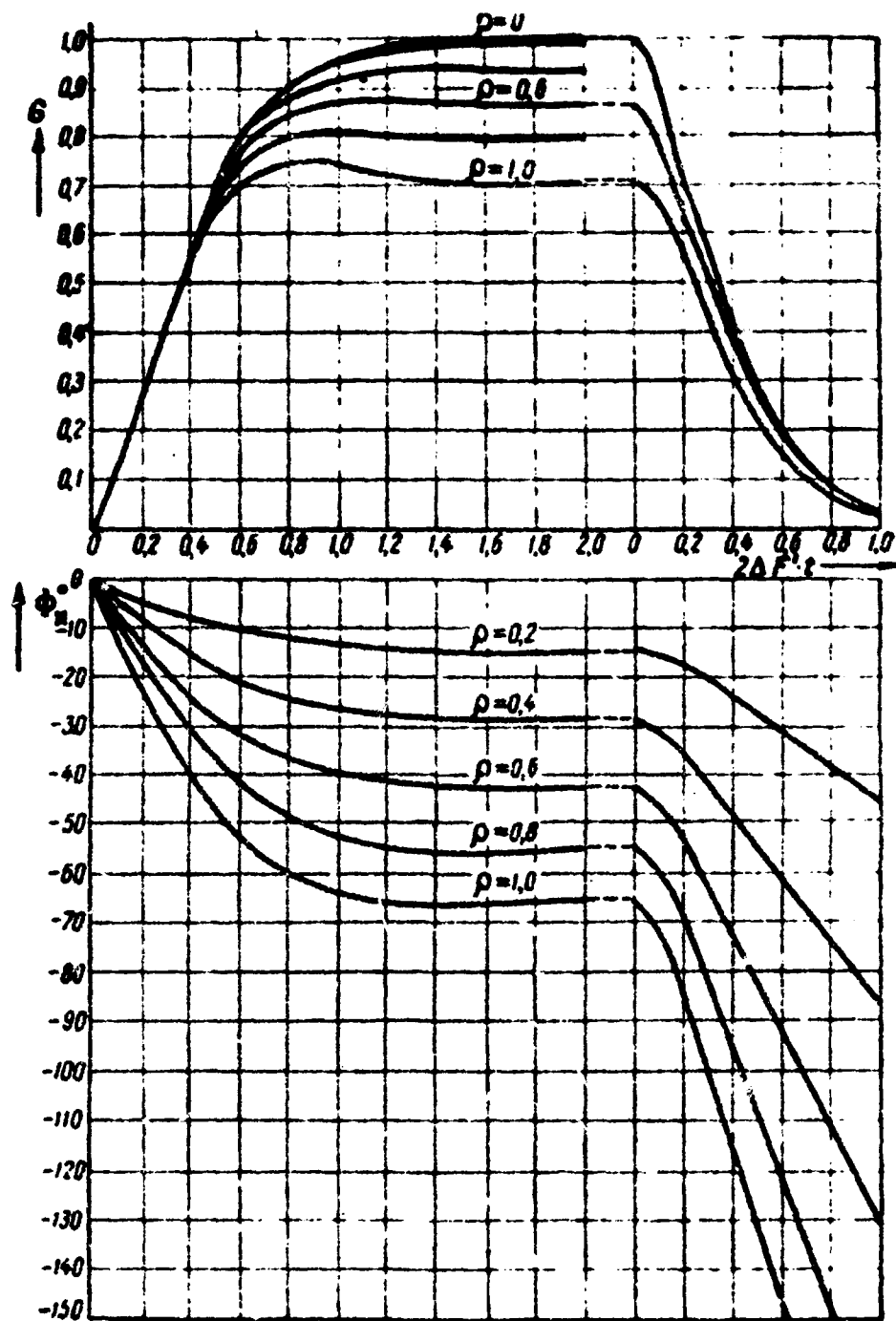


Fig. 5.2. Graphs for the modulus and phase of the envelope at the output of a two-stage tuned amplifier to which a radio pulse is applied.

and the difference in the phase shifts of the envelopes

$$\psi_p = \Phi_{p1} - \Phi_{p2} \quad (5.6)$$

at the output of the channels, when identical radio pulses are applied to the inputs. The quantities a_p and ψ_p (the subscript denoting pulsed operation) are functions of time and characterize the running unbalance of the envelopes, due to the non-identity of the amplifying channels of the radio direction finder.

Knowing the running unbalance for different instants of time, it is possible to determine the values of the running error for the same instants of time.

2. READING OF THE BEARING IN THE CASE OF A PULSED RADIO SIGNAL

When receiving pulsed radio signals, the pattern on the screen is a "smeared" figure made of successively traced ellipses with a common center.

During the time of action of the pulsed radio signal and during the time of the transient due to this radio signal, the

instantaneous values of the error change. With this, the operator reads the bearing with a certain error which is averaged over the time of the signal. It is obvious that this error is greatly influenced by the instantaneous values of the error during those instants of time, when the length of the pattern reaches a sufficient quantity, for example not less than 0.707 of the maximum length. Therefore, for further analysis, it is necessary to determine the time dependence of the length of the line or the major semi-axis of the ellipse when a radio pulse is received by a two-channel direction finder. For the circuit with pre-amplification (see Fig. 3.2) the length of the major semi-axis of the ellipse equals the sum of the moduli of the envelopes at the output of the channels

$$p = G_1(t) + G_2(t). \quad (5.7)$$

For the circuit with post-amplification (see Fig. 3.1) the length of the major semi-axis, subject to certain assumptions (see Section 4.2), can be determined from the formula

$$p = \sqrt{\frac{G_1(t) + G_2(t)}{2}}. \quad (5.8)$$

Thus, one can find from (5.7) and (5.8) the instants of time when the length p has a maximum, and also determine that interval of time, in which p amounts to not less than 0.707 of the maximum. However, this is a rather complicated task, since the moduli

of the envelopes at the output of the channels are determined by complex functions of the channel parameters and depend on the types of the stages in the channels.

, In order to find the major semi-axis of the ellipse for small detunings of the channels relative to each other, we can replace the radio direction finder (see Figs. 3.1 and 3.2) by a single equivalent channel, which has an input envelope with a modulus proportional to the length of the pattern. The bandwidth of such an equivalent channel is equal to the arithmetic mean of the bandwidths of the real channels, i.e., $2\Delta\Omega'_{av}$, and the resonant frequency of this channel is different from the frequency of the signal by the amount

$$\rho_{av} = \frac{1}{2} \left[\frac{\Delta\omega_1}{\Delta\Omega'_{av}} + \left(\frac{\Delta\omega_1}{\Delta\Omega'_{av}} - \frac{\Delta\omega}{\Delta\Omega'_{av}} \right) \right], \quad (5.9)$$

which is the arithmetic mean of the detunings of the real channels relative to the signal frequency. It is then possible to obtain the numerical values of the parameters of the envelope from the curves of Figs. 5.1 and 5.2, assuming that the latter have been plotted for the equivalent channel.

We note also that in direction finding by means of pulsed radio signals, the reading of the bearing can be also taken on the basis of the direction of the point of the pattern that is

farthest away from the center of the screen, corresponding to ... taking the reading on the basis of the instantaneous indicator value at the instant of the maximum length of the pattern. Obviously in this case the error will represent the instantaneous value during the corresponding instant of time.

For the circuit with pre-amplification, the instantaneous value of the apparatus error is determined by the running phase unbalance, in accordance with formula (5.6), i.e., $\Delta = \psi_p(t)$.

3. ERRORS IN THE CIRCUIT WITH PULSED AMPLIFICATION

(See Fig. 3.1)

After determining the parameters a_p and ψ_p , which characterize the ... running unbalance, from formulas (5.5) and (5.6), it is possible to determine the instantaneous values of the error by formula (3.13). However, in a circuit with post-amplification the error depends also on the value of the measured phase difference φ . It is therefore necessary, as an example, to specify certain values of φ . Let us take such a values of φ , for which the error has the maximum for specified parameters of channel non-identity.

Fig. 5.3 shows the variation of the instantaneous values of the maximum apparatus error on the non-identity of single-

stage channels during the time of action of a pulsed radio signal. The abscissas represent the dimensionless time

where

$$\Delta F'_{av} = \frac{\Delta \Omega'_{av}}{2\pi}.$$

The curves on Figs. 5.3a and 5.3b correspond to the case when the bandwidths of the channels are the same ($\xi = 1.0$), but a detuning exists between channels. The curves on Fig. 5.3c correspond to the case when there is no detuning between channels, $\Delta \omega / \Delta \Omega'_{av} = 0$, but the channels have different bandwidths, and the hatched lines correspond to unequalized channel gains, owing to the unequal bandwidths, while the solid lines correspond to equalized gains, for example, by changing the transconductances of the tubes.

It is seen from the curves that the error increases most substantially during the time of action of the trailing front (on the curve, the start of the trailing front is indicated by a thin vertical line). It is known, however, that in this case the length of the pattern on the screen decreases rapidly, and this reduces the influence of the trailing front on the reading error.

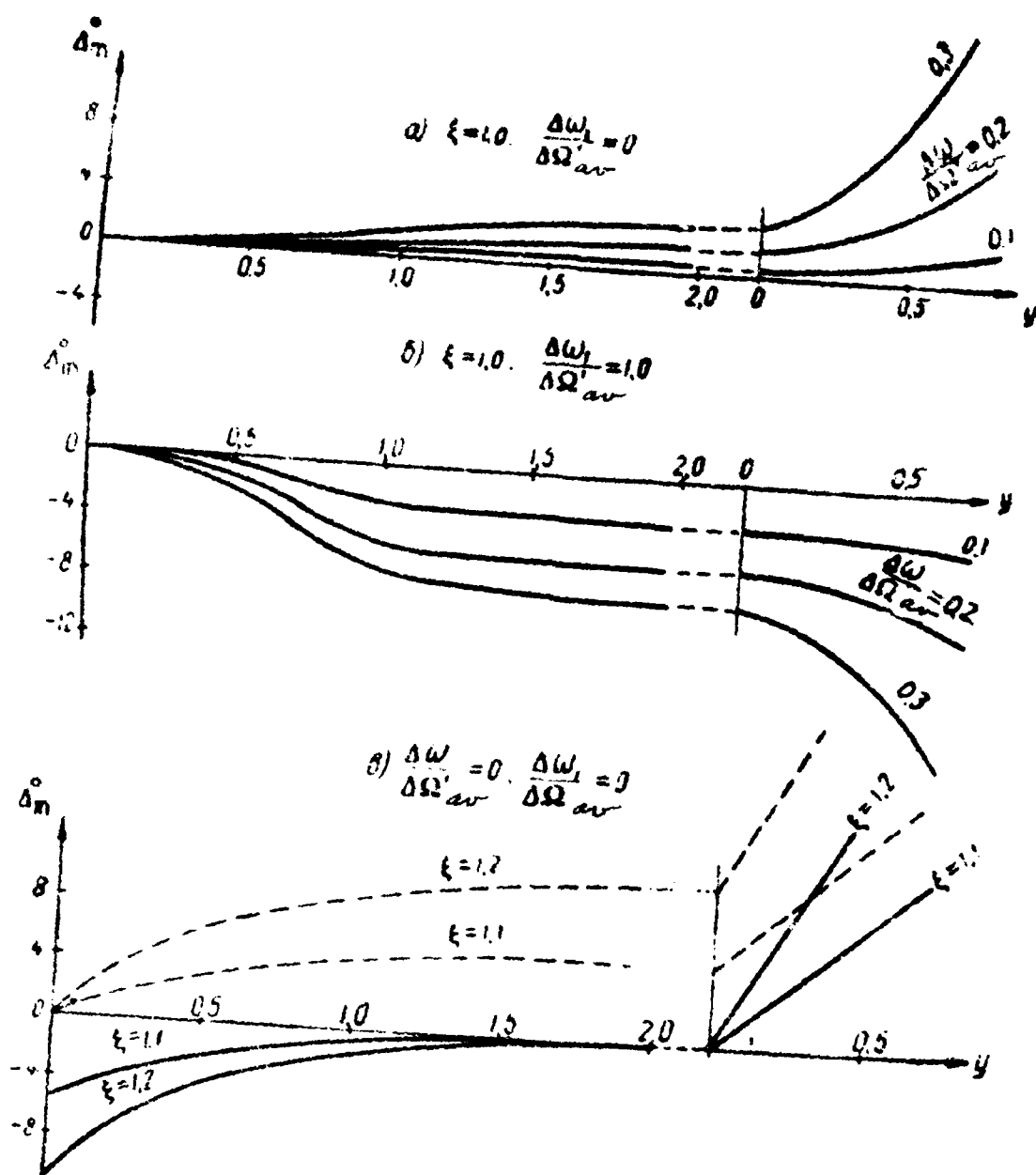


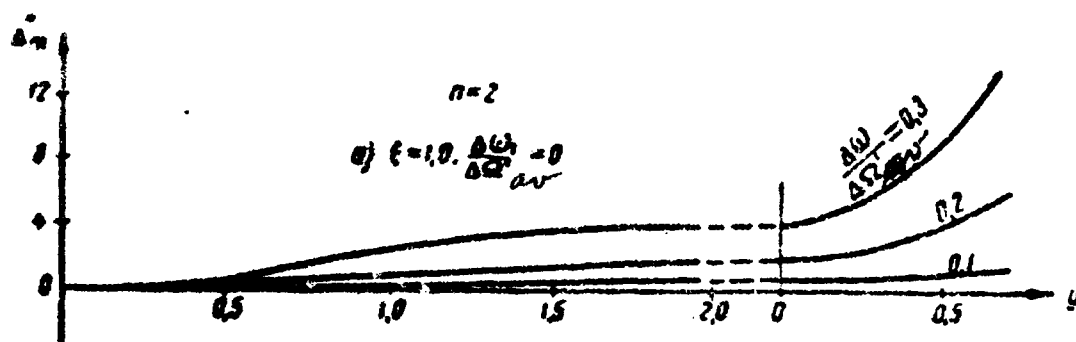
Fig. 5.3. Change in the instantaneous values of the maximum error due to non-identity of single-stage channels during the time of action of a pulsed radio signal.

Fig. 5.4 shows analogous curves for the instantaneous values of the maximum apparatus error due to the non-identity of two-stage amplifier channels, having the same bandwidth as the corresponding single-stage channel.

If the bearing reading is taken to be the average reading during the time of action of the pulsed radio signal, when the length of the pattern amounts to not less than 0.707 of the maximum size, then the error in reading will in this case also be an average, which can be determined from the curves for the instantaneous error, using the formula

$$\Delta_{av} = \frac{\int_{t_1}^{t_2} \Delta(t) dt}{t_2 - t_1}, \quad (5.10)$$

where t_1 and t_2 -- instants of time that determine the averaging interval.



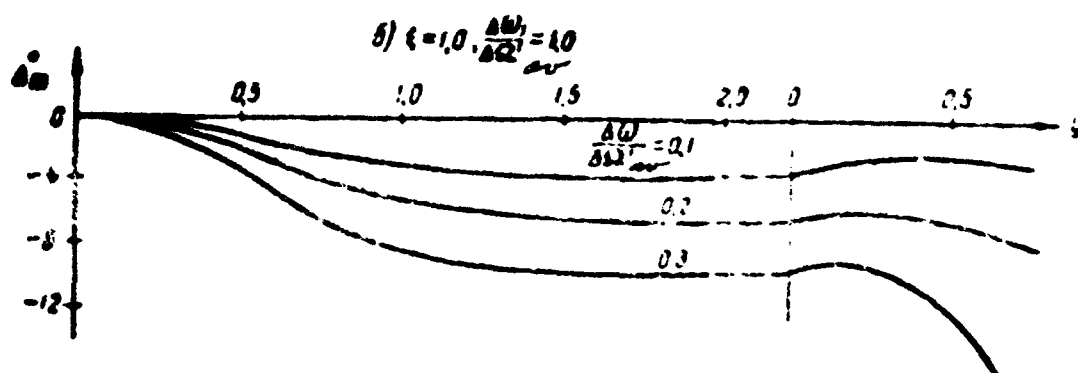


Fig. 5.4. Instantaneous values of the maximum error due to differences in the bandwidths of single-stage channels during the time of action of a pulsed radio signal.

If the reading is based on the point of the pattern that is farthest away from the center, then the error will represent the value of the instantaneous error during the instant when the length of the pattern reaches a maximum, i.e.,

$$\Delta_{p \max} = \Delta(t) \text{ for } p = p_{\max}.$$

Fig. 5.5 shows curves of the instantaneous values of the maximum error due to differences in the bandwidths of single-stage channels during pulsed radio signals of different durations.

For our graphs, formula (5.10) for determining the average maximum error of direction finding by means of a pulsed signal, becomes

$$\Delta_{m \text{ av}} = \frac{\int_{y_1}^{y_2} \Delta(y) dy}{y_2 - y_1}. \quad (5.11)$$

An analytical determination of this error by formula (5.11) is ~~xxxx~~ impossible, owing to the ~~difficult~~ serious mathematical difficulties, and therefore the calculations were carried out graphically.

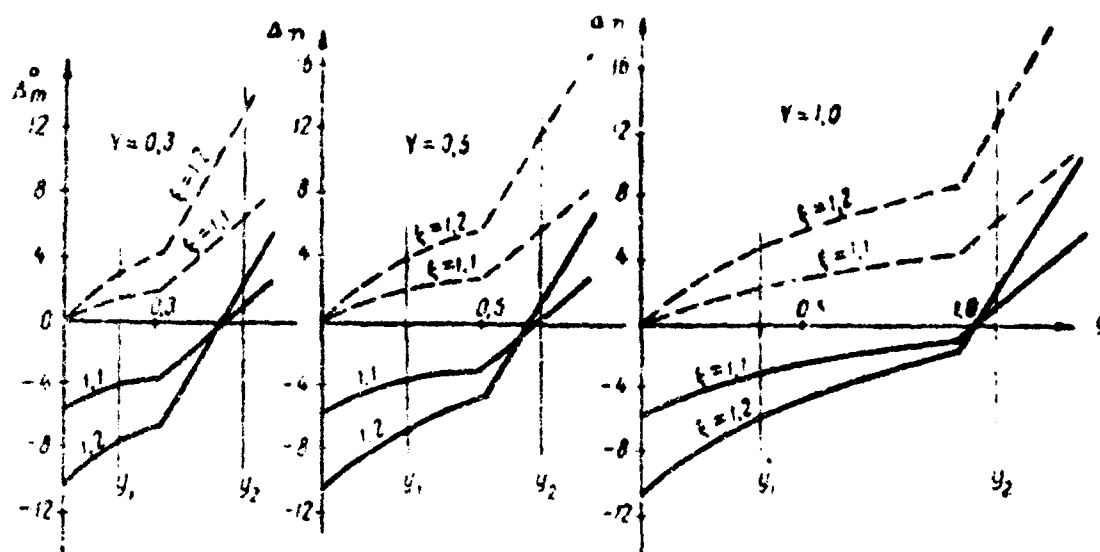


Fig. 5.5. Curve showing the instantaneous values of the maximum error due to differences in bandwidths of single-stage channels in the case of radio pulses of different durations.

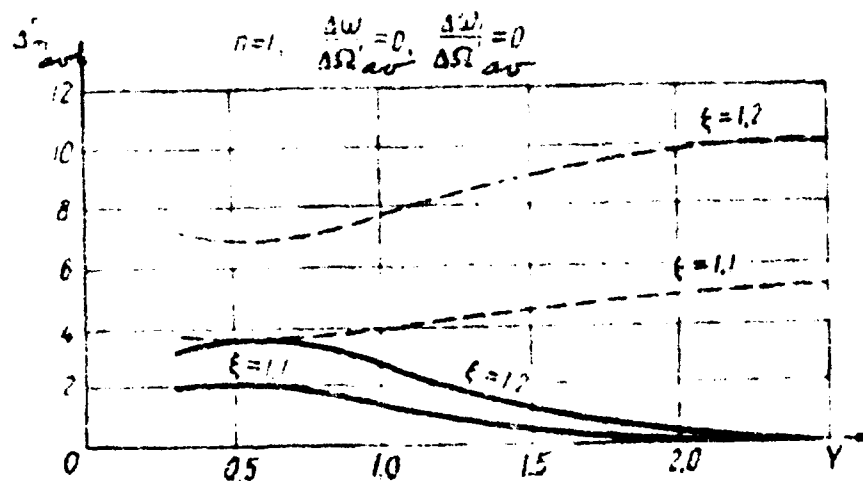


Fig. 6.6. Influence of the duration of the averaging on the averaged maximum error due to inequality of the bandwidths of single-stage amplifying channels.

Fig. 6.6 shows by means of thin vertical lines the chosen, regardless of time, y_1 and y_2 , between which the averaging was carried out. The dashed lines correspond to unequalized resonant gains of the channels, and the continuous lines to equalized ones. The results of the graphical averaging are shown in Fig. 6.7.

Fig. 6.7 shows a curve for the dependence of the maximum direction-finding error by means of a pulsed radio signal, when the readings are taken during the instant of the maximum length of the pattern on the screen, of the pulse duration. The dependence was investigated for the same cases that were analyzed in the preceding curves. For the case of unequalized resonant gains of channels, the errors Δ_{max} and Δ_{min} decrease with shortening of the pulse in the case of differences in the bandwidths. The error Δ_{min} changes most.

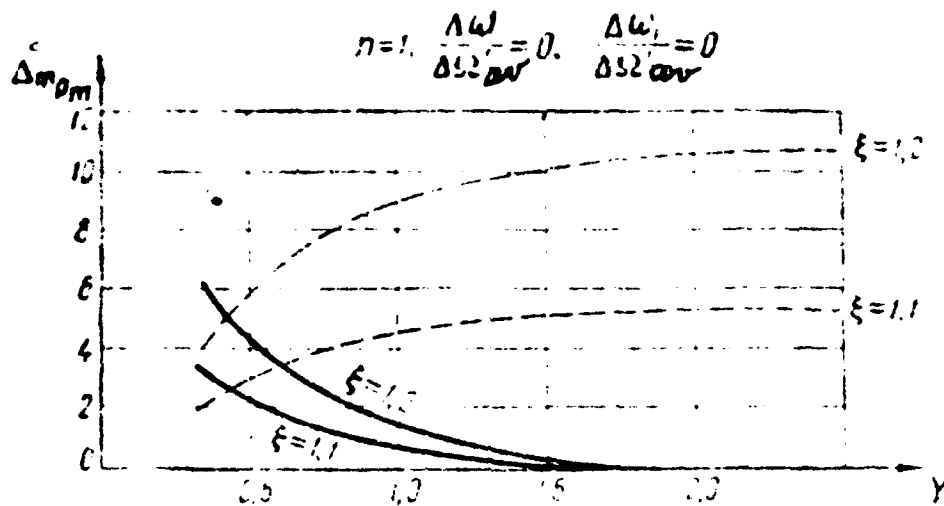


Fig. 7. Influence of the parameter ξ on the function Δm_{0m} in the inequality of the boundary conditions of single-frequency oscillations. Dashed lines for $\xi \neq 1$, solid lines for $\xi = 1$.

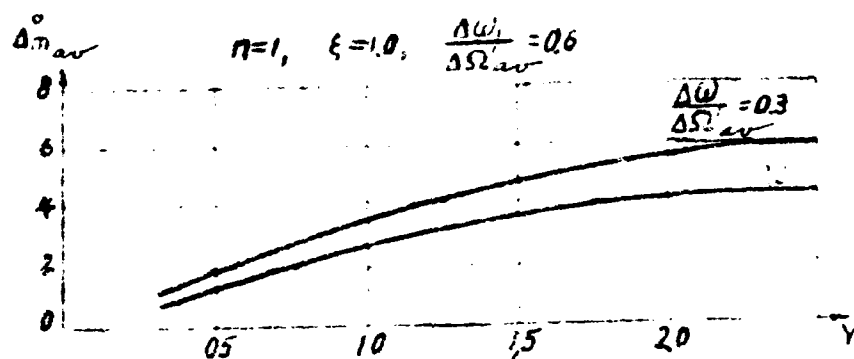


Fig. 8. Influence of the parameter $\Delta\omega/\Delta\Omega_{av}$ on the function Δm_{av} in the inequality of the boundary conditions of single-frequency oscillations.

For the case of $\Delta\omega/\Delta\Omega_{av} = 0$, the curves Δm_{0m} and Δm_{av} are shown with reference to Fig. 7, although the

are relatively small in absolute magnitude.

Fig. 5.8 shows the dependence of the averaged maximum error $\Delta_{m_{av}}$ on the duration of the pulse for identical bandwidths of single-stage channels, but for different detunings between them, while Fig. 5.9 shows the dependence of the error $\Delta_{m_{pm}}$ on the duration of the pulse for the same conditions.

It is seen that the averaged error $\Delta_{m_{av}}$ and the error obtained when the reading is made on the basis of the farthest point of the pattern, $\Delta_{m_{pm}}$, decrease with reduction in the radio pulse.

It must be borne in mind that in the case of pulses that are shorter than optimum duration, the ratio between the signal and noise gets worse.

An analysis of errors due to non-identity of two-stage amplifying channels, having the same bandwidth as single-stage ones, yields analogous results for direction finding by means of a radio pulse. This can be seen from the comparison of the curves of the instantaneous values of the errors, shown respectively on Figs. 5.3a, 5.3b and 5.4a, 5.4b. One can therefore expect that the results will have the same character also for $n > 2$.

If the pulse duration is twice the optimum value, then the errors will be practically equal to the errors in direction finding by means of a continuous signal, but if the duration is less than optimum, then the values of the errors will also be somewhat less.

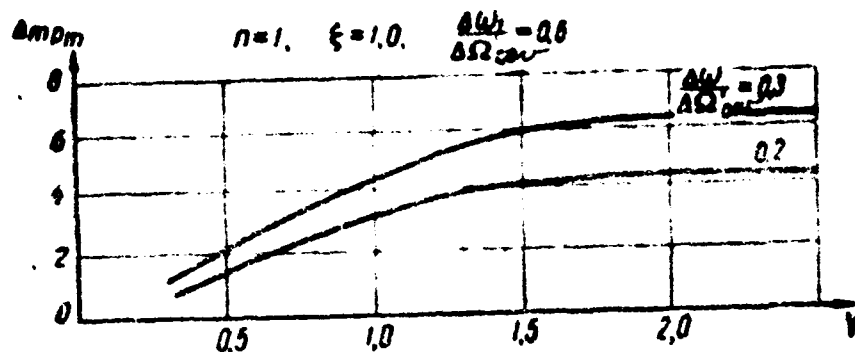


Fig. 5.9. Dependence of the error Δm on the pulse duration for different detunings between channels.

One can therefore assume that the errors due to non-identity of the amplifying channels with multiple-stage tuned amplifiers do not exceed, during direction finding by means of a short radio signal, the corresponding errors obtained with continuous radio signals.

This conclusion holds also for the circuit with pre-amplification (see Fig. 5.2).

To supplement the analysis of the apparatus errors, we note that in practice two-channel amplification is usually effected by means of superheterodyne receivers with a one heterodyne common to the two channels.

Fig. 5.10 shows a characteristic block diagram of a receiving-indicating unit of a radio direction finder with long base.

The main amplification here is produced ahead of the "sum -- difference" stage, with some amplification being produced past this stage.

Fig. 5.11 shows a block diagram of a two-channel receiving-indicating unit of the short-wave radio direction finder, intended for direction finding with transmitters operating with continuous, telegraph and pulse signals.

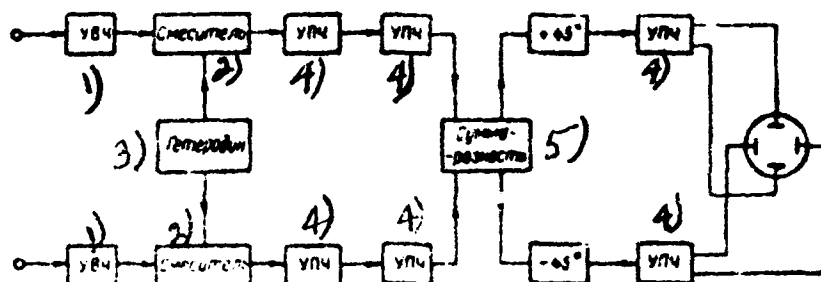


Fig. 5.10. Block diagram of two-channel receiver.

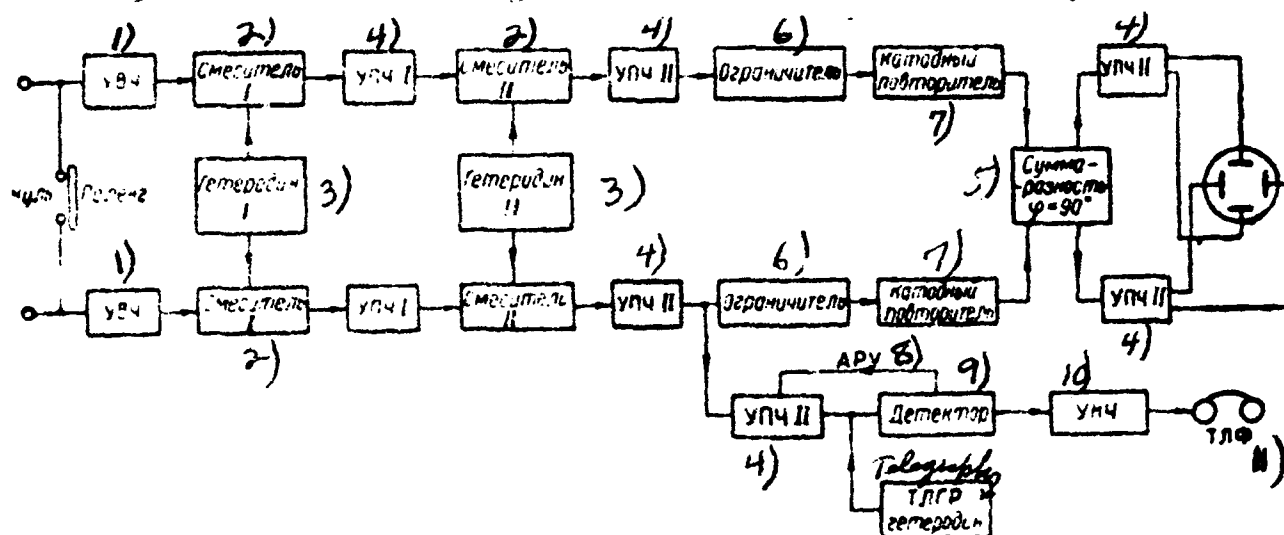


Fig. 5.11. Block diagram of short-wave two-channel receiving-indicating unit for direction finding with continuous, telegraph, and pulsed radio signals.

1) high frequency amplifier; 2) mixer; 3) heterodyne;
4) intermediate frequency amplifier; 5) sum--difference;
6) limiter; 7) cathode follower; 8) automatic gain control;
9) detector; 10) low frequency amplifier; 11) telephone;
12) telegraph heterodyne.

We see that the apparatus contains two principal amplifying channels with double frequency conversion and an audio channel. The first intermediate frequency is 2.5 Mcs. At such a relatively high intermediate frequency, good suppression of UHF image signal is insured. The received frequencies, ranging from 5 to 25 Mcs, are broken up into six bands so as to insure optimum density of radio stations in each of the bands and to insure accuracy of tuning of the frequency on the scale, not worse than 10 kc. The tuning is by means of a five-**gang** variable capacitor, the sections of which are carefully symmetrized beforehand. At the input of the principal channels is connected a "zero-bearing" switch to monitor the equality of the channels.

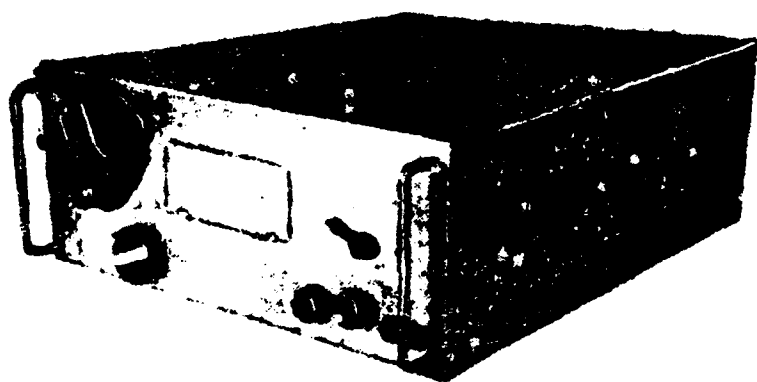


Fig. 5.12. View of two-channel radio receiver.

Following the second intermediate frequency amplifiers, the frequency of which is 112 kcs, each of the principal channels contains a limiter. The purpose of the limiter is to produce equal and constant voltage amplitudes at the outputs. This insures normal conditions for the operation of the "sum -- difference" unit and for the following elements of the indicator unit, particularly when the

input signal amplitudes increase considerably. Identical tuned networks are used in all stages of the principal channels.

The limiters are followed in the channels by cathode followers, and therefore the output of the receiving portion has a low resistance, thereby reducing phase shift in the cables that join the amplifying channels with the indicator portion. The indicator portion contains the "sum -- difference" device with phase-shifting RC network, output paraphase stages of the intermediate-frequency amplifier, and the cathode ray tube.

Structurally, the apparatus consists of a receiver block, an indicator block, and a power supply block. Fig. 5.12 shows the appearance of a two-channel receiver. We see that on the front panel of the receiver are grouped the control devices: scale with band switch, tuning knob, knob with flag indicator for the "zero-bearing" switch, tumbler switch to connect the telegraph heterodyne, knob for loudness control, and a spare knob, intended for equalizing the amplitudes of the voltages past the amplifying channels. With the spare knob it is possible to convert the ellipse into a line.

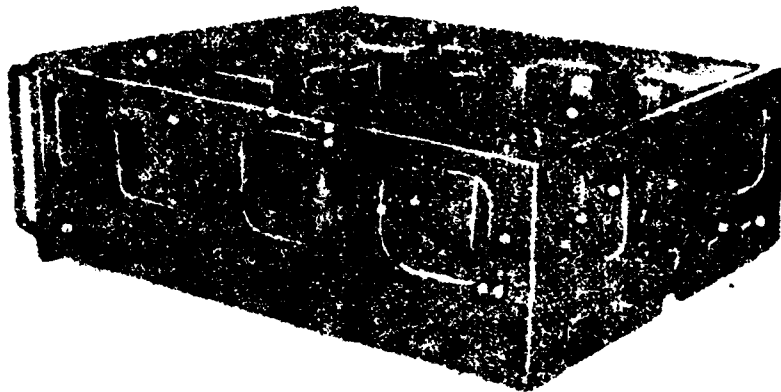


Fig. 5.13. Is shows the chassis of the receiver, taken out of the case. On the rear are seen four high frequency disconnects under a coaxial cable, two of which serve to connect the antennas and two to connect the indicator.

Chapter VI

APPARATUS ERRORS OF PHASE METERS OPERATING AT LOW FREQUENCY

1. CHOICE OF PHASE METER CIRCUIT

There are many known circuits capable of insuring the measurement of the phase shift into low frequency voltages (see Chapter I). However, by far not all these circuits can be used in a short-wave direction finder indicator (with frequency conversion). It is desirable above all that the phase meter insure direct reading of the bearing on the indicator scale. This makes it necessary to forego the use of circuits that require manual compensation during the measurement.

Phase meters with automatic compensation, based on the servo-mechanism system principle, are used in those cases when the time delay of the indicator device need not be changed during the process of operation. Otherwise it is more convenient to use phase meters based on electronic tubes, operating with current rectification. Here it is easy to obtain the necessary time delay of the phase meter, by suitable choice of the time constant of the filter at the output of the rectifying device. In the case of necessity it is also easy to vary the time delay by switching the filter capacitors in and out.

In choosing the phase meter circuit it is necessary to call attention to the possibility of insuring the required measurement accuracy. The most dangerous errors are those arising through instability of the circuit parameters and the power supply parameters. Balanced circuits have definite advantages in this respect.

The deviation of the actual parameters of the circuit from the nominal ones leads to the appearance of the systematic apparatus error. The apparatus error can be taken into account in principle during the calibration. However when the error has a complicated variation on the measured bearing, complete elimination of the error is impossible. It is therefore important that the absolute value of the apparatus error be sufficiently small. This necessitates the maintenance of definite tolerances for the parameters of the phase meter circuit.

In certain types of phase meters errors may occur when the signal amplitude varies. Obviously these errors should be sufficiently small when the signal amplitude varies within limits that insure automatic gain control.

In many cases a short-wave direction finder must measure the bearing within a short time interval. In this connection, it is required that the phase meter produce rapid readings whenever necessary.

2. PHASE METERS WITH READING BY MEANS OF A CATHODE RAY TUBE

Fig. 6.1 shows a possible block diagram of a phase meter for a short-wave direction finder. The signal voltage and the reference voltage are shifted in phase by an angle ϕ , which must be measured. These voltages are applied to a phase-sensitive element, the output of which is a rectified voltage proportional to the amplitude of the signal and to the cosine of the phase shift, i.e., to the quantity $U_{\text{sig}} \cos \phi$.

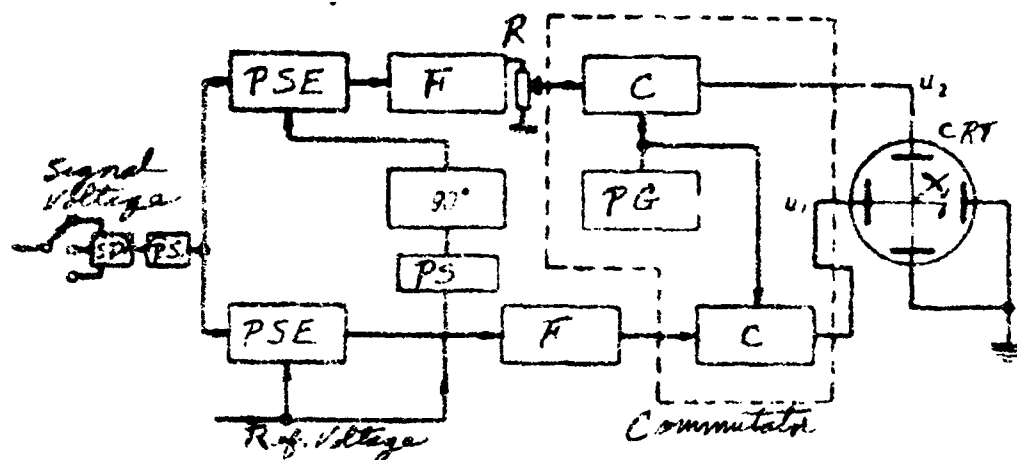


Fig. 6.1. Block diagram of a phase meter using a cathode ray tube.

PSE -- phase sensitive element, 90° -- phase shifter, producing a phase shift of 90° in the reference voltage.

SF -- standard phase shift, F -- filter, C -- chopper, PG -- pulse generator, CRT -- cathode ray tube, R -- regulator for the gain of the first channel, PS -- continuous phase shifter for initial adjustment.

The reference voltage is applied to the second phase sensitive element after being shifted in phase by 90° . Consequently its output will be a direct voltage proportional to $U_{\Sigma} \sin \varphi$. The difference of the outputs of the phase-sensitive elements insures the required time delay of the phase meter.

The rectified voltages, after passing through the commutator (Fig. 1a), are applied to the vertical and horizontal plates of a cathode ray tube and shift the ^{light} spot from the center to the edge of the screen. The choppers, controlled by the pulse generator, disconnect periodically the voltages applied to the plates. Consequently the spot will move on the screen in a radial direction, and will trace a straight line which serves as an indicator of the bearing. The slope of this line on the screen is determined by the voltage ratio

$$\gamma = \arctg \frac{U_2}{U_1} = \arctg \frac{U_{\Sigma} \sin \varphi}{U_{\Sigma} \cos \varphi} = \varphi. \quad (6.1)$$

Thus, one reads the phase shift directly on the cathode ray tube, and consequently this determines the bearing. The principal block of this phase meter, which determines the quality of its operation, is the phase sensitive element.

One can use as phase sensitive elements phase detectors with sinusoidal reference voltage and phase commutators with rectangular reference voltage.

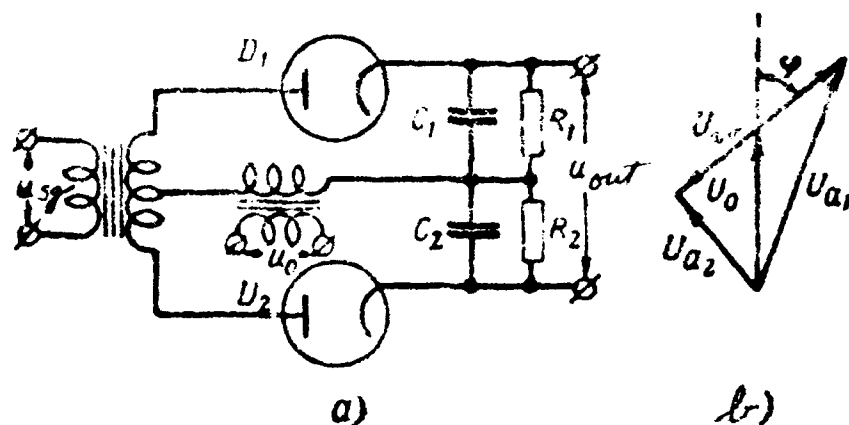


Fig. 6.2. Principal diagram of a phase detector and the vector diagram of the voltages in its circuits.

The principal diagram of a half-wave phase detector is shown in Fig. 6.2.

The voltage U_0 is applied to the plates of the two diodes in phase, while the voltage U_{sg} is applied in phase opposition. The amplitude of the voltage in the circuit of diode D_1 is, according to the vector diagram (see Fig. 6.2b)

$$U_{a1} = \sqrt{U_0^2 + \frac{U_{sg}^2}{4} + 2U_0 \frac{U_{sg}}{2} \cos \varphi}. \quad (6.2)$$

Analogously, the amplitude in the circuit of diode D_2

$$U_{a2} = \sqrt{U_0^2 + \frac{U_{sg}^2}{4} - 2U_0 \frac{U_{sg}}{2} \cos \varphi}. \quad (6.3)$$

If the voltage U_{sg} is taken to be considerably smaller than the voltage U_0 , expressions (6.2) and (6.3) can be represented in the form

$$U_{a1} = U_0 \sqrt{1 + m^2 + 2m \cos \varphi} \cong U_0 \left(1 + \frac{m^2}{2} + m \cos \varphi \right), \quad (6.4)$$

$$U_{a2} = U_0 \sqrt{1 + m^2 - 2m \cos \varphi} \cong U_0 \left(1 + \frac{m^2}{2} - m \cos \varphi \right), \quad (6.5)$$

where

$$m = \frac{U_{\text{сг}}}{2U_0}. \quad (6.6)$$

The dc voltage delivered to the detector and load is proportional to the amplitude of the signal voltage. The voltage at the output of the circuit is

$$u_d = K_d (U_{a1} - U_{a2}) = K_d U_{\text{сг}} \cos \varphi, \quad (6.7)$$

where K_d is the detection coefficient of the diode.

A phase detector can be built also with amplifier tube operating in the nonlinear portion of the grid characteristic.

Fig. 6.3 shows the principal diagram of the phase detector using a square-law triode. In this circuit the triode operates in the quadratic portion of the characteristic so that the dependence of the plate current on the grid voltage can be represented by the equation

$$i_a = I_0 + \beta u_g + \gamma u_g^2. \quad (6.8)$$

Eq. (6.8) is valid only for small voltages u_g . In the left arm of the circuit is the alternating voltage

$$u_{g1} = U_0 \sin \omega t + U_{\text{сг}} \sin (\omega t + \varphi). \quad (6.9)$$

In the right arm is respectively a voltage

$$u_{g_2} = U_0 \sin \omega t - U_{\omega} \sin(\omega t + \varphi). \quad (6.10)$$

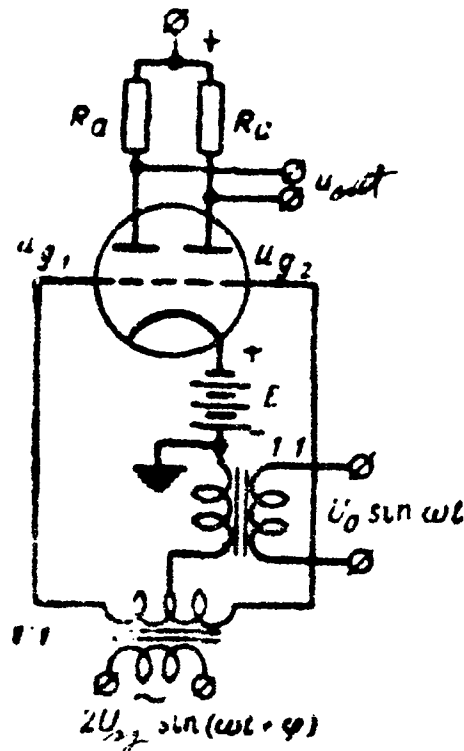


Fig. 6.3. Phase detector using a triode with quadratic characteristic.

The plate current of the left triode is

$$i a_1 = I_0 + \beta U_0 \sin \omega t + \beta U_{\omega} \sin(\omega t + \varphi) + \gamma [U_0 \sin \omega t + U_{\omega} \sin(\omega t + \varphi)]^2. \quad (6.11)$$

Analogously, the plate current of the right triode is

$$i a_2 = I_0 + \beta U_0 \sin \omega t - \beta U_{\omega} \sin(\omega t + \varphi) + \gamma [U_0 \sin \omega t - U_{\omega} \sin(\omega t + \varphi)]^2. \quad (6.12)$$

The output voltage is equal to the difference of the plate voltages of

the left and right triode

$$u_{out} = 2R_a [\beta U_{az} \sin(\omega t + \varphi) - \gamma U_0 U_{az} \cos(2\omega t + \varphi) + \gamma U_0 U_{az} \cos \varphi]. \quad (6.13)$$

The dc component of the output voltage is

$$u_{out} = 2R_a \gamma U_0 U_{az} \cos \varphi. \quad (6.14)$$

A major drawback of this circuit is the difficulty of selecting identical triodes. The balancing of the circuit is considerably more complicated than in a diode phase detector, since it is necessary to make the three parameters, which determine the characteristic, equal to each other. In this connection, in spite of the relatively large gain, a triode phase detector is not advantageous for use.

If it is desirable to incorporate amplification in the phase-sensitive element, it is better to use phase commutators with rectangular reference voltage.

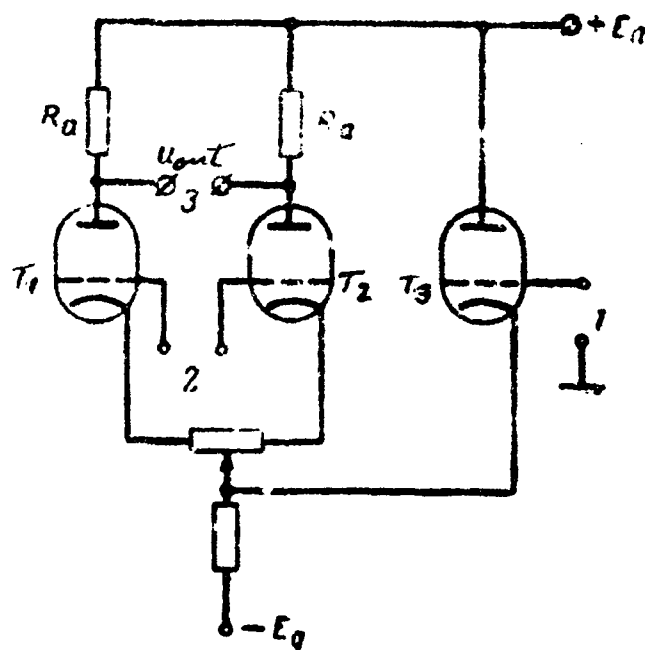


Fig. 6.4. Phase commutator employing triodes.

1 -- output of reference voltage, 2 -- input of signal voltage,
3 -- output.

Fig. 6.4 shows a circuit of a triode phase commutator. The commutation is carried out in the cathodes of tubes T_1 and T_2 . To insure clean commutation, the rating of tube T_3 should be greater than those of T_1 and T_2 .

Even more gain is produced by a pentode phase commutator (Fig. 6.5). The commutation is carried out here in the screen grids. To facilitate ~~xxx~~ cutoff, the plate voltage is taken to be smaller than the screen voltage. The diode D_1 is intended for fixing the zero level of the reference voltage. Both circuits (Figs. 6.4 and 6.5) are of the half-wave type.

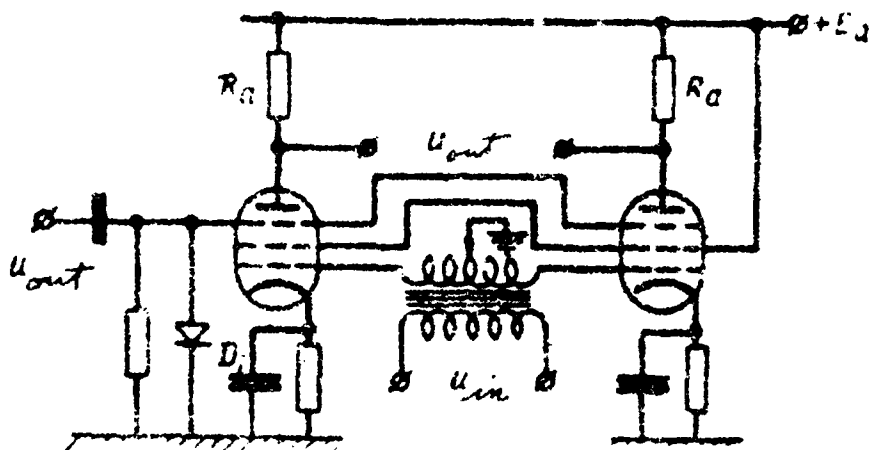


Fig. 6.5. Phase commutator using pentodes.

Fig. 6.6 shows oscillograms that characterize the operation

of a half-wave phase commutator. It is seen that the output voltage can be obtained from the input voltage x by multiplication by a specially chosen commutating function (see Fig. 6.6a). This circumstance makes it possible to represent the output voltage in the following form

$$u_{out} = u_{in} u_{com} \quad (6.15)$$

In this circuit u_{com} represents a sequence of rectangular pulses of duration equal to half the period ($1/2$). The amplitude of these pulses depends on the gain of each tube of the phase commutator (T_1 or T_2).

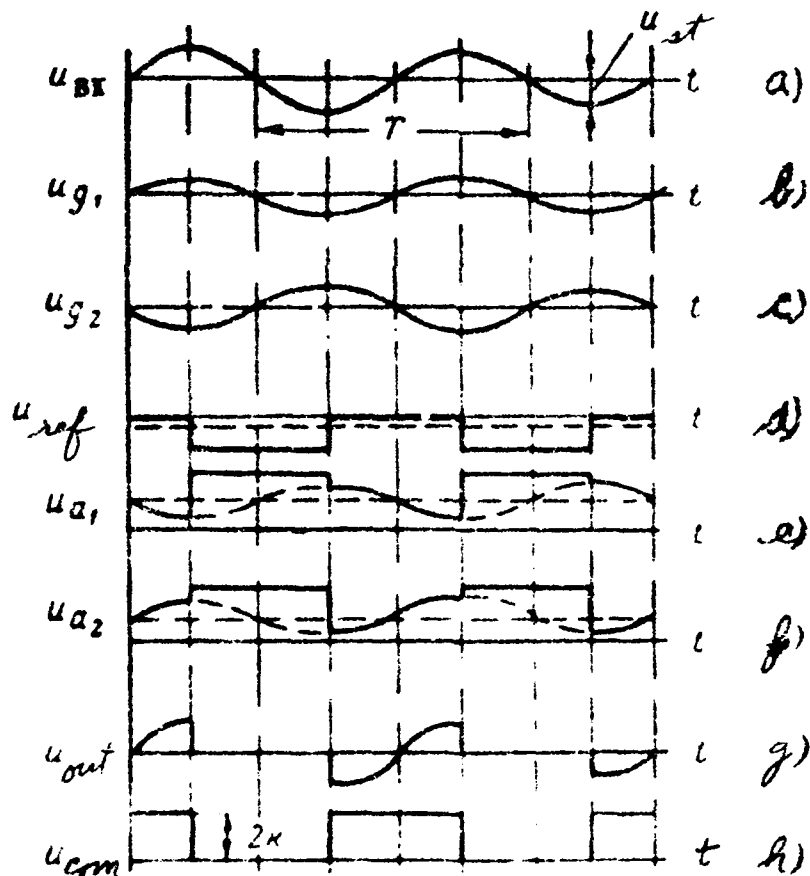


Fig. 6.6. Voltage oscillograms and current oscillograms in the phase commutator circuit.

(a) Input voltage (signal), (b) and (c) — voltages at the grids of tubes T_1 and T_2 , (d) — reference voltage, (e) and (f) — input voltage of tubes T_1 and T_2 , (g) — output voltage, (h) — commutating function).

Let us investigate the spectrum of the input voltage. For this purpose we represent the commutating function in the form of a Fourier series

$$u_{com} = K + \frac{4K}{\pi} \cos\left(\frac{2\pi}{T}t\right) - \frac{4K}{3\pi} \cos\left(3\frac{2\pi}{T}t\right) + \dots \quad (6.16)$$

where K characterizes the gain.

The input voltage is sinusoidal

$$u_{in} = U_{sz} \cos\left(\frac{2\pi}{T}t + \varphi\right). \quad (6.17)$$

Substituting the values of u_{com} and u_{in} from (6.16) and (6.17) in (6.15) we obtain, after trigonometric transformations

$$u_{out} = KU_{sz} \cos\left(\frac{2\pi}{T}t + \varphi\right) + \frac{2K}{\pi} U_{sz} \cos \varphi + \frac{2K}{\pi} U_{sz} \cos\left(2\frac{2\pi}{T}t + \varphi\right) - \frac{2K}{3\pi} U_{sz} \cos\left(2\frac{2\pi}{T}t - \varphi\right) - \frac{2K}{3\pi} U_{sz} \cos\left(4\frac{2\pi}{T}t + \varphi\right) + \dots \quad (6.18)$$

The dc component at the output is

$$u_0 = \frac{2K}{\pi} U_{sz} \cos \varphi. \quad (6.19)$$

In addition to the dc component, the output contains harmonics of frequency ω , 2ω , 4ω , etc., which are eliminated with the aid of filters.

In conclusion we note that both the phase detector and the

phase commutator can be constructed of the full-wave type. In this case the output will not contain the first harmonic of the working frequency and the lowest harmonic will have a frequency 2ω . This can be a substantial advantage in those cases, when the working frequency is quite low, and the time delay of the filter of the phase meter must be sufficiently small. Full-wave circuits are more complicated than single-wave circuits and are more difficult to balance.

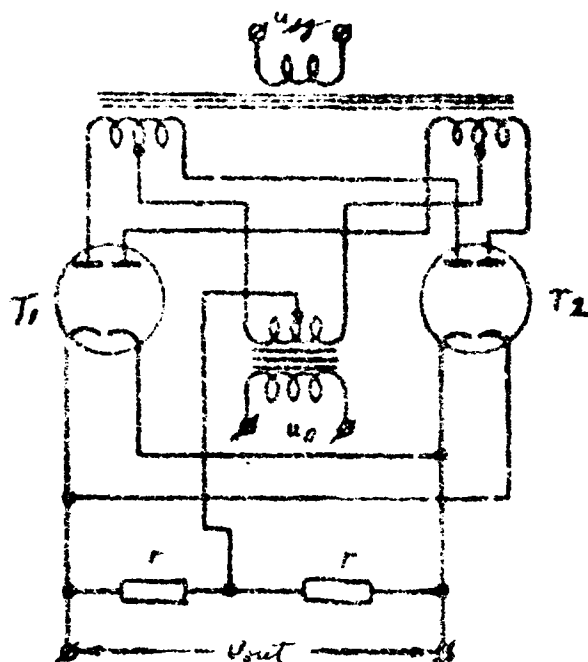


Fig. 6.7. Full-wave phase detector.

A diagram of a full wave phase detector is shown in Fig. 6.7.

Let us proceed now to a more detailed analysis of several of the characteristics of a phase meter based on diode phase detectors.

3. PHASE METER ERROR DURING CHANGE IN SIGNAL AMPLITUDE

In a phase meter containing phase detectors based on linear diodes, the fluctuations in the signal amplitude cause an error in the phase measurement. At a constant reference-voltage amplitude, the fluctuations of the signal amplitude are equivalent to a variation in the quantity $m = U_{sg}/2U_0$. Calibration of the indicator scale may be carried out in accordance with formula

$$\operatorname{tg} \varphi_0 = \frac{\sqrt{1+m^2-2m \sin \varphi} - \sqrt{1+m^2-2m \sin \varphi}}{\sqrt{1+m^2+2m \cos \varphi} - \sqrt{1+m^2-2m \cos \varphi}}. \quad (6.20)$$

It is seen from the formula that at phase angles $\varphi = 45^\circ \pm n45^\circ$, where $n = 0, 1, 2, 3, \dots$, the indicator readings are independent of the value of m . At all intermediate phases ~~indications~~ the indications vary with m .

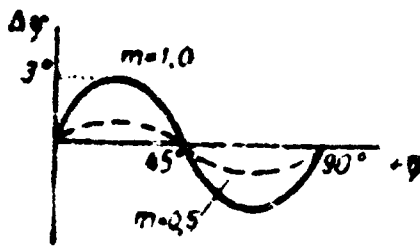


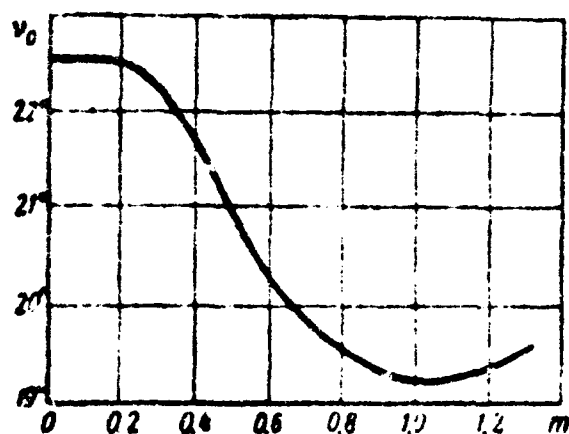
Fig. 6.8. Dependence of the phase meter error on the ~~stage~~ measured phase difference.

The graph 6.8 shows the variation of the indicator readings at different initial phases as the value of m changes from 0 to 1.0.

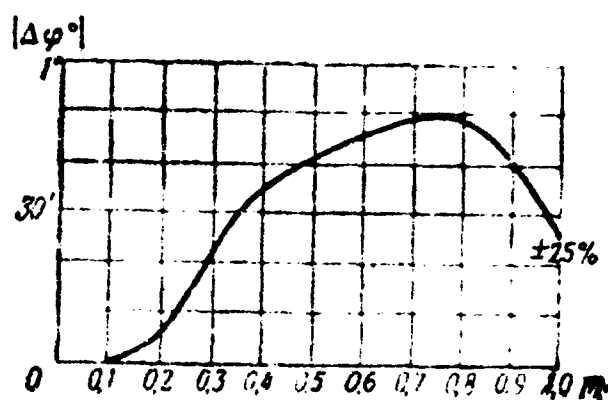
It is seen from the graph that the maximum error is obtained at $\varphi = 22.5^\circ \pm 45^\circ$. The maximum error is equal to 3° at $m = 1$.

In the indicated range of variation of signal amplitude, the variation of the phase meter readings depends on the selected value of m .

On the graph (Fig. 6.9) plotted from formula (6.20) are shown the values of the indicator reading, corresponding to a phase $\varphi = 22.5^\circ$ at different values of m . With this graph it is possible to determine the fluctuations in the indicator reading after specifying an average value of m and the range of variation of m as a percentage of the average value. Fig. 6.9 shows also that by reducing the average value of m it is possible to reduce considerably the dependence of the indicator reading on the signal amplitude. Thus, at $m = 0.1$ the readings of the phase meter remain almost constant as the amplitude of the signal is doubled.



6.9



6.10

Fig. 6.9. Dependence of the phase meter readings on the signal amplitude at a constant phase difference.

Fig. 6.10. Dependence of the phase meter error as the signal fluctuates by $\pm 25\%$.

Fig. 6.10 shows the dependence of the maximum variation of the phase meter readings on the selected value of m as the signal amplitude changes by $\pm 25\%$ from the average value.

It must be noted that upon considerable changes in the signal amplitude at the receiver input, the readings of the phase meter may change because of distortion of the form of the signal by the linear elements of the receiver. Therefore automatic gain control of the receiver must be calculated in such a way as to make the signal amplitude not exceed the permissible value.

The dependence of the phase meter readings on the signal amplitude shows that it is possible to obtain correct readings at large signal attenuation. This follows from the graph of Fig. 6.9. At $m \leq 0.15$ the phase meter readings remain practically constant with decreasing m . All that changes is the length of the line on the screen of the tube.

4. APPARATUS ERROR OF THE PHASE METER

The apparatus error is a result of the fact that the real parameters of the circuit always differ in practice from the nominal values. Phase detectors ~~have~~ have an apparatus error which is due both to the asymmetry of the halves of each phase detector, and the difference between the two phase detectors that are used in the phase meter. In an analysis of the apparatus error it is necessary to take into account the presence of an initial setting of the

phase meter, which makes it possible to reduce the influence of the instability of different circuit parameters.

The initial setting may be produced with the aid of a standard phase shifter as a control voltage is applied to the input in place of a signal. In view of the fact that the standard phase shifter, with continuous phase variation, is frequently too complicated, it is possible to use a stepped phase shifter with three positions, 0, 45, and 90°. Since the phase meter operates at a constant frequency, such a phase shifter, made up of resistances and capacitances is quite simple.

The phase meter has three control devices, which make it possible to obtain at the initial setting exact readings at 0, 90, and 45° in three corresponding positions of the ^{standard} phase shifter.

The first two adjustments establish the phase in the signal channel and in the reference voltage channel, and the third regulates the ratio of the output voltages of the two phase detectors.

An analysis of the relations that take place in this phase meter yield an expression for the indicator reading as a function of the measured phase angle φ , with allowance for possible deviations in the values of the circuit components and for the influence of the initial setting. The phase meter reading will be

$$\alpha = \arctg \frac{MK_{d1}U_{01} \left[\sqrt{1 + m_1'^2 + 2m_1' \sin \left(\varphi + \arcsin \frac{m_1'' - m_1'}{2} \right)} - \right]}{K_{d2}U_{02} \left[\sqrt{1 + m_2'^2 + 2m_2' \cos \left(\varphi \pm \beta - \arcsin \frac{m_2'' - m_2'}{2} \right)} - \right]}$$

$$\frac{-\sqrt{1+m_1'^2-2m_1'\sin\left(\varphi+\arcsin\frac{m_1''-m_1'}{2}\right)}}{-\sqrt{1+m_2'^2-2m_2'\cos\left(\varphi\pm\beta-\arcsin\frac{m_2''-m_2'}{2}\right)}}, \quad (6.21)$$

where U_0 , U_{02} -- amplitudes of the reference voltage in the first and second phase detector,

K_{d1} , K_{d2} -- transfer functions of the first and second phase detector.

In turn, we have,

$$M = \frac{K_{d2}U_{02}\left[\sqrt{1+m_2'^2+2m_2'\cos\left(45^\circ\pm\beta\pm\Delta-\arcsin\frac{m_2''-m_2'}{2}\right)}-\right.}{K_{d1}U_{01}\left[\sqrt{1+m_1'^2+2m_1'\sin\left(45^\circ\pm\Delta+\arcsin\frac{m_1''-m_1'}{2}\right)}-\right.} \\ \left.-\sqrt{1+m_2'^2-2m_2'\cos\left(45^\circ\pm\Delta\pm\beta-\arcsin\frac{m_2''-m_2'}{2}\right)}\right] \\ \left.-\sqrt{1+m_1'^2-2m_1'\sin\left(45^\circ\pm\Delta+\arcsin\frac{m_1''-m_1'}{2}\right)}\right]}. \quad (6.22)$$

In these formulas the parameters pertaining to the first phase detector are marked by the subscript 1, and those pertaining to the second are marked by a subscript 2. Accordingly, m_1' and m_1'' denote the ratio of the signal to the reference voltage in the circuits of the first and second diodes of the first phase detector. Analogously, for the second phase detector these ratios will be m_2' and m_2'' .

The angles β and Δ denote the error in the phase shift of

the control signal for 90 and 45° at the setting of the standard phase shifter.

Thus, formula (6.21) takes into account the joint influence of the inequality of the transfer functions of first and second phase detectors, and the differences in the gains of the channels of the reference voltage of the phase detectors; it also takes into account the asymmetry in the transformer branches of the signal in the two phase detectors and the differences in the signal amplitude to the reference voltage in the first and second phase detectors, as well as the errors in the phase shifter at phase shifts of 45 and 90°.

The influence of the control devices and the phase meter tuning devices are simultaneously taken into account.

An analysis of formula (6.21) yields an expression for the measurement error $\Delta\varphi = (\varphi - \varphi')$.

Neglecting terms of higher order of smallness, we obtain

$$\begin{aligned} \Delta\varphi \approx m_n [0.5\gamma(1 - \cos\varphi)\cos\varphi - 0.104\sin 2\varphi(\gamma - 1) - \\ - 0.5(1 - \sin\varphi)\sin\varphi](1 - \alpha) + \left[\pm \Delta \sin 2\varphi \pm \frac{\beta}{2} \sin 2\varphi \pm \right. \\ \left. \pm \beta \sin^2\varphi \right], \end{aligned} \quad (6.23)$$

where m_n -- nominal value of the ratio of the signal amplitude to the reference-voltage amplitude,

$\gamma = m'_1/m'_2$ -- characterizes the degree of non-identity of the operating modes of the first and second phase detectors,

$\alpha = m'_1/m_1$ -- characterizes the asymmetry of the signal transformer arms in both circuits.

Formula (6.23) shows that the overall error in the measurement consists of two terms, the first representing the ^{intrinsic} phase meter error, and the second the error due to inaccuracy of the standard phase shifter.

Fig. 6.11 shows, in polar coordinates, the dependence of the intrinsic phase meter error on the measured phase difference.

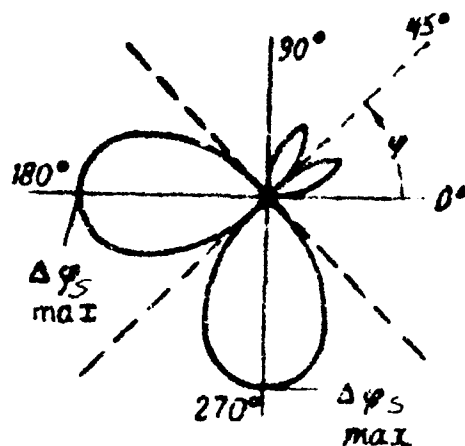


Fig. 6.11. Apparatus error of the phase meter proper.

As can be seen, the intrinsic error has a maximum for phase difference values of 180 and 270° :

$$\Delta\varphi_{s \max} = m_n \gamma (1 - \alpha). \quad (6.24)$$

Assuming $\gamma = 1.2$ and $(1 - \alpha) = 0.1$, corresponding to approximately 5% accuracy in the manufacture and adjustment of the circuit, we obtain

$$\Delta\varphi_{s \max} = \pm 6 m_n \quad (6.25)$$

when $m_n \leq 0.1$ we obtain a maximum error of 0.6° .

We can conclude from the analysis of the apparatus error of the phase meter that a) the overall apparatus error of the phase meter is the sum of the intrinsic error in the error of the phase shifter,

b) both the intrinsic error and the standard error depends on the measured phase difference

c) the intrinsic error is equal to zero when the phase differences are 0° , 45° , and 90° ,

d) the intrinsic error has a maximum when the phase difference values are 180° and 270° .

The magnitude of the maximum intrinsic error is proportional to m_n , and consequently can be reduced upon a judicious choice of the phase meter operating conditions.

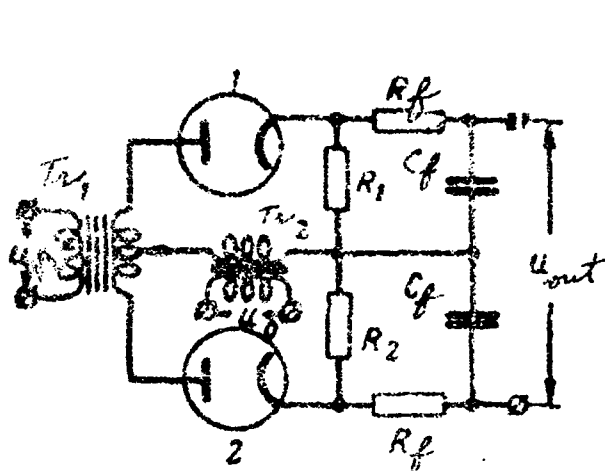
For $m_n \leq 0.1$ it is enough to ensure 5% accuracy in the manufacture and balancing of the phase detector, to obtain a phase meter error less than 1° .

5. TRANSIENT TIME OF PHASE METER READINGS

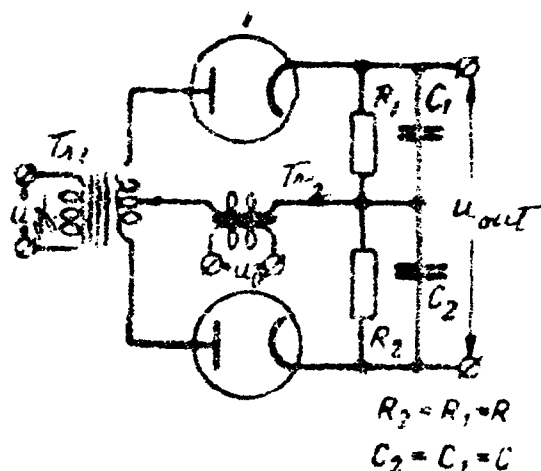
The phase detector output contains RC filters, intended to reduce the amplitude of the alternating component to an acceptable value, determined by the permissible ripple coefficient.

If the ripple factor is too large, the line that indicates the bearing on the tube screen becomes smeared out, and this

reduces the reading accuracy. The alternating voltage at the output of the phase detectors is also due to noise. In the case of white noise, the line on the tube is subject to random fluctuations, which make the reading difficult. The intensity of this fluctuation can be reduced by increasing the time delay of the filter. However, an increase in the time constant of the filter is limited by the requirement that the transient time of the phase meter reading be short.



6.12



6.13

Fig. 6.12. Diagram of phase detector in time-delay detection.

Fig. 6.13. Diagram of phase detector in peak detection.

Let us consider the sequence of determination of the transient time of the readings, t_t , for different filter systems.

In ~~analogous~~ a time-delay phase detector, as shown in Fig. 6.12, the transient time for the case $R_f \gg R_{1,2}$ is independent of the signal phase and is determined fully by the time constant of

the filter $R_f C_f$. It is possible to determine the transient time with sufficient degree of accuracy from the formula

$$t_t \approx 3R_f C_f. \quad (6.26)$$

Let us now determine the transient time in the case of peak detection (Fig. 6.13). Fig. 6.14 shows oscillograms for this case.

In the absence of a signal ~~the~~ capacitances C_1 and C_2 are charged approximately to a voltage equal to the amplitude of the reference voltage, U_0 . When a signal appears, the amplitude of the voltage acting in the circuit of diode 1 increases to a value $U_{a1} > U_0$, while in the circuit of diode 2 it decreases to $U_{a2} < U_0$.

The capacitance C_1 is charged almost instantaneously through diode 1 and the internal resistance of the transformers (time constant rC_1 is small). The diode 2, after the appearance of the signal, becomes cutoff, since the voltage on capacitance C_2 , applied with negative polarity to its anode, exceeds the amplitude of the acting voltage U_{a2} .

The capacitance C_2 is freely discharged through resistance R (time interval t_0 in Fig. 6.14) until the voltage across the capacitance is equalized with the amplitude of the acting voltage ($\vec{U}_{a2} = \vec{U}_0 - (1/2)\vec{U}_{sg}$), accurate to ~~ms~~ within one cycle of the working frequency.

Let us determine the transient time t_0 for the most unfavorable case, $\phi = 0$. The voltage across the capacitance C_2 varies as

$$U_0 e^{-\frac{t}{R_2 C_2}}.$$

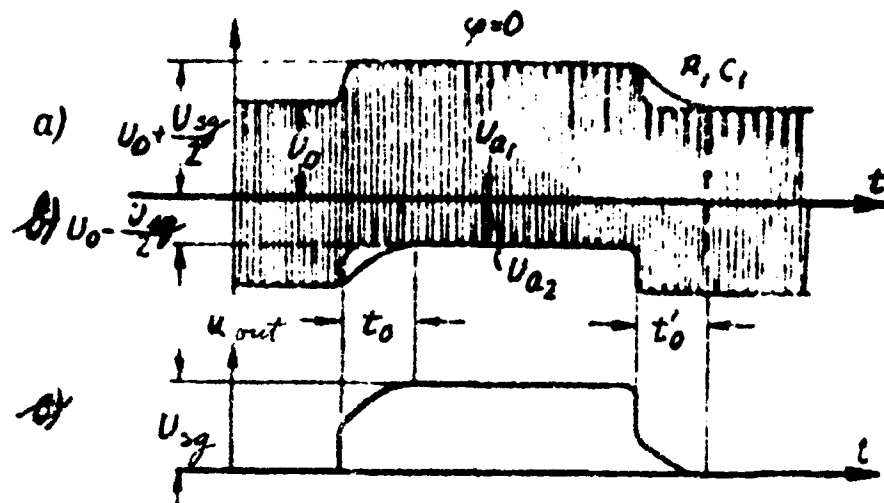


Fig. 6.14. For the determination of time to fix reading with pulse signal (dashed line shows voltage modulation in circuits of first and second diodes, solid line show voltage per capacitances C_1 and C_2)

(a) and (b) -- voltage oscillograms for first and second diode circuits, respectively;

(c) -- oscillogram of output voltage.

During the instant t_0 the voltage across the capacitance C_2 will be $U_0 - U_{sg}/2$. Then

$$U_0 e^{-\frac{t_0}{R_2 C_2}} = U_0 - \frac{1}{2} U_{sg}$$

where U_{sg} is the signal amplitude.

Hence

$$e^{-\frac{t_0}{R_2 C_2}} = 1 - m, \quad (6.27)$$

where

$$m = \frac{U_{sg}}{2U_0}; \quad m < 1.$$

From Eq. (6.27) we determine

$$t_0 = -R_2 C_2 \ln(1 - m). \quad (6.28)$$

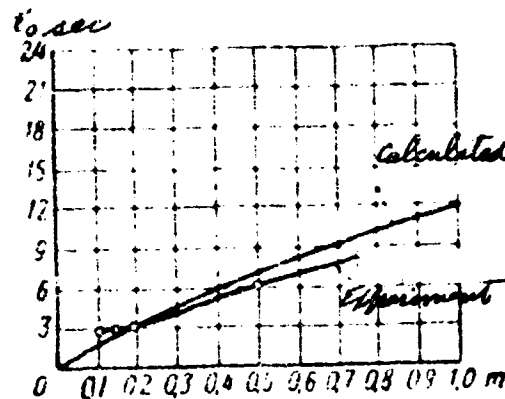
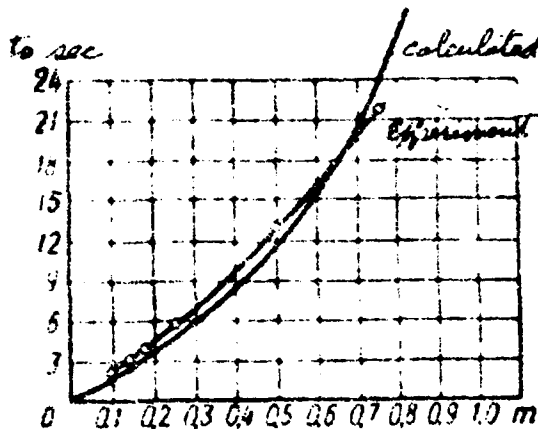


Fig. 6.15. Dependence of the transient time on the choice of operating conditions of the phase detector with peak detectors.

Fig. 6.16. Dependence of the transient time on the choice of conditions.

Taking $m \ll 1$ and considering $R_2 C_2 = R_1 C_1 = RC$, we get

$$t_0 \approx RCm. \quad (6.29)$$

Analogously, we obtain the transient time

$$t'_0 = -RC \ln \left(\frac{1}{1+m} \right). \quad (6.30)$$

for $m \ll 1$ we get

$$t'_0 \approx RCm. \quad (6.31)$$

Thus, the transient time of the readings in a peak detector is determined not only by the time constant RC , but depends also on the relation between the signal voltage and the reference voltage, as well as on the measured phase difference.

Taking the reference voltage sufficiently large compared with the signal voltage, it is possible to reduce considerably the transient time of the readings, for an equal ripple coefficient. This circumstance makes the circuit with peak detectors quite superior. The dependence of t_0 and t'_0 on m , established by formulas (6.28) and (6.30), is shown graphically in Figs. 6.15 and 6.16. The same graphs show the experimental results.

The experiment was carried out with an indicator symbolized as shown in Fig. 6.1, with phase detectors (see Fig. 6.2). The signal voltage was maintained constant at 20 volts.

The reference voltage was varied from 13.3 to 96 volt, corresponding to m ranging from 0.75 to 0.104. One of the phase detectors was turned on. The transient time was determined with a stop watch, being the time necessary for the line on the tube

to build up to total length. The time constant RC was taken to be 17 seconds.

Experiment has confirmed the dependence of the transient time on the ratio of the effective voltages.

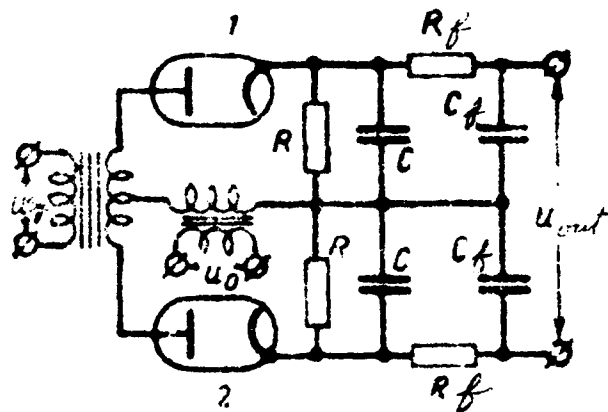


Fig. 6.17. Diagram of phase detector with complex filter.

The quantitative discrepancy between the experimental and theoretical curve is small and is essentially due to inaccuracies in measurement.

Let us examine the time variation of the transient time in the presence of an additional filter at the output of the phase detector (Fig. 6.17), under the condition $R_f \gg R$. In the absence of a signal the capacitance C_f , like C , is charged to a voltage U_0 . When a signal appears, the effective voltage U_a increases and the capacitance C is charged almost instantaneously.

The corresponding capacitance C_f is charged through a resistance R_f , and its charging time is approximately $3R_fC_f$.

In the second arm of the first detector, after cutoff of

diode 2, the capacitances C and C_f are discharged through resistances R and R_f .

Approximately within a time t_0 , the voltage across C reaches a steady state value. The capacitance C_f continues to discharge, and the time constant is approximately $R_f C_f$. The voltage is built up within a time of approximately $3 C_f R_f$. The total buildup time of the readings is determined by the formula

$$t_{\Sigma} \approx mRC + 3R_f C_f$$

6. OPERATION OF THE PHASE METER IN THE PRESENCE OF NOISE

Let us consider certain singularities of a phase detector circuit, which distinguish its operation in the presence of noise from ordinary detector circuits. Assume that a variety of sinusoidal noises, at frequencies close to the signal frequency, are applied to the phase meter input simultaneously with the signal. Such a phenomenon occurs when the signal of the radio station is modulated in amplitude. It is possible to consider analogously the action of white noise.

The voltage acting on the circuit of the first diode (see Fig. 6.12) is given by the formula

$$u_{a1} = \sqrt{\left[U_0 + U_{\omega} \cos \varphi + \sum_{i=1}^n U_{\omega_i} \cos (\omega_i - \omega) t \right]^2 + \left[U_{\omega} \sin \varphi + \sum_{i=1}^n U_{\omega_i} \sin (\omega_i - \omega) t \right]^2} \sin [\omega t + \xi(t)], \quad (6.32)$$

where U_{ni} — amplitude of the voltage of the i -th noise,

ω_i — frequency of the i -th noise.

ω — frequency of the signal.

$\xi(t)$ — phase modulation of the effective voltage.

We introduce the following notation

$$\frac{U_{ni}}{U_0} = m_i; \quad \frac{U_{nk}}{U_0} = m_k; \quad \frac{U_{\text{eff}}}{U_0} = m.$$

We then obtain after certain transformations

$$u_{a1} = U_0 \sqrt{1 + m^2 + 2m \cos \varphi + \sum_{i=1}^n m_i^2} \times$$

$$\times \left[\sqrt{1 + \frac{2 \sum_{i=1}^n m_i \cos (\omega_i - \omega) t}{1 + m^2 + 2m \cos \varphi + \sum_{i=1}^n m_i^2} + \frac{2 \sum_{i=1}^{n-1} \sum_{k=i+1}^n m_i m_k \cos (\omega_i - \omega_k) t}{1 + m^2 + 2m \cos \varphi + \sum_{i=1}^n m_i^2}} + \right.$$

$$\left. + \frac{2 \sum_{i=1}^n m m_i \cos [(\omega_i - \omega) t - \varphi]}{1 + m^2 + 2m \cos \varphi + \sum_{i=1}^n m_i^2} \right] \sin [\omega t + \xi(t)]. \quad (6.33)$$

Assume that the voltage on the detector load duplicates the form of the envelope of the actual voltage. Let also the reference voltage exceed considerably the signal voltage and the noise voltage. Then the voltage across the load is given approximately by

$$u_{d1} \approx K_d U_0 \sqrt{1 + m^2 + 2m \cos \varphi + \sum_{i=1}^n m_i^2} + K_d U_0 \times$$

$$\times \left[\frac{\sum_{i=1}^n m_i \cos(\omega_i - \omega)t + \sum_{i=1}^n m m_i \cos[(\omega_i - \omega)t - \varphi] + \sum_{i=1}^{n-1} \sum_{k=i+1}^n m_i m_k \cos(\omega_i - \omega_k)t}{\sqrt{1 + m^2 + 2m \cos \varphi + \sum_{i=1}^n m_i^2}} \right]. \quad (6.34)$$

To obtain an analogous expression for the load voltage of the second diode, it is enough to reverse the signs of m , m_i , and m_k in formula (6.34).

The output voltage of the phase detector is the difference in the voltages across the loads of the ~~second and first~~ first and second detector. Obviously, under the conditions indicated above ($m \ll 1$) the spectrum of the alternating component of the output voltage of the phase detector will contain predominately the components of the beats between the frequency of the reference voltage ω and the noise $(\omega_i - \omega)$.

Combination frequencies of the type $(\omega_i - \omega_k)$ are practically absent from the output. This increases the interference immunity of the phase detector compared with the detection cir-

cuits without reference voltage.

Let us now consider the effect of pulse noise on the phase detection.

Assume that the input of the phase meter is subjected simultaneously to a signal and to a noise, the oscillogram of which is shown in Fig. 6.18. Noise of this type is frequently produced by atmospheric discharges.

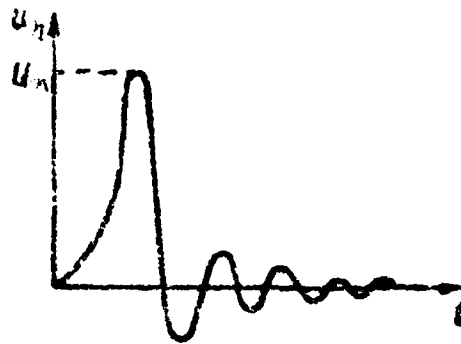


Fig. 6.18. Oscillogram of a pulsed noise.

The duration of the principal pulse is approximately equal to half the period of the working frequency. In the case of time-delay detection (see Fig. 6.12) the effect of such a single noise is very insignificant, since the change in the output voltage past the filter is negligible, if the amplitude of the noise is comparable with that of the signal. In the case of peak detection, to the contrary, single pulse noises greatly interfere with the measurements.

This is explained by the fact that the capacitance C_1 in

the circuit of diode 1 (see Fig. 6.13) is charged through the diode, since the noise combines with the effective voltage of the signal. The increase in the voltage across capacitance C_1 is almost equal to the amplitude of the noise. At the same time, the capacitance in the circuit of diode 2 remains practically with the same charge. The increment in the output voltage is approximately equal to the amplitude of the noise. This causes a pip on the line of the tube screen. After the noise action stops, the capacitance is discharged through the load resistances and the line gradually returns to its previous position. The angle of the pip in the line is determined by the formula

$$\Delta \varphi_m \approx \frac{\sqrt{2}}{2} \frac{U_n}{U_{sg}}. \quad (6.35)$$

Formula (6.35) is correct when $U_n \ll U_{sg}$.

Let us consider now the effect of a single noise on a phase detector built in accordance with the circuits shown in Fig. 6.17. As in the case of peak detection, the capacitance C in the cathode of diode 1 increases its voltages by an amount equal to the amplitude of the noise. After the noise stops, the diode is cutoff and the capacitance C is discharged through the resistances R and R_f , charging thereby the capacitance C_f . The voltage on the capacitance C_f increases slowly, and then drops again to the steady-state value (Fig. 6.19).

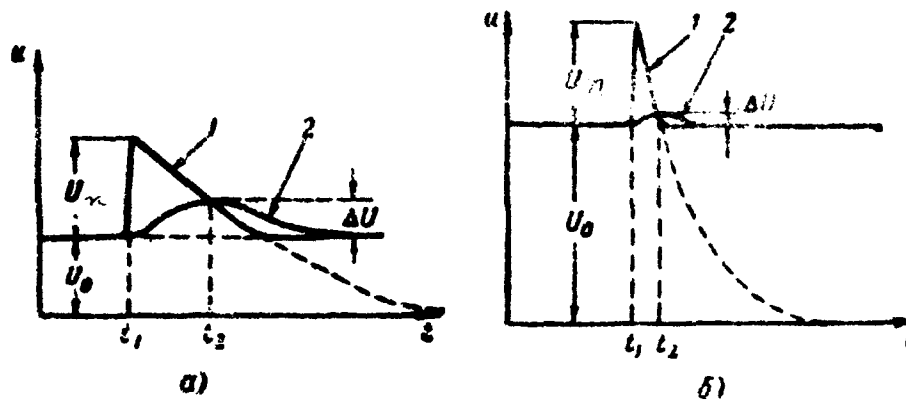


Fig. 6.19. On the determination of the effect of pulsed noise on the phase meter reading.

(a) Small reference voltage, (b) -- large reference voltage, 1 -- voltage across capacitance C , 2 -- voltage across capacitance C_f .

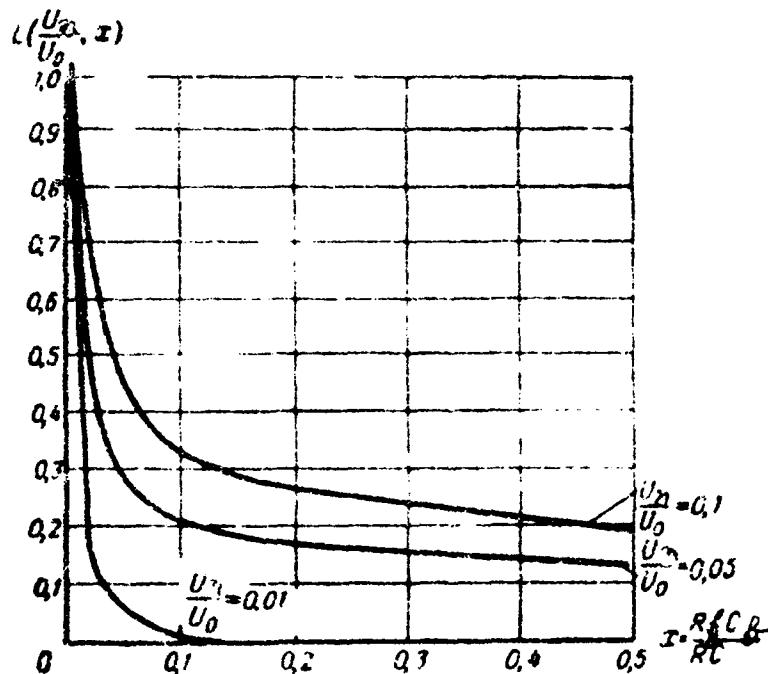


Fig. 6.20. Values of the function that determines the

error of the phase meter for single noise pulses.

The maximum increase ΔU of the voltage across the capacitance C_f determines the angle of slope of the line, and consequently the effect of the noise. It can be shown that this quantity depends not only on the amplitude of the noise, but also on the amplitude of the reference voltage. Actually, prior to the arrival of the noise both capacitances C and C_f were charged equally, approximately to voltage U_0 . After the cessation of the noise the capacitance C is discharged to a voltage $U_0 + U_n$, with the diode cutoff. The rate of discharge of capacitance C depends on the initial voltage $U_0 + U_n$ and increases with increasing U_0 . Since the capacitance C_f has been previously charged to a voltage U_0 , the rate of its charge and discharge is determined only by the noise voltage U_n .

The maximum voltage across capacitance C_f is reached in that case, when the voltages across the capacitances C and C_f are approximately equalized (instant t_2 , Fig. 6.19). Actually, the voltage u_{Cf} becomes maximum, when $du_{Cf}/dt = 0$. This means that the current through the resistance R_f is equal to 0, and consequently, the voltages across C and C_f are equal to each other (see Fig. 6.17). By increasing U_0 we increase the rate of discharge C at an unchanged rate of discharge C_f . Therefore the equalization of the voltages occurs earlier and the voltage across C_f has a smaller

increase. In order to verify this it is enough to compare the curves of Figs. 6.19a and 6.19b, which are constructed for different values of the reference-voltage amplitude U_0 and equal values of U_n .

A detailed analysis shows that the angle of the throw of the line on the screen of the cathode ray tube, for the case under consideration, is determined by the equation

$$\Delta\varphi = \frac{\sqrt{2}}{2} \frac{U_n}{U_0} L\left(\frac{U_n}{U_0}; \frac{R_f C_f}{RC}\right). \quad (6.36)$$

The function L , which is a function of $R_f C_f / RC$, is shown on Fig. 6.20 for different values of U_n / U_0 .

The analysis given makes it possible to choose the parameters of the phase meter in such a way, that for a given buildup time the effect of different noises can be substantially reduced.

BIBLIOGRAPHY

1. Adamskiy, V.K., Radio Receiving Centers, Svyaz'dat, 1949.
2. Ayzenberg, G.Z. Antennas for Main Line Radio Communication, Svyaz'dat, 1948.
3. Al'pert, Ya. L., Ginzburg, V.L., Feynberg, Ye. L., Propagation of Radio Waves, Gostekhizdat, 1959.
4. Al'pert, Ya. L. Propagation of Radio Waves in the Ionosphere, Gostekhnizdat, 1949.
5. Aseyev, B.P. Phase Relations in Radio Engineering, Svyaz'dat, 1951.
6. Dolukhanov, M.P., Propagation of Radio Waves, Svyaz'dat, 1951.
7. Yevtyanov, S.I. Transients in Receiving and Amplifying Circuits. Svyaz'dat, 1948.
8. Karmalin, P.V. Physical and Technical Principles for Marine Radio Direction Finding, Morskoy transport, 1946.
9. Cramer, H. Mathematical Methods of Statistics (Russian Translation), IL, 1948.
10. Pestryakov, V.B. Radio Navigation Angle Measuring Systems. Gosenergoizdat, 1955.
11. Pistol'kors, A.A., Antennas, Svyaz'dat, 1949.
12. Starik, M. Ye. and Kukes I.S. Radio Direction Finders, Voenmorizdat, 1941.
13. Snirkov, V.V. Calculation of Antenna-Angle Measuring

System of Direction Finders of the Adcock Type, Voenizdat, 1947.

14. Bain W. C., The calculation of wave — interference errors on a direction — finder employing cyclical differential measurement of phase. «PIEE», vol. 100, part III, № 67, 1953.

15. Orme W., Möglichkeiten und Grenzen der Richtmessung mit Vorn. Ant. len, Deutsche Luftfahrtforschung, Untersuchungen und Mitteilungen, № 612, 1942.

16. Ross W., Lateral deviation of radio waves reflected at the ionosphere. Radio research spec. Rep. № 19, London, 1949.

17. Ross W., Bramley E. N., Ashwell G. E., A phase-comparison method of measuring the direction of arrival of ionospheric radio waves. «PIEE», vol. 98, part III, № 54, VII, 1951.

18. Rundfleisch H., Die Großbasis peilanlage «Wullenwever», «Nachrichtentech. Z.», 1956, 9, № 3, 119—123.

19. Walden S., Locke A. F. L., Barrett J. O. G., Pritts W. J., The development of a high — frequency cathode — ray direction — finder for naval use, «Journ. IEE», vol. 94, part III, № 54, p. 294—301, 1951.

5-107

B. I. D.